EFFECT OF LIPOTOXICITY ON ER STRESS, AUTOPHAGY AND APOPTOSIS IN SKELETAL MUSCLE AND REGULATION BY ADIPONECTIN

ESTHER RAI

A THESIS SUBMITTED TO THE FACULTY OF GRADUATE STUDIES IN PARTIAL FULFILLMENT OF THE REQUIREMENTS FOR THE DEGREE OF MASTER OF SCIENCE

GRADUATE PROGRAM IN BIOLOGY
YORK UNIVERSITY
TORONTO, ONTARIO

January 2015

Abstract

Obesity is a key factor contributing to the “metabolic syndrome” which increases the risk for type 2 diabetes, cardiovascular disease and liver complications. In obese conditions, lipotoxicity is a serious concern as the accumulation of lipids and lipid-intermediates in non-adipose tissue such as skeletal muscle, heart, liver and pancreas, leads to cellular dysfunction and activation of stress responses. In this study, I have examined how palmitate-induced lipotoxicity, effects the cellular processes ER stress, autophagy and apoptosis, in L6 rat skeletal muscle cells. I have elucidated cross-talk mechanisms between these processes, and have demonstrated that palmitate induces excessive protein accumulation, thereby stimulating ER stress, activation of the UPR and subsequent apoptosis. Autophagy may be recruited as a compensatory mechanism to help the cell cope with the stress of protein overload through its degradative pathway. Additionally, adiponectin may increase autophagic flux, thereby contributing to cytoprotective effects of reducing ER stress and apoptosis.

Acknowledgements

I would like to take this opportunity to first and foremost thank Dr. Gary Sweeney, my supervisor, whose constant support, encouragement and advice, I will always be grateful for. It is with his guidance, expertise and patience that I have been able to arrive at this milestone in my academic career and his good nature, humor and steady backing have made the journey a truly valuable, enjoyable experience that has helped me to realize my potential as a researcher.

Next, I would like to express my heartfelt gratitude to my committee members: Dr. John McDermott, Dr. Andrew Donini, Dr. Chun Peng and Dr. Michael Connor, for their time and support in the discussion and revision of my thesis. Thank you also to my in-lab supervisors, Dr. Min Park and Dr. Subat Turdi for their meticulous efforts in training and advising me.

A very big thank you to all past and present members of the Sweeney Lab. Your friendship and day-to-day support has meant so much to me during the past two years and I could not have made it to this point without you. A special thank you to Penny Ahlstrom, Sanjana Sen, Dr. Keith Dadson, Dr. Carol Chan and Dr. Helen Chasiotis for always being there for me and willing to lend a helpful hand, or an attentive ear. Thank you to Dr. Scott Kelly, Adrienne Dome and Cristalina Del Biondo for your behind-the-scenes support at the university and to the Go Safe staff for keeping me safe on the late nights.

Lastly, but not in the least, a sincere thank you to my loving family. To my parents, Daniel and Elizabeth Rai, for their love and steadfast support of my endeavours, to my sister Desiree Chester, for constantly inspiring and motivating me, to my brother-in-law, Trevor Chester, for being my continued cheerleader, and to my boyfriend, Danny Ray Dadula, who held my hand throughout, thank you. This could not have been possible without you all.

Table of Contents

Chapter 2: Materials and Methods

Chapter 3: Effect of Palmitate on ER Stress, Autophagy and Apoptosis and Regulation by Adiponectin

Chapter 5: Summary

List of Abbreviations

3-MA	3-Methyladenine
ACD	Autophagic cell death
ACS	Acyl CoA synthase
Ad	Adiponectin
AdipoR	Adiponectin receptor
AdKO	Adiponectin knockout
ADP	Adenosine diphosphate
AIF	Apoptosis-inducing factor
AMBRA1	Activating molecule in BECN1-regulated autophagy 1
AMEM	Alpha-minimum essential medium
AMPK	Adenosine monophosphate-activated protein kinase
ANGPTL2	Angiopoietin-like protein 2
ANOVA	Analysis of variance
APAF1	Apoptotic protease-activating factor 1
ASK	Apoptosis signal-regulating kinase
ATF	Activating transcription factor
ATG	Autophagy protein
ATP	Adenosine triphosphate
BAK	BCL-2 antagonist or killer
BAX	BCL-2-associated X protein
BCA	Bicinchoninic acid
Bcl-2	B cell lymphoma 2
BH3	Bcl-2 homology domain 3
BID	BH3-interacting to domain death agonist
BiP	Binding immunoglobulin protein
BMI	Body mass index
BSA	Bovine serum albumin
C/EBP	CCAAT/enhancer-binding protein
CAD	Caspase-activated DNase
CCL2	(C-C motif) chemokine ligand 2
CDC	Cell division cycle protein 16 homolog
Chl	Chloroquine
CoA	Coenzyme A
CHOP	CCAAT/enhancer-binding protein homologous protein
CIH	Chronic intermittent hypoxia
CV	Cresyl violet
CXCCL5	(C-X-C motif)-chemokine ligand 5
DAG	Diacylglycerols
DAPI	4’,6-diamidino-2-phenylyindole
DMSO	Dimethyl sulfoxide
DTT	Dithithreitol
EMCL	Extramyocellular lipids
eIF2	Eukaryotic translation initiation factor 2
EndoG	Endonuclease G
ER	Endoplasmic reticulum
ERA	ER-containing autophagosomes
ERAD	ER-associated degradation
Ero1	ER oxidoreductin 1

EV	Empty vector
FA	Fatty acid
fAd	Full length adiponectin
FAK	Focal adhesion kinase
FADD	Fas-associated protein with death domain
FasL	Fas ligand
FasR	Fas receptor
FBS	Fetal bovine serum
FFA	Free fatty acid
FIP200	FAK family kinase-interacting protein of 200 kDa
gAd	Globular adiponectin
GADD34	Growth arrest and DNA damage-inducible protein 34
GAP	GTPase-activating protein
GFP	Green fluorescent protein
GLUT4	Glucose transporter type 4
GRP78	Glucose-regulated protein
GTP	Guanosine-5'-triphosphate
H_2O_2	Hydrogen peroxide
HEK293	Human embryonic kidney 293 cells
HFD	High-fat diet
HMW	High molecular weight
HRP	Horse-radish peroxidase
ICAD	Inhibitor of CAD
IKKβ	IκB kinase
IL	Interleukin
IMCL	Intramyocellular lipids
iNOS	Inducible nitric oxide synthase
IR	Insulin receptor
IRE1	Inositol-requiring enzyme-1
IRS	Insulin receptor substrate
JNK	c-Jun N-terminal kinases
LAMP-2A	Lysosome-associated membrane protein type 2A
LC3	Microtubule-associated protein 1A/1B-light chain 3
LMW	Low molecular weight
MAPK	Mitogen-activated protein kinase
MCP1	Monocyte chemoattractant protein 1
MEF	Mouse embryonic fibroblast
MMW	Medium molecular weight
MOMP	Mitochondrial outer membrane permeabilization
mtDNA	Mitochondrial DNA
mTORC2	Mammalian target of rapamycin complex 2
MTS	3-(4,5-dimethylthiazol-2-yl)-5-(3-carboxymethoxyphenyl)-2-(4-sulfophenyl)-2H-tetrazolium
MTT	3-(4,5-dimethylthiazol-2-yl)-2,5-diphenyltetrazolium
MuRF1	Muscle RING-finger protein 1
NaF	Sodium fluoride
NAMPT	Nicotinamide phosphoribosyltransferase
NCK	Noncatalytic region of tyrosine kinase
NF-κB	Nuclear factor-κB
NLRP3	NOD-like receptor
NO	Nitric oxide

NOD	Nucleotide-binding oligomerization domain
PAGE	Polyacrylamide gel electrophoresis
Pal	Palmitate
PARP	Poly ADP ribose polymerase
PAS	Pre-autophagosomal structure
PBS	Phosphate-buffered saline
PDK	Phosphoinositide-dependent kinase
PE	Phsphatidylethanolamine
peIF2α	Phospho-eIF2 alpha
PERK	Protein kinase-like ER kinase
PH	Pleckstrin-homology
PI3K	Phosphatidylinositol-3-kinase
PINK1	PTEN-induced putative kinase 1
PIP2	Phosphatidylinositol 4,5-bisphosphate
PIP3	Phosphatidylinositol 3,4,5-triphosphate
PKB	Protein kinase B
PKC	Protein kinase C
PolyQ72	Polyglutamine 72
PP1	Protein phosphatase 1
PPARα	Peroxisome proliferator-activated receptor alpha
pPERK	Phospho-PERK
PTB	Phosphotyrosine-binding
PTEN	Phosphatidylinositol-3,4,5-trisphosphate 3-phosphatase
PVDF	Polyvinylidene fluoride
Rap	Rapamycin
RBP4	Retinol-binding protein 4
RFP	Red fluorescent protein
RIP	Ribosome inactivating protein
RIPA	Radioimmunoprecipitation
ROS	Reactive oxygen species
Sal	Salubrinal
SDS	Sodium dodecyl sulfate
SEM	Standard error of the mean
SERCA	Sarco/ER Ca^{2+}-ATPase
SFRP5	Secreted frizzled-related protein 5
SH2	Src homology
siRNA	Small interfering RNA
SMAC	Second mitochondria-derived activator of caspase
TG	Triacylglycerol
ThT	Thioflavin T
TBC1D4	(tre-2/USP6, BUB2, cdc16) domain family member 4
TEM	Transmission Electron Microscopy
TNF	Tumour necrosis factor
TRAD	TNF receptor type 1-associated death domain
TRAF2	TNF receptor-associated protein factor 2
TUNEL	Terminal deoxynucleotidyl transferase dUTP nick end labeling
TZD	Thiazolidinedione
UCP	Uncoupling protein
ULK1	UNC-51-like kinase 1
UPR	Unfolded protein response
USP6	Ubiquitin specific peptidase 6

VMP1	Vacuole membrane protein 1
VPS34	Vacuolar protein sorting 34
WHO	World Health Organization
wt	Wild type
XBP1	X-box binding protein 1
XIAP	X-linked inhibitor of apoptosis protein

List of Figures

Chapter 1: Introduction

Chapter 3: Effect of Palmitate on ER Stress, Autophagy and Apoptosis and Regulation by Adiponectin

Chapter 5: Summary

Chapter 1: Introduction

1.1. The Prevalence and Health Risks of the Obesity Epidemic

Over the past decades, with an increase in caloric intake and sedentary lifestyle, obesity has risen to become a global pandemic [1]. Categorized as a body mass index (BMI) of over 30 (i.e. weight (kg)/height (m^2)), a 2008 evaluation by the World Health Organization has estimated that 500 million adults aged 20 or older worldwide are obese and 900 million are overweight (BMI of 25.0-29.9). This means that approximately 35% of the global adult population are overweight or obese, and indicates that since 1980, obesity rates have doubled [2].

This trend is well represented in Canada, with the overall prevalence of obesity having increased from 10% in 1970 to 23% in 2004 (i.e. 8% to 23% in men and 13% to 22% in women) [3]. Another report states that between 1985 and 2011, the prevalence of adult obesity in Canada has escalated from 6.1% to 18.3%. Breaking it down, there has been an increase from 5.1% to 13.1% in individuals with a BMI of 30.0–34.9 (obese class I), from 0.8% to 3.6% in the BMI group of 35.0–39.9 (obese class II), and from 0.3% to 1.6% in those with BMI of ≥ 40.0. Furthermore, it is predicted that by 2019, adults classified as overweight or obese are predicted to outnumber normal-weight adults in half of the Canadian provinces [4].

These alarming increases are particularly disconcerting as obesity is known to lead to numerous adverse disorders such as dyslipidemia, hypertension and glucose intolerance. Such abnormalities which are often grouped under the umbrella term “metabolic syndrome” increase the risk for cardiovascular disease, type 2 diabetes and liver complications such as non-alcoholic fatty liver disease [5]. In addition, obesity has been linked with gastrointestinal and

reproductive cancers, osteoarthritis and sleep apnea. Collectively, these mean that obesity reduces life expectancy, increases disability and impairs productivity [1].

1.2. Adipose Tissue, Skeletal Muscle and the Consequences of Increased Adiposity

Adipose tissue consisting of adipocytes, endothelial cells, fibroblasts, leukocytes and macrophages is primarily found in subcutaneous and visceral depots, but it also occurs in organs such as the heart and kidneys, and in the bone marrow, lungs and the adventitia of major blood vessels [6]. One of the chief functions of adipose tissue is to sequester excess fuel as fat in adipocytes. In conditions of obesity however, adipocytes experience challenges and limitations on their lipid storage and processing capabilities. Beyond a critical threshold, the adipocyte begins exhibiting signs of stress, including hypertrophy and mechanical stress, hyperplasia, compositional changes of lipids and other nutrients, hypoxia, disruption of mitochondrial function, production of reactive oxygen species, apoptotic signaling, increased fatty acid (FA) release, altered adipokine signaling, inflammation and endoplasmic reticulum (ER) stress. Overlap occurs between several of these processes – many of them feeding into and influencing each other to contribute to the development of metabolic dysfunction [7].

Many studies have found that the excess circulating fatty acids in the blood plasma of obese individuals lead to the deposition of lipids or lipid-intermediates in non-adipose tissue such as heart and skeletal muscle, liver and pancreas [8-10]. In skeletal muscle, lipids are categorized as extramyocellular lipids (EMCL) which are localized in adipose cells between myofibers, and intramyocellular lipids (IMCL) which are found within muscle cells. IMCL consist of lipid droplets containing triacylglycerols (TAG) and cholesterol esters, as well as lipid metabolites, such as long-chain acyl CoAs, diacylglycerols (DAG) and ceramides. Both EMCL and IMCL expand in obese conditions, causing buildup of lipid byproducts and consequent

lipotoxic effects. Indeed, elevated TAG content and greater numbers of lipid droplets have been documented in muscle biopsies from obese people, while long-chain acyl CoAs, diacylglycerols and ceramides have been noted to accumulate in skeletal muscle of obese humans, genetically obese mice (*ob/ob and db/db*) and obese Zucker rats [11].

Investigating the biological effects of excessive lipids on skeletal muscle is of particular interest because the changes in cell signaling that are induced bring about adverse outcomes such as insulin resistance and inflammation. These metabolic consequences are especially important in this tissue as skeletal muscle is the primary site of insulin-stimulated glucose disposal [12]. An additional point of concern that is gaining more recognition in recent years, is the observation that excessive adiposity can lead to apoptosis and atrophy, which is involved in the development of various skeletal muscle myopathies that are often observed in obese patients [13].

1.2.1. Insulin Resistance

Approximately 45% of lean body mass is composed of skeletal muscle, which collectively accounts for about 80% of insulin-stimulated glucose disposal in the body. With skeletal muscle being such a major contributor to whole-body energy expenditure, its responsiveness to insulin is crucial for regulating whole-body insulin sensitivity [14-16]. In healthy individuals, insulin promotes glucose uptake through a cascade of phosphorylation events that culminate in the translocation of GLUT4 transporters from the cytoplasm to the plasma membrane, which then allow glucose to enter the cell [12, 17].

Insulin binds to the α subunit of its insulin receptor (IR), inducing a conformational change that results in the autophosphorylation of tyrosine residues present in the β subunit [18].

Members of the insulin receptor substrate family (IRS) then bind to IR via phosphotyrosine-binding (PTB) domains [19]. Receptor binding leads to the phosphorylation of key tyrosine residues on IRS proteins, which then bind to downstream substrates such as class I phosphatidlyinositol-3-kinase (PI3K) through the Src homology 2 (SH2) domain of the p85 regulatory subunit. The catalytic subunit p110 is then activated and phosphorylates lipid substrates such as phosphatidylinositol 4,5-bisphosphate (PIP2) to form phosphatidylinositol 3,4,5-triphosphate (PIP3) at the plasma membrane. Akt is recruited to the plasma membrane via pleckstrin-homology (PH) domain interaction with PIP3, and a conformational change in Akt occurs that allows its subsequent phosphorylation. Specifically, interaction with the activating kinase phosphoinositide-dependent kinase (PDK) phosphorylates Akt at threonine (308) in its kinase-domain activation loop, causing partial activation of Akt/protein kinase B (PKB). However the complete activation of Akt requires phosphorylation at serine (473) located in the hydrophobic C-terminal domain by mammalian target of rapamycin complex 2 (mTORC2). The essential step of GLUT4 translocation to the plasma membrane, is mediated via Akt phosphorylation of AS160 (i.e. Akt substrate of 160kD) which is also known as TBC1D4 (i.e. member 4 of TBC1 (tre-2/USP6, BUB2, cdc16) domain family). Phosphorylation occurs at T642 and phospho S/T Akt (PAS) sites, with the (R/K)X(R/K)XXS*/T* recognition motif. Phosphorylation of TBC1D4 increases binding to 14-3-3 proteins, which may inhibit Rab-GAP function towards downstream Rabs, and promote GTP loading, activation of Rabs and the movement of GLUT4 from intracellular compartments to the plasma membrane [20].

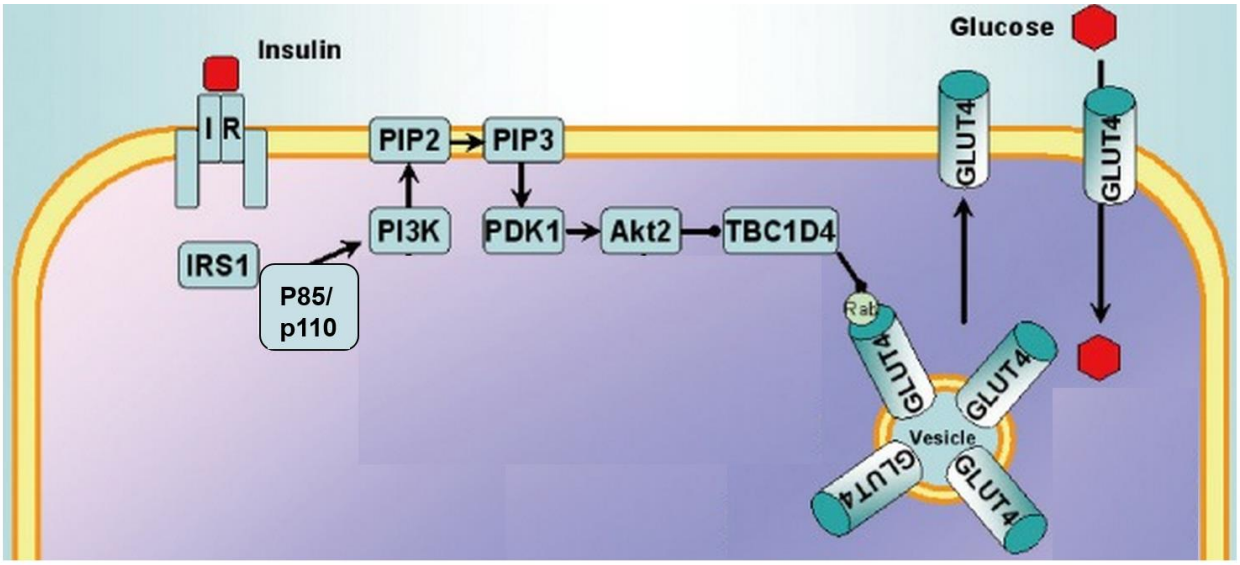

Figure 1.1. Regulation of insulin-stimulated glucose uptake. Insulin binds to IR which triggers a cascade of phosphorylation events, culminating in the translocation of GLUT4 transporters from the cytoplasm to the plasma membrane, which then allow glucose to enter the cell. Adapted from O'Neill [20].

In addition to its regulatory role in glucose uptake, insulin is also important for suppressing lipolysis i.e. the hydrolysis of fats into fatty acids and glycerol, in adipose tissue during the fed state. However, in obesity, the impairment of insulin action means that even in the fed state free fatty acids (FFA) are released into the circulation [21]. The abnormal accumulation of circulating FFA and lipid metabolites such as DAG and ceramides in skeletal muscle are postulated to be involved in activating protein kinase C (PKC) α, θ, and ε isoforms as well as IκB kinase (IKKβ) and c-Jun N-terminal kinases (JNK). These catalyze the phosphorylation of serine/threonine sites of the insulin receptor and substrates IRS1 and IRS2 (instead of the tyrosine sites), and decrease subsequent phosphorylation of Akt/PKB. The remainder of the signaling pathway downstream of these events therefore becomes inhibited, leading to reduced or abrogated GLUT4 translocation and glucose uptake [12, 22, 23]. Indeed, studies have shown that when rat L6 myotubes are incubated with palmitate, a common saturated fatty acid, insulin stimulated glucose uptake and translocation of GLUT4 to the cell surface is inhibited, indicating that deposition of fatty acids in insulin target tissues lead to loss of insulin sensitivity and cause insulin resistance [17]. This resistance to insulin action, brought

on by obesity, is instrumental in the pathogenesis of type 2 diabetes as it induces hyperglycemia when compensatory insulin hypersecretion fails. Therefore, from the standpoint of adiposity, central fat accumulation, intraorgan lipid deposition and plasma free fatty acid accumulation, are all important mediators in the development of insulin resistance and metabolic dysfunction [1].

1.2.2. Inflammation and Adipokine Imbalance

Insulin resistance in the obese state is typically accompanied by chronic, low-grade inflammation. Exposure to fatty acids induce an inflammatory response in insulin sensitive tissues that is characterized by increased generation of reactive oxygen species (ROS), activation of mitogen activated protein kinases (MAPK) and nuclear factor-κB (NF-κB), and elevations in inflammatory cytokines [17]. Cytokines secreted by adipose tissue are collectively called adipokines and metabolic dysfunction that results from excess adipose tissue mass is thought to be partly attributable to an imbalance in the expression of pro- and anti-inflammatory adipokines, which either induce inflammatory responses and metabolic dysfunction or help to resolve inflammation and exert protective effects on obesity-linked metabolic disorders [6].

Most adipokines are pro-inflammatory and are upregulated in obesity, thereby exacerbating obesity-linked metabolic and cardiovascular diseases. They include tumour necrosis factor (TNF), interleukin-6 (IL-6), resistin, retinol-binding protein 4 (RBP4), lipocalin 2, IL-1S, angiopoietin-like protein 2 (ANGPTL2), CC-chemokine ligand 2 (CCL2), CXC-chemokine ligand 5 (CXCL5) and nicotinamide phosphoribosyltransferase (NAMPT) [6]. Adipose tissue also secretes a smaller number of anti-inflammatory proteins, such as adiponectin and SFRP5. Adiponectin is particularly interesting as its expression profile in obesity and states of metabolic dysfunction is opposite to the pro-inflammatory adipokines; many rodent and human studies

have found that its level decreases with increasing BMI, plasma glucose and insulin, as well as serum triglycerides, in spite of an increase in adipose mass [6, 12]. When administered to diabetic or obese experimental organisms, it has been shown to protect against several metabolic disorders. For example, *ob/ob* mice given adiponectin demonstrated improvement in fatty liver disease through suppression of pro-inflammatory TNFα production [24], streptozotocin-induced diabetic mice treated with hydrodynamic injection of adiponectin-expressing plasmid DNA exhibited a reduction in hyperglycemia brought about by increased hepatic glucose uptake [25], and mice fed a high fat/sucrose diet and given adiponectin treatment showed increased fatty acid oxidation in muscle tissue and reduced plasma levels of glucose, free fatty acids and triglycerides [26]. A more in-depth review of adiponectin and its protective effects will be covered in a later section.

1.2.3. Skeletal Muscle Myopathies

Although the role of obesity in inducing insulin resistance in skeletal muscle has been extensively studied, obesity's part in promoting apoptosis and atrophy in skeletal muscle as well as in impairing muscle differentiation and regeneration is also worth consideration [11, 27].

A recent study of the gastrocnemius muscle in diet-induced obese male Wistar rats showed that dyslipidemia may be a mechanism for the activation of inflammatory and stress-activated signaling pathways, which lead to apoptosis and atrophy in skeletal muscle [27]. Obese rats demonstrated significant increases in pro-inflammatory TNF-R1 and TNF-R2, which contributed to the activation of the NF-κB pathway and the subsequent induction of the E3 ligase, MuRF-1, which is involved in all models of atrophy. Additionally, physical evidence of atrophy in obese rats was also illustrated by a reduction in fibre cross-sectional area in the gastrocnemius muscle. Apoptosis was shown to have a role in obesity-related skeletal muscle

atrophy as obese animals demonstrated a significant increase in cleaved caspase 3 and PARP cleavage downstream of caspase 3 activation [27].

Accumulation of toxic lipid metabolites and inflammation caused by obesity have also been found to compromise muscle satellite cell function that results in impaired muscle maintenance and regeneration [28]. In vitro studies have found that fatty acids, diacylglycerols and ceramides induce apoptosis and reduce myoblast proliferation and differentiation, perhaps by activating myostatin, a growth factor that limits the size of muscles [11], and by inhibiting the expression or activity of myogenic regulatory factors MyoD and myogenin [13]. Additionally ceramides and pro-inflammatory cytokines have been shown to inhibit muscle growth in part by inhibiting the IGF-1/Akt /mTOR pathway [29-31]. Hence lipotoxicity arising from obesity might be shown to have negative implications for differentiation during muscle regeneration in obese animals [11].

1.3. Stress-Activated Cellular Responses Induced by Obesity: ER Stress, Autophagy and Apoptosis

As mentioned in section 1.2, excess lipid accumulation brought on by obesity can lead to the activation of cellular stress responses [7]. In recent years, the relationships between three of these cellular processes, namely, ER stress, autophagy and apoptosis, have come under investigation, not only because of their prominent role in obesity but also because they have been found to be involved in the development of several other pathologies such as neurodegenerative disorders like Alzheimer's and Parkinson's, cancer, cardiovascular disease and diabetes mellitus [5, 32, 33]. Under conditions of health, each of these processes have imperative roles in maintaining cellular homeostasis, but disease states and various adverse stimuli such as DNA damage, pathogens, hypoxia, hyperglycemia and lipotoxicity, can cause

their dysregulation and induce stress signaling pathways that often involve cross talk between them [5, 32-35].

1.3.1. ER stress

1.3.1.1. Function and Signaling Pathway

In the eukaryotic cell, the endoplasmic reticulum (ER) organelle has important roles in protein and lipid biosynthesis, folding of newly synthesized peptides, modification of secreted proteins, detoxification of xenobiotics and the maintenance of calcium homeostasis [36, 37]. It efficiently processes approximately one third of all proteins produced, but when the amount of nascent proteins exceeds its processing capacity, unfolded or misfolded proteins accumulate and disrupt ER homeostasis causing ER stress [36]. This usually results from various physiological and pathological insults including high protein demand, viral infections, environmental toxins, inflammatory cytokines and mutant protein expression [38]. The unfolded protein response (UPR) is then activated as a cellular self-defense mechanism that reduces ER stress by reducing protein synthesis, increasing protein folding and increasing the degradation of misfolded proteins [39].

These actions are mediated by three ER transmembrane proteins, namely, double stranded RNA-dependent protein kinase-like ER kinase (PERK), inositol-requiring enzyme-1 (IRE1), and activating transcription factor 6 (ATF6). When glucose-regulated protein (GRP78), an ER chaperone, becomes dissociated from these proteins' luminal domains, due to recruitment for protein folding, the UPR is triggered [40].

The first response to lessen ER stress is a reduction in protein translation and ER workload, mediated by PERK. PERK becomes homodimerized and autophosphorylated, and

then phosphorylates the α subunit of eukaryotic translation initiation factor 2 (eIF2), which reduces global protein synthesis and translation. The expression of transcription factor ATF4 is increased and genes involved in antioxidant response and amino acid transport are induced. Finally PERK activation may lead to the expression of pro-apoptotic transcription factor CCAAT/enhancer-binding protein (C/EBP) homologous protein (CHOP) and induction of Gadd34 (growth arrest and DNA damage-inducible protein 34), which results in negative feedback of eIF2α phosphorylation and attenuation of PERK signaling [7, 40, 41].

The second pathway of the UPR involves IRE1 which also becomes homodimerized and autophosphorylated, and cleaves the X-box binding protein 1 (XBP1) mRNA. The spliced form of XBP1 is translated and translocated to the nucleus, where it initiates several transcriptional programs involved in protein folding, maturation and degradation [7, 41].

The third pathway of the UPR takes effect when the basic leucine zipper domain protein ATF6 is activated, and becomes translocated to the Golgi. It is cleaved by site 1 and site 2 proteases, releasing its N-terminal cytosolic domain, which then enters the nucleus and regulates ER chaperone expression, induces XBP1 expression, and increases induction of ER-associated degradation (ERAD) proteins by forming a heterodimer with spliced XBP1 [7, 40, 41].

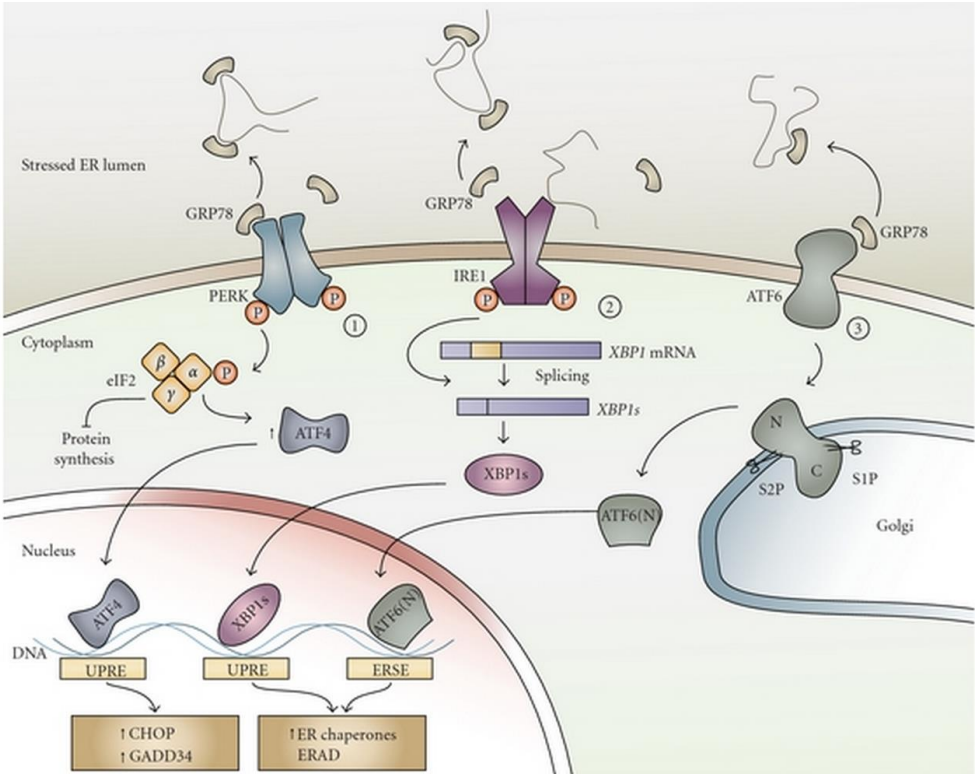

Figure 1.2. ER stress and activation of the UPR pathways. In response to ER stress, GRP78 becomes dissociated from the luminal domains of PERK, IRE1 and ATF6 and triggers the UPR, which induces a transcriptional program focused on re-establishing homeostasis. Taken from Basseri & Austin [40].

1.3.1.2. Role in the Complications of Obesity

Many studies have investigated the role of ER stress in the pathogenesis of obesity and there are many lines of thought regarding the potential pathways and mechanisms that might be involved. For example, all three branches of the UPR have been shown to induce inflammation, which is a key marker of obesity, through activation of NF-κB and/or JNK signaling. Specifically, when PERK is activated and protein translation is reduced, IKB levels become reduced as well, as does the inhibition of NF-κB activity. The cytosolic domain of IRE1α can associate with TNF receptor–associated factor 2 (TRAF2) to activate the JNK pathway, and by interacting with the adaptor protein Nck (noncatalytic region of tyrosine kinase) and a protein complex composed of IKK and TRAF2, it can activate the NF-κB pathway. A link between ATF6 and the activation of

NF-κB has also been demonstrated as when ATF6 is genetically and pharmacologically inhibited, NF-κB activation has been found to be suppressed [7].

In addition, in-vitro models of lipotoxicity induced by palmitate in various cell types, have shown that it increases ER stress by several mechanisms. In pancreatic β-cells palmitate disrupts the calcium homeostasis in the ER by causing calcium efflux [42]. In mouse insulinoma cell line MIN6 it significantly reduced the rate of ER-to-Golgi protein trafficking, thereby contributing to impaired protein exit and increased protein overload [43], in H9c2 cells palmitate increased protein aggregation, phosphorylation of PERK and eIF2α, and caused abnormal extension and swelling of the rough endoplasmic reticulum [44], and in HepG2 cells palmitate treatment significantly increased levels of XBP1mRNA splicing and CHOP expression, in addition to activating JNK and decreasing Akt phosphorylation, suggesting that ER stress-mediated JNK activation may be involved in insulin resistance in the liver [45].

Similarly, studies in skeletal muscle using high-fat diet or palmitate have been shown to activate the UPR. Mice fed a diet containing 70% fat and <1% carbohydrates for 6 weeks demonstrated higher levels of UPR markers BiP and IRE1 alpha in the soleus and in the tibialis anterior muscles, and mice fed a diet containing 46% fat and 36% carbohydrates for 20 weeks also showed more GRP78, IRE1 alpha, phospho-PERK, CHOP, and both spliced and unspliced forms of XBP1 in the plantar flexors[46]. The mediation of insulin resistance by palmitate-induced ER stress was also demonstrated in skeletal muscle. When treated with palmitate, L6 myotubes showed increased phosphorylation of UPR proteins PERK and eIF2α, and decreased insulin-stimulated phosphorylation of Akt (Ser473) [47].

1.3.2. Autophagy

1.3.2.1. Function and Mechanisms

Autophagy is a general term for the evolutionarily conserved catabolic process that captures cytoplasmic components for lysosomal degradation [48]. Three types of autophagy have been characterized: 1) macroautophagy which involves the formation of a double-membraned vesicle called the autophagosome, 2) chaperone-mediated autophagy which involves the binding of proteins containing a KFERQ motif to a chaperone protein for translocation to the lysosomes, where it binds to lysosome-associated membrane protein type 2A (LAMP-2A) receptor and is subsequently internalized and degraded, and 3) microautophagy which involves the direct sequestration of cellular components by the lysosome through the invagination of the lysosomal membrane [5]. Mizushima [48] notes however, that unless specifically indicated, the general use of the term “autophagy” typically refers to macroautophagy, and it is this process that is investigated in this thesis.

Autophagy has been called a “double-edged sword” [49] as it can either be beneficial or detrimental to the cell, depending on the context. On one hand, basal autophagy is essential for maintaining cellular homeostasis and for the turnover of cytosolic components, as it degrades long-lived proteins, defective organelles and intracellular pathogens, thereby protecting the cell and replenishing it with molecules for future anabolic purposes [5, 48]. Additionally, when faced with nutrient starvation, cells use autophagy as a stress adaptation that circumvents cell death by enabling adaptive protein synthesis from degraded macromolecules [50]. Autophagy has also been implicated in providing protection against aging and pathologies such as cancer, neurodegeneration and cardiac disease [5]. However, on the other hand, prolonged or excessive autophagy can result in an alternative pathway to cell death, called autophagic or

type II cell death [50], that arises when the autophagic process catabolizes excess cytoplasm and indispensable cell components [51].

Autophagy consists of distinct stages, each of which is facilitated by numerous proteins. The process is initiated with the formation of a small vesicular sac in the cytoplasm called the isolation membrane or phagophore, that then encloses a portion of cytoplasm containing targeted organelles, proteins etc. to form the characteristic double-membraned autophagosome [5]. Though the origin of the autophagosomal membrane is undecided, possible sources include the endoplasmic reticulum (ER), mitochondria, golgi and plasma membrane [52]. This is followed by the fusion of the autophagosome with a lysosome, creating the autophagolysosome, that then leads to the degradation of the sequestered cellular constituents by lysosomal enzymes, and the release of amino acids and other compounds into the cytoplasm for recycling or energy production [5].

Autophagosome formation utilizes 18 different Atg proteins and is comprised of three major steps: initiation, nucleation and elongation/enclosure [5]. The initiation step is controlled by the ULK1 (UNC-51-like kinase 1)–FIP200 (FAK family kinase-interacting protein of 200 kDa) ATG13 ATG101 complex. The serine/threonine kinase mammalian target of rapamycin (mTOR), interacts with and inactivates ULK1 by phosphorylation. Under starvation conditions, autophagy is induced via the inactivation of mTOR that results in ULK1 activation and phosphorylation of Atg13 and FIP200. The nucleation step involves the lipid kinase vacuolar protein sorting 34 (VPS34)-Beclin 1-class III phosphatidylinositol 3-kinase (PI3K) complex that also includes Vps15, Atg14L and Ambra-1. This complex is usually inactivated by anti-apoptotic proteins from the BCL-2 family, but when it is active it enables the nucleation of the isolation membrane. The final elongation and enclosure step requires the recruitment of two ubiquitin-like protein conjugation systems. Firstly, the conjugation of Atg12–Atg5 is mediated by ligases Atg7 and

Atg10. Atg5 also associates with Atg16 to form the Atg12–Atg5–Atg16 complex. Second, the microtubule-associated protein light chain 3 (LC3) which is the mammalian homolog of yeast Atg8 is cleaved at its carboxyl terminus by Atg4, giving rise to the soluble, cytosolic form LC3-I, which is then conjugated to phosphatidylethanolamine (PE) through the action of Atg7 and Atg3. This lipid conjugated form, LC3-II, is localized to the autophagosomal membrane, and allows the closure of the autophagic vacuole [5, 51]. LC3 is to date the only protein that has been identified on the inner membrane of the autophagosome and hence is the most commonly used protein marker for autophagic vacuoles, with an increase in LC3II showing an increase in autophagsome formation [48].

Another protein important in the assessment of autophagy is p62, which delivers ubiquitinated proteins to the autophagosome for degradation by binding to the polyubiquitin chains and LC3 [53]. p62 is then preferentially degraded by autophagy [48]. Autophagic flux is said to increase when LC3-II levels increase and p62 levels show a corresponding decrease. Two additional proteins which participate in the recruitment of molecules to the isolation membrane are the transmembrane proteins, ATG9 and vacuole membrane protein 1 (VMP1), which recycle between the golgi, endosomes and autophagosomes, probably shuttling lipids for degradation [51]. The next stage of autophagy, the fusion between autophagosomes and lysosomes is believed to be mediated by several SNARE-like proteins, and finally, in the autolysosome, various lysosomal enzymes hydrolyse proteins, lipids and nucleic acids [51].

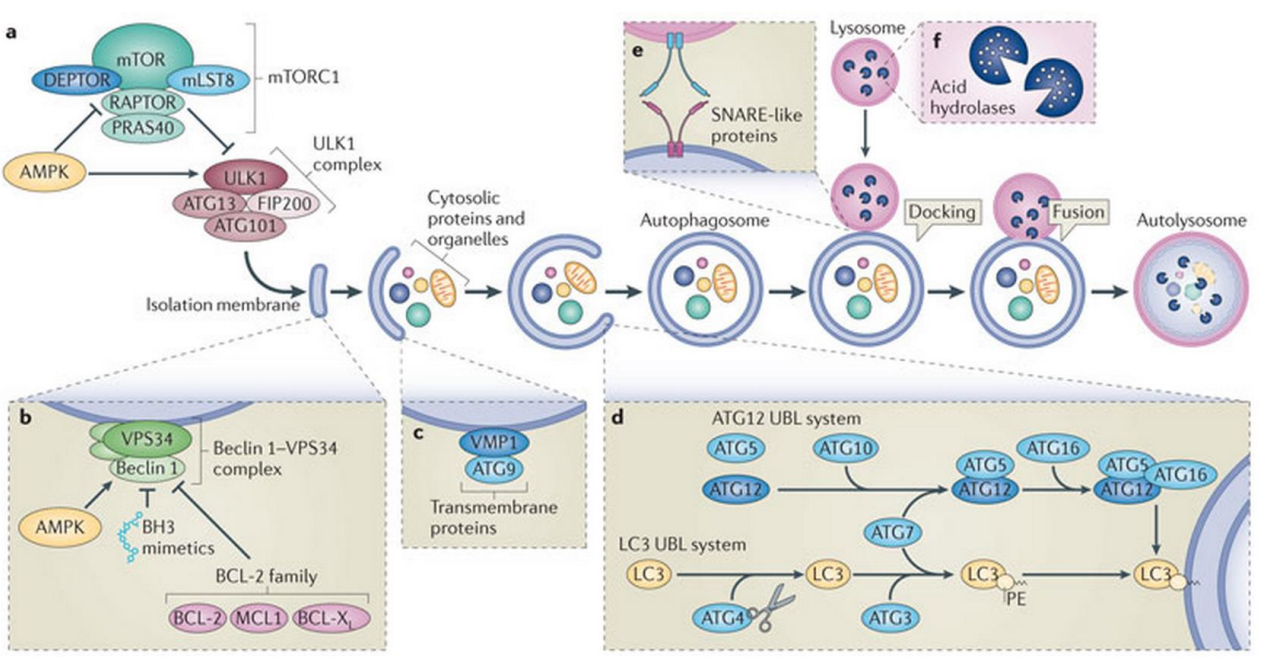

Figure 1.3. The major stages of autophagy. (a) The initiation step of autophagsome formation is controlled by the ULK1-FIP200-ATG13-ATG101 complex, and inhibited by mTOR. (b) The nucleation step involvesVPS34-Beclin 1-class III PI3K complex, which is inactivated by anti-apoptotic BCL-2 family proteins. (c) Transmembrane proteins ATG9 and VMP1 recruit molecules to the isolation membrane. (d) The elongation and enclosure step of autophagosome formation requires two ubiquitin-like protein conjugation systems. Firstly, the conjugation of Atg12–Atg5 is mediated by ligases Atg7 and Atg10. Atg5 also associates with Atg16 to form the Atg12–Atg5–Atg16 complex. Second, LC3 is cleaved by Atg4 to form LC3-I, which then undergoes lipid conjugation through the action of Atg7 and Atg3 to form LC3-II, which is then localized to the autophagosomal membrane. (e) Fusion between autophagosomes and lysosomes is mediated by SNARE-like proteins. (f) Various lysosomal enzymes hydrolyse proteins, lipids and nucleic acids in the autolysosome. Taken from Marino et al [51].

1.3.2.2. Role in the Complications of Obesity

Obesity has been known to inhibit effective autophagy by activating anti-autophagic Akt and mTOR signaling pathways and down-regulating autophagic genes such as Ulk1/Atg1, Atg5, Atg7, and Atg6/Beclin1 [54]. This defective autophagy is capable of promoting obesity-related inflammation through several mechanisms including p62 accumulation that leads to TRAF6 oligomerization and NF-*κ*B activation [55], and impaired autophagy of damaged mitochondria, i.e. mitophagy, that upregulates reactive oxygen species and inflammasome activation [56].

In addition, recent studies have demonstrated autophagy's importance in whole-body lipid and glucose homeostasis [5, 57]. In this way, autophagy's roles in the pathogenesis of obesity, in which such homeostasis is disrupted, has come under investigation. For example, Singh et al [58] have shown that when lipid availability is moderately increased, hepatic autophagy facilitates lipophagy i.e. the degradation of lipid droplets to provide free fatty acids for ATP production, in this way regulating lipid content and metabolism, and providing a mechanism for the prevention of steatosis. The movement of lipids through the autophagic pathway was evidenced by fluorescence and electron microscopy of hepatocytes that showed co-localization of lipids with autophagosomes and lysosomes, and immunogold staining which demonstrated that LC3 associated with lipid droplets. Additionally, when autophagy was inhibited by genetic knockdown of Atg5 or pharmacological treatment with 3-methyladenine, RALA255-10G hepatocytes treated with oleic acid for between 2 to 8 hours showed significantly increasedcellular triglyceride content. The impairment of autophagy resulted in decreased lipolysis and fatty acid β-oxidation, and excessive retention of triglycerides and cholesterol in lipid droplets [58].

However the same authors also reported that lipophagy was unable to cope with abnormal, sustained availability of lipids. Mice were fed a high-fat diet for 16 weeks (34g per 100g diet fat, 0.03g per 100g diet cholesterol with 60% of the total kcal in fat), and electron microscopy of their liver tissue demonstrated a reduced association of autophagic vacuoles with lipid droplets in response to starvation [58]. This reduction in the efficiency of interaction between the autophagic system and lipid droplets may be due to the alteration of membrane structure by lipid accumulation, that decreases fusion efficiency between autophagosomes and lysosomes [5].

Other studies have shown that a deficiency in autophagy could lead to insulin resistance that is a core component of metabolic disorders brought on by obesity such as type 2 diabetes. Ebato et al [59] have reported that in the pancreas, basal autophagy is important for maintaining normal islet architecture and function. They found that mice deficient for Atg7, demonstrated degeneration of islets, substantial beta cell death and diminished beta cell mass. This translated to impaired glucose tolerance and insulin secretion when these mice were challenged with high-fat diet. On the other hand, INS-1 beta cells, treated with the FFA oleate, and the beta cells of diabetic db/db and high-fat-fed C57BL/6 mice showed increased induction of autophagy, thereby suggesting that inductive autophagy might be an adaptive response of beta cells to increased insulin resistance in obesity [59].

1.3.3. Apoptosis

1.3.3.1. Function and Regulatory Mechanisms

Apoptosis is a highly regulated type of programmed cell death or cell suicide characterized by morphological changes, including nuclear condensation (pyknosis), fragmentation (karyorrhexis) and plasma membrane blebbing [60]. It is important in multicellular organisms for various processes such as normal cell turnover, proper development and functioning of the immune system, hormone-dependent atrophy, embryonic development and chemical-induced cell death [61, 62].

During the process of apoptosis, the cell shrinks, cytoplasm becomes dense, organelles become more tightly packed, and chromatin condenses. Extensive plasma membrane blebbing is followed by nuclear fragmentation and the separation of the cell components into apoptotic bodies that consist of cytoplasm with tightly packed organelles with or without a nuclear

fragment. Macrophages, parenchymal cells, or neoplastic cells then phagocytose these apoptotic bodies and degrade them within phagolysosomes [62].

There are two main pathways in the cell for the initiation of apoptosis: 1) the extrinsic death-receptor pathway, and 2) the intrinsic mitochondrial pathway [51]. The extrinsic pathway utilizes transmembrane receptors that contain a cytoplasmic domain of about 80 amino acids termed the “death domain”, which is responsible for transmitting the death signal from the cell surface to intracellular signaling pathways. Some of the ligands and corresponding death receptors identified to date are FasL/FasR, TNF-*α*/TNFR1, Apo3L/DR3, Apo2L/DR4 and Apo2L/DR5, among which the FasL/FasR and TNF-*α*/TNFR1 models have the best characterized signaling cascades. First, ligands bind with the death receptors, leading to the recruitment of adapter proteins that exhibit corresponding death domains. Specifically, the binding of Fas ligand to Fas receptor results in the binding of the adapter protein FADD, and the binding of TNF ligand to TNF receptor results in the binding of the adapter protein TRADD with subsequent recruitment of proteins FADD and RIP. FADD then associates with procaspase-8, leading to caspase 8 dimerization and activation [51]. Once active, caspase 8, an “initiator caspase” [61], can directly cleave and activate “effector or executioner caspases” caspase 3 and caspase 7 [60, 63], leading to caspase-dependent apoptosis. There is potential for cross talk here with the intrinsic apoptotic pathway, as activated caspase 8 can also truncate the BH3-only protein BID (BH3-interacting domain death agonist), which translocates to the mitochondria and causes organelle damage [51].

The intrinsic pathway of apoptosis is characterized by one central injurious event – mitochondrial outer membrane permeabilization (MOMP) [51]. Non-receptor-mediated stimuli activate B cell lymphoma 2 (Bcl-2) homology 3 (BH3)-only proteins, which stimulate MOMP by inducing the oligomerization of BCL-2-associated X protein (BAX) and/or BCL-2 antagonist or

killer (BAK) in the outer mitochondrial membrane. This forms supramolecular channels that enable the release of two groups of soluble proapoptotic proteins from the mitochondrial intermembrane space into the cytosol. Among the first group is cytochrome *c* that binds apoptotic protease-activating factor 1 (APAF1), inducing its oligomerization and forming a structure called the apoptosome that recruits and activates “initiator caspase”, caspase 9. Caspase 9 cleaves and activates “effector or executioner caspases”, caspase 3 and caspase 7, leading to caspase-dependent apoptosis. In addition, second mitochondria-derived activator of caspase (SMAC/DIABLO) and OMI are also released from the mitochondria to promote apoptosis by neutralizing the caspase inhibitory function of X-linked inhibitor of apoptosis protein (XIAP) [51, 62]. The second group of proapoptotic proteins are released from the mitochondria later in the timeline of apoptosis, after the cell has committed itself to death, and function in a caspase-independent manner. This group consist of apoptosis-inducing factor (AIF) and endonuclease G (EndoG) which translocate to the nucleus, to cause DNA fragmentation and condensation of chromatin [62]. PUMA and NOXA are two other BCL2 family members that have been shown to have proapoptotic roles. Overexpression of PUMA *in vitro* was demonstrated to be accompanied by increased BAX expression, BAX conformational change, translocation to the mitochondria, cytochrome *c* release and reduction in mitochondrial membrane potential [64], while NOXA has been shown to localize to the mitochondria, interact with anti-apoptotic Bcl-2 family members, and thereby activate caspase 9 [65].

The extrinsic and intrinsic apoptotic pathways converge on the “execution pathway” that constitutes the final phase of apoptosis [62]. This pathway is initiated by activation of the “execution or effector caspases”, caspase 3, caspase 6 and caspase 7, and results in DNA fragmentation, degradation of cytoskeletal and nuclear proteins, cross-linking of proteins, formation of apoptotic bodies, expression of ligands for phagocytic cell receptors and finally uptake by phagocytic cells [62].

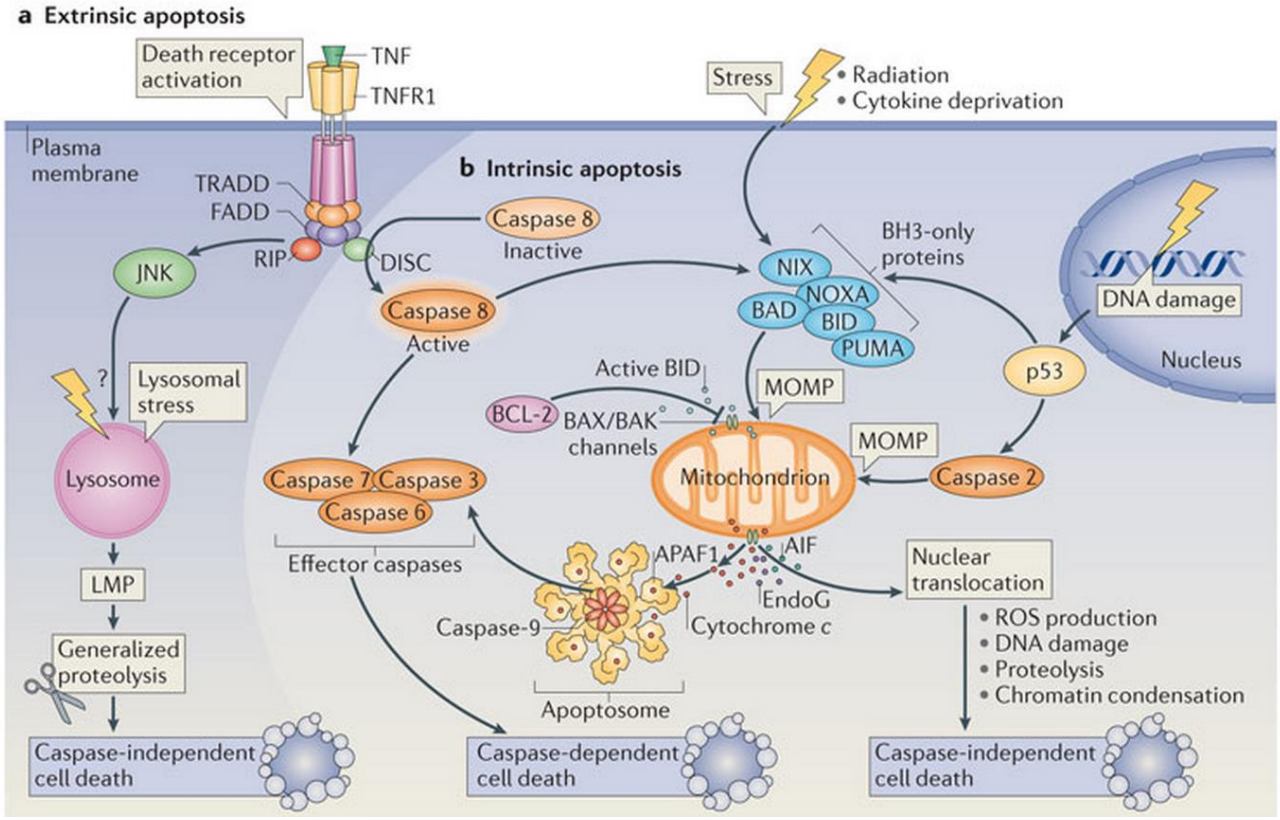

Figure 1.4. The two main pathways for the initiation of apoptosis (a) the extrinsic death-receptor pathway, and (b) the intrinsic mitochondrial pathway. Taken from Marino et al [51].

1.3.3.2. Role in the Complications of Obesity

Lipoapoptosis, a type of programmed cell death induced specifically by lipid overload in conditions of obesity, has been described in many studies. When fatty acid (FA) influx into non-adipose cells chronically exceeds oxidative capacity, the FA surplus is forced to enter available pathways of nonoxidative metabolism. Initially, they may be esterified to relatively harmless triacylglycerols (TG) but ultimately, hydrolysis of these TG stores will only lead to exacerbated accumulation of fatty acyl CoA, providing additional substrate for other lipotoxic nonoxidative FA metabolic pathways [66].

De novo ceramide biosynthesis, which involves the condensation of palmitate and serine, is the best characterized of these. Ceramide causes apoptosis by activating NFκB which

increases the expression of inducible nitric oxide synthase (iNOS) and increases the formation of nitric oxide (NO). Alternatively, ceramide may decrease Akt phosphorylation, thereby preventing its inactivation of pro-apoptotic BCL2 family members Bad, Bax, Bid and Bim. In addition ceramide has also been shown to inhibit mitochondrial respiratory chain complexes I and III, causing harmful mitochondrial alterations [67]. The apoptotic effect of ceramide has been demonstrated in various cell types, such as pancreatic beta cells [68], cardiomyocytes [69], hepatocytes [70] and skeletal muscle [71].

The consequences of lipoapoptosis in the heart can lead to heart failure as was illustrated by a study that utilized cardiomyocyte-specific acyl CoA synthase (ACS)-overexpressing mice [72]. ACS-overexpression increased fatty acid transport across the plasma membrane of cardiomyocytes, and led to elevated levels of cardiac TG and ceramide, as well as cytosolic cytochrome-c release from mitochondria. The mice exhibited initial cardiac hypertrophy, followed by the development of left-ventricular dysfunction and premature death [72].

In insulin-sensitive tissues, such as skeletal muscle and adipocytes, lipoapoptosis was implicated in the inhibition of insulin-stimulated glucose utilization. In L6 myotubes, palmitate increased apoptosis and decreased glucose uptake, but the addition of effector caspase inhibitors [Ac-DEVD-aldehyde (DEVD-CHO), Z-DQMD-FMK] restored >80% of insulin-stimulated glucose uptake [71]. In3T3-L1 adipocytes, ceramide was found to decrease insulin-stimulated glucose uptake by decreasing GLUT4 translocation, through the inhibition of Akt activity [73].

1.4. Cross talk and Links Between ER Stress, Autophagy and Apoptosis

1.4.1. ER Stress Induces Autophagy as a Rescue Mechanism

When the cell experiences ER stress, it activates a number of pathways to help alleviate protein overload and restore homeostasis. As previously described, the UPR is the chief cellular response that acts to down regulate protein synthesis and up regulate protein folding and degradation [39]. However, it has been proposed that autophagy is another mechanism that may also be induced to help cells cope with ER stress by contributing to the elimination of unfolded or aggregated proteins [74]. Indeed, ER stress can stimulate the assembly of autophagosomes. Polyglutamine- and drug-induced ER stress has been found to facilitate the conversion of LC3I to LC3II, a key step for autophagosome formation [75], and in yeast atg11Δ cells that have an inherent defect in pre-autophagosomal structure (PAS) assembly, it was found that induction of ER stress by tunicamycin facilitated PAS formation, as observed by following the localization of GFP-Atg8 (yeast homolog of LC3) with autophagic vesicles [76].

Additionally, Ogata et al [39] found that treating SK-N-SH neuroblastoma cells with ER stressors tunicamycin and thapsigargin markedly induced the formation of autophagosomes, which were recognizable by the formation of green fluorescent protein (GFP)-LC3-labeled puncta, that represented the autophagosomal conversion of LC3I of LC3II. The group reported that the IRE1-JNK pathway appeared to be involved in the activation of autophagy following ER stress as they found that autophagy was inhibited in IRE1-deficient MEF cells or cells treated with JNK inhibitor SP600125 [39]. Evidence has also been provided to show that PERK-eIF2-dependent Atg12 upregulation is required for induction of autophagy in response to polyglutamine protein accumulation. When a dominant-negative form of PERK was utilized or phosphorylation of eIF2 was prevented by genetic substitution of its Serine 51 with Ala,

polyglutamine protein-induced autophagy was inhibited. This suggested that controlling the expression of autophagy-related genes by eIF2 downstream targets could be one of the mechanisms connecting both the UPR and autophagy [74, 75]. Additionally H9c2 cells treated with palmitate alone demonstrated more autophagic flux, evidenced by LC3 and p62 expression, than cells treated additionally with salubrinal, an ER stress inhibitor [44]. Therefore autophagic flux may indeed be mediated by ER stress.

1.4.2. Prolonged or Excessive ER Stress Induces Apoptosis

Though pro-apoptotic outputs like CHOP production occur as a result of UPR signaling, activation of the UPR is generally accepted as being a primarily adaptive and prosurvival response of the cell to try to manage ER stress. Indeed, the combined actions of the IRE1α, PERK, and ATF6α pathways are predominantly initially protective as they collectively work to reduce translation, enhance ER protein-folding capacity and clear misfolded ER proteins [35]. Rutkowski et al [77] proposed that the preliminary outweighing of proapoptotic factors by prosurvival factors may be partially due to the greater stability of prosurvival UPR effector molecules like GRP78 at both the mRNA and protein levels [77]. Hence the cell initially attempts to adapt to ER stress and regain homeostasis by increasing chaperone levels to facilitate protein folding or increasing protein degradation to get rid of terminally misfolded proteins. However if these measures are not successful at assuaging ER stress, and ER stress becomes prolonged or excessive, as would happen in cases where lethal ER toxins are present or when production of terminally misfolded proteins persists, protective outputs would diminish. Proapoptotic UPR signaling would then proceed unchecked, and the cell might also be left vulnerable to other damaging stimuli like hypoxia and nutrient starvation, ultimately leading to cell death via apoptosis [35].

Many studies have investigated CHOP's role in mediating ER-stress induced apoptosis. Several genes have been found to be induced in CHOP's transcriptional program including GADD34 and ERO1. GADD34, a regulatory subunit of protein phosphatase 1 (PP1) targets PP1 to dephoshorylate eIF2, which then enables protein synthesis to start up again. If the protein folding capacity of the stressed ER has not yet been restored, such a de-inhibition of translation will only act to intensify ER stress by exacerbating ER protein load and improper disulphide bond formation of unfolded proteins [78]. Increased expression of ERO1 by CHOP causes hyperoxidizing conditions in the ER which also expedites apoptosis via oxidative stress [79, 80]. CHOP has also been found to regulate the expression of some Bcl-2 family proteins that govern mitochondrial outer membrane permeabilization (MOMP). Though the mechanism is unknown, CHOP appears to suppress the expression of antiapoptotic Bcl-2, while promoting the transcription of proapoptotic BH3-only protein Bim [74]. Puma and Noxa are other proapoptotic BH3 family proteins that are transcriptionally regulated by ER stress. They are called sensitizers of apoptosis as they interact with various anti-apoptotic proteins, inhibiting their effects and inducing MOMP [81].

Among the three branches of the UPR, PERK signaling which involves the induction of CHOP, is generally agreed upon to have proapoptotic effects. Indeed, Lin et al [82] demonstrated that sustained PERK signaling impaired cell proliferation and promoted apoptosis. However the effects of the IRE1 and ATF6 pathways appear to be more ambiguous. ATF6 signaling has been stated to be largely prosurvival and adaptive, however by its ability to upregulate CHOP during prolonged ER stress, it can also be pro-apoptotic [81]. IRE1 signaling has been regarded as an adaptive response that occurs early in the UPR and diminishes with prolonged ER stress [83], but it has also been postulated to have a role in proapoptotic pathways via the IRE1a-TRAF2-JNK axis which plays parts in upregulating the proapoptotic activity of Bid and Bim (i.e. other Bcl-2 family proteins) and in modulating TNFa release that

activates death receptor signaling [81].

1.4.3. Interplay Between Autophagy and Apoptosis

1.4.3.1. Autophagy Precedes and Inhibits Apoptosis

There are many links between autophagy and apoptosis, and crosstalk is often observed. This is because many stimuli that ultimately cause apoptosis also initiate autophagy which, as previously described, often precedes apoptosis as one of the cellular mechanisms attempting to adapt to and cope with stress. Therefore, in general, autophagy is believed to protect against the induction of apoptosis [45].

When agents inducing cellular stress cause mitochondrial damage and MOMP, proapoptotic factors are released into the cytoplasm, including catabolic hydrolases such as apoptosis inducing factor (AIF) or endonuclease G (EndoG), and caspase activators such as cytochrome *c* and SMAC (second mitochondria-derived activator of caspase) [84]. Release of these proapoptotic factors may be reduced via activation of mitophagy i.e. the specific autophagic elimination of damaged mitochondria. This is accomplished via the dissipation of the inner mitochondrial transmembrane potential that occurs during MOMP and leads to the inhibition of PINK1 (PTEN-induced putative kinase 1) proteolysis. PINK1 then accumulates at the surface of damaged mitochondria and recruits the E3 ubiquitin ligase PARKIN (Parkinson's disease protein) to ubiquitinate proteins in the outer mitochondrial membrane, thereby targeting the mitochondria for degradation [85]. Mitophagy of damaged, apoptosis-inducing mitochondria can therefore delay the onset of apoptosis, by increasing the threshold for apoptosis induction [51]. In addition, autophagy has been shown to selectively target specific proapoptotic proteins in the cytoplasm such as active caspase 8 [86]. These proteins are ubiquitinated, which

facilitates their interaction with selective autophagy receptors, such as p62, that also binds LC3. In this way targeted proteins are selectively brought to the autophagosome for degradation [87].

1.4.3.2. Apoptosis Inhibits Autophagy beyond a Critical Threshold of Stress

If the intensity or duration of stress surpasses a cell's ability to cope, adaptive mechanisms including autophagy are overtaken by apoptosis. Furthermore, once apoptosis is initiated caspase activity acts to inactivate the autophagic pathway and shut down its cytoprotective function, in order to further enhance cell death [51]. This can occur through caspase-mediated digestion of several essential autophagy proteins, such as ATG3 [88], Beclin 1[89, 90] and AMBRA1 (activating molecule in BECN1-regulated autophagy 1) [91]. Additionally, studies have found that autophagy protein fragments leftover from caspase cleavage may acquire pro-apoptotic functions. For example, when caspase 3, caspase 6 or caspase 9 cleaved Beclin 1 in Ba/F3 cells, a carboxy-terminal fragment was produced that localized to mitochondria, causing permeabilization and the release of cytochrome *c* [89].

1.4.3.3. Autophagy Induces Cell Death via Apoptosis, Independent of Autophagic Cell Death

Though autophagy is recognized as a cytoprotective mechanism, there are certain cases in which it might lead to cell death. One of these is the previously described autophagic cell death (ACD), which occurs when extreme autophagy degrades the cytoplasm excessively and catabolizes indispensable portions of cells [51]. It is important to note, as indicated in a recent review by Marino et al [51], that strictly speaking, the term ACD should refer to cell death specifically caused by increased autophagic flux, rather than by apoptosis or necroptosis. It should not be confused with cell death simply accompanied by autophagy. Also, the authors note that ACD will be circumvented when autophagy is inhibited [51]. However, there is some

disparity in the field regarding what constitutes ACD, as Kroemer and Levine [92] point out that the term has simply been used to describe cell death with autophagy.

Regardless, beyond ACD, research has shown that autophagosomes or autophagic proteins, rather than the autophagic degradative process, are capable of inducing true apoptosis [51]. Autophagsomes may serve as a platform for the activation of caspase 8, through the formation of an intracellular death-inducing signaling complex composed of caspase 8, FADD and ATG5, that colocalizes with LC3 and p62 [93]. ATG12 has been shown to interact with anti-apoptotic BCL-2 family members, via stimulation by proapoptotic stressors such as C6 ceramide or tunicamycin, thereby inhibiting their function and enhancing mitochondrial apoptosis [94]. In addition, ATG7 has been shown to induce intrinsic apoptosis following lysosomal photodamage by causing lysosomal membrane permeabilization [95], that may trigger MOMP through the release of cathepsin proteases into the cytosol [51].

1.4.3.4. Autophagy Protects Against ER Stress-Induced Apoptosis

As discussed in Section 1.4.1., autophagy may be activated as an adaptive response to alleviate ER stress, and many studies have in fact demonstrated autophagy's ability to inhibit apoptosis induced by ER stress. For example, ATG5 wild type and ATG5-deficient MEF cells exposed to tunicamycin, a stimulator of ER stress, exhibited ER-stress dependent caspase 3 activation and cell death, which was augmented in the autophagy-impaired ATG5-deficient group [39]. In H9c2 cells co-treated with palmitate and bafilomycin, an inhibitor of autophagy, the extent of cell death was analyzed via Annexin V and caspase-3 expression. It was found to be increased when palmitate-induced autophagy was inhibited by bafilomycin treatment [44]. [better to rework this sentence and simplify] Exacerbation of cellular damage imposed by ER stress through the obstruction of autophagy was also demonstrated in SK-N-SH cells that exhibited marked chromatin condensation and fragmentation when treated with tunicamycin in

the presence of 3-MA, another inhibitor of autophagy [39]. Conversely, using rapamycin to induce autophagy through inhibition of mTOR function, has been shown to make H9c2 cells [44] and HeLa cells [39] more resistant to ER stress-induced cell death. Additionally, beta-cell apoptosis caused by ER stress arising from accumulation of misfolded proinsulin in diabetic Akita mice with a mutation in proinsulin, was reduced when they were treated with rapamycin [96]. All these reports therefore support the idea that autophagy is a cellular self-protective mechanism against ER-stress induced apoptosis [44].

1.5. Adiponectin

1.5.1. Structure

Adiponectin (also known as ACRP30 and ADIPOQ) is a 30kD protein that is primarily secreted by adipocytes and is highly abundant in the blood, occurring at levels of approximately 3-30ug/ml. It consists of an amino-terminal signal sequence followed by a collagen-like domain and a carboxyl-terminal globular domain. The monomers can form trimers (low molecular weight i.e. LMW form), hexamers (medium molecular weight i.e. MMW form) and oligomers (high molecular weight i.e. HMW form). The mixture of these different oligomeric forms circulating in the plasma is termed full length adiponectin (fAd), but an additional form, globular adiponectin (gAd) containing only the carboxyl-terminal, may be generated by the enzymatic cleavage of adiponectin [6, 97, 98].

1.5.2. Role in the Complications of Obesity and Functional Significance

The level of circulating adiponectin has an inverse relationship with BMI, plasma glucose and insulin, and serum triglycerides, in spite of an increase in adipose mass [6, 12]. Many studies have recognized the central role that the reduction of adiponectin action has in

metabolic syndrome and obesity-related diseases, as decreased plasma adiponectin levels have been associated with type 2 diabetes [99], dyslipidemia [100], cardiovascular disease [101], hypertension [102], cancer [103] and non-alcoholic steatohepatitis [104]. Two mechanisms have been proposed for impaired adiponectin effects in such disease conditions; the first is the absolute decrease of circulating adiponectin and the other is decreased adiponectin sensitivity, both of which may be caused in part by obesity-related increases in oxidative stress and inflammation [105].

Though adiponectin action is naturally impaired in many metabolic disease states, research has shown that increasing adiponectin effects is possible through various strategies such as the exogenous administration of adiponectin through injection or *in vitro* treatment, the increase of adiponectin expression using compounds like TZDs, the activation of AdipoRs using small molecule compounds and antibodies, and the increase of AdipoR expression levels such as by implementing PPARα activation by its agonist Wy-14,643 [105]. Indeed, upregulating adiponectin action has been demonstrated to confer protective effects through its antidiabetic, insulin-mimetic, insulin-sensitizing, anti-inflammatory and anti-atherosclerotic properties [106-108].

An example of this is the study done by Yamauchi et al [109] that used KKAy mice (KK mice overexpressing the agouti protein), as a model of the metabolic syndrome and obesity-related type 2 diabetes. It was found that plasma adiponectin levels were decreased in these mice when fed a high-fat diet (HFD), and insulin resistance was pronounced. However glucose tolerance test results obtained after replenishment of adiponectin showed a significant amelioration in hyperglycemia and hyperinsulinemia, providing evidence of adiponectin's insulin-sensitizing and anti-diabetic actions [109].

More recent work has shown that adiponectin's ability to combat insulin resistance may occur in part due to its stimulation of autophagy and antioxidant potential. Liu et al [110] found that adiponectin treatment not only reduced oxidative stress, but also reinstated high-fat diet-induced autophagic flux in adiponectin knockout (AdKO) mice. In addition, when autophagy was impaired *in vitro* through pharmacological inhibition or in a cell line overexpressing an inactive mutant of ATG5, insulin sensitivity was reduced. Collectively these findings elucidate the vital connections between adiponectin action, autophagy, oxidative stress and insulin sensitivity.

Furthermore, in skeletal muscle, adiponectin has been found to exert its anti-diabetic properties by directly stimulating glucose utilization via increased glucose uptake and increased GLUT4 translocation [111]. These processes are mediated by various receptors and downstream signaling events. Briefly, adiponectin binds to its two primary receptor isoforms AdipoR1 and AdipoR2, although T-cadherin is another alternative adiponectin receptor that competitively binds only the hexameric and HMW forms of adiponectin [98, 112]. APPL1 (adaptor protein containing pleckstrin homology domain, phosphotyrosine binding (PTB) domain and leucine zipper motif) is the best characterized protein that binds with adiponectin receptors to sequentially activate downstream signaling pathways involving adenosine monophosphate-activated protein kinase (AMPK), p38 mitogen-activating protein kinase (MAPK), peroxisome proliferator-activated receptor alpha (PPARα) and RAS-associated protein Rab5 [113]. The importance of APPL1 was first demonstrated [113] by showing that APPL1 knock down with siRNA abolished adiponectin-stimulated GLUT4 translocation and glucose uptake in muscle cells.

The anti-inflammatory and cardioprotective effects of adiponectin have been linked to its ability to decrease ER stress and apoptosis. In H9c2 cardiomyocytes, adiponectin has been shown to reduce genes associated with ER stress such as HSPa5, ATF6 and GRP94, as well

as genes associated with inflammation such as TNFalpha and MCP1 [114]. In addition adiponectin can reduce cardiomyocyte cell death induced by palmitate, therefore contributing to its ability to protect against metabolic dysfunction-associated heart failure [115].

Moreover, adiponectin has been shown to have positive effects on lipid metabolism as it increases fatty acid uptake and oxidation, increases ceramide catabolism and decreases the esterification of fatty acids to triglycerides [116]. As an example, one study showed that in mouse skeletal muscle, low doses of gAd increased expression of molecules involved in fatty-acid transport, combustion and energy dissipation such as CD36, acyl-CoA oxidase and uncoupling protein (UCP)2, which ultimately led to a decrease in skeletal muscle triglyceride content [109].

1.6. Research Objectives, Experimental Model and Hypothesis

In light of the serious health implications posed by obesity-mediated lipotoxicity, the goals of my project have been to:

1) examine how lipotoxicity, induced by palmitate, influences ER stress, autophagy and apoptosis in skeletal muscle cells.
2) investigate the cross talk between ER stress, autophagy and apoptosis
3) explore how adiponectin regulates these processes.

Briefly, I have used an *in-vitro* model of lipotoxicity, induced by treatment of L6 rat skeletal muscle cells with palmitate, a common saturated free fatty acid. I have used well established methods and also developed new approaches in our laboratory to accurately examine autophagy, ER stress and apoptosis. Full length recombinant adiponectin (fAd) was utilized to study the direct effects this adipokine has on the cellular processes described above.

My hypothesis is that palmitate-induced lipotoxicity will increase ER stress in skeletal muscle cells, with subsequent development of apoptosis. I also propose that autophagy will be activated as a compensatory cellular mechanism to alleviate ER stress. Finally, I expect that fAd will directly increase autophagic flux and that this will contribute to its cytoprotective effects.

Chapter 2: Materials and Methods

2.1. Cell Culture and Treatment of L6 cells

Rat L6 myoblasts were grown and maintained under 5% CO_2 at 37°C in alpha-minimum essential medium (5.5mM glucose AMEM; Wisent, St.Bruno, QC) containing 10% (v/v) fetal bovine serum (FBS; Wisent, St.Bruno, QC) and 1% antibiotic-antimycotic (Wisent, St.Bruno, QC). When differentiation of L6 wild type (wt) myoblasts into myotubes was necessary, plated cells were cultured in 2% FBS AMEM for approximately 5-7 days.

Prior to experimental treatments, cells were starved for 4h in 0.5% FBS AMEM. Palmitate (Pal) treatment (sodium palmitate; Sigma-Aldrich) pre-conjugated with fatty-acid free bovine serum albumin (BSA; Sigma-Aldrich) in 2:1 molar ratio,was administered at 250μM to model lipotoxicity, and an equal volume of a solution consisting of 0.5% FBS AMEM supplemented with fatty-acid free BSA was administered to control cells. Tunicamycin (Tun; Sigma-Aldrich) was used as a positive control to induce ER stress, at 8 μg/ml. Rapamycin (Rap; Sigma-Aldrich) was used as a positive control to induce autophagy at 1 μM. Hydrogen peroxide (H2O2; Sigma-Aldrich) was administered to cells at a concentration of 500μM as a positive control for apoptosis. Where necessary, 1h prior to adding the palmitate treatment or control BSA solution, cells were pretreated with 30μM salubrinal (Sal; Sigma-Aldrich) to inhibit ER stress by keeping the UPR active through prevention of dephosphorylation of peIF2α. When it was necessary to inhibit autophagy, 50μM chloroquine (Chl; Invitrogen) was added to cells 1h prior to treatment, to inhibit the fusion of autophagosomes to lysosomes. Where necessary, 1h prior to adding the palmitate treatment or control BSA solution, cells were pretreated with 5μg/ml recombinant full length adiponectin (fAd), that had been produced in a mammalian expression

system (i.e. human embryonic kidney 293 cells; HEK293), to enable the post-translational modifications necessary for proper biological activity of fAd as indicated in Fang et al [117].

2.2. Thioflavin T (ThT) Fluorescence Assay

ER stress was analyzed using ThT (Sigma-Aldrich), a benzothiazole dye that exhibits enhanced green fluorescence upon binding to protein aggregates. A measured increase in ThT fluorescence directly correlates to the amount of accumulated proteins and the degree of UPR activation [36].

Confocal Microscopy

L6 wt myoblasts were grown on cover slips in 6 or 12 well plates and were treated as required. ThT solution was added in the last 40 minutes of the treatment at 5µM. Following the end of the treatment time, the media was aspirated and the cells were gently rinsed with phosphate-buffered saline (PBS; Wisent) two times. They were then fixed with 4% paraformaldehyde (Sigma-Aldrich) for 30 min in the dark at room temperature. Following fixation, the cells were gently rinsed three times with PBS. Using Vecta Shield mounting medium for fluorescence with DAPI (Vector Laboratories Inc., Burlingame, CA), the cover slips were mounted onto slides and analyzed using a confocal microscope within a day's time.

Spectrometry

L6 wt myotubes were grown in a 24 well plate and were treated as required. ThT solution was added in the last 40 minutes of the treatment at 5µM. Following the end of the treatment time, the media was aspirated and cells were rinsed with PBS, which was also aspirated. A volume of 150µl of 0.1% Triton X in PBS was added, and the cells were scraped on ice. A volume of 100ul was pipetted into a 96 well black bottom plate and the fluorescence signal of the ThT dye was

measured using a spectrometer (485nm/535nm, 1s reading). The values were normalized to protein concentration obtained using BCA protein assay kit (Thermo Scientific).

2.3. GRP78mcherry Fluorescence Microscopy and Quantification

To monitor the transcriptional output of the UPR in response to ER stress, a reporter construct, mCherry protein under the control of the GRP78 promoter, was used.
The -304GRP78-mCherry sequence from the vector supplied by Dr. Allen Volchuk (University of Toronto) was PCRed with restriction sites introduced on each end. At the 5' end we introduced an AgeI site, at the 3' we introduced a PacI site. Upon PCR and purification, we TOPO cloned and then excised the fragment using AgeI/PacI sites and ligated it into the retroviral cloning vector pQCXIP using the same sites. The viral vector was then transfected into HEK-derived packaging cell line, EcoPack 2-293 (Clontech), expressing the MMLV Gag, Pol and Env proteins. The culture medium containing the virus was collected 48 hours post transfection. 100 ul of the collected supernatant, or viral soup, was directly applied to L6 cells in presence of polybrene (4ug/ml) in 10 cm culture dish on the next day after being seeded. Cells were incubated with the virus for 24 hours in the incubator, and the medium was replaced with fresh growth medium containing the selection antibiotic, puromycin (2ug/ml) (Sigma Aldrich). The pool of cells resistant to the antibiotic was then selected and maintained. The L6 GRP78mcherry stable cell line exhibits low basal mCherry expression and a marked increase in red fluorescence following initiation of ER stress [118].

For microscopy analysis, L6 GRP78mcherry myoblasts were grown on cover slips in 6 or 12 well plates, and treated as required. At the end of the treatment time, the media was aspirated, the cells were rinsed with PBS, fixed with 4% paraformaldehyde for 20 min in the dark at room temperature, and rinsed with PBS again. The cover slips were mounted on slides using DAKO fluorescent mounting medium (DAKO North America Inc, CA). Images were

obtained using a confocal microscope and Image J software was used to quantify mean fluorescence of 30-50 cells per condition.

2.4. Cell Lysis and Western blotting

After the required treatments, cells were washed in PBS and solubilized in RIPA buffer (50mM Tris, 150mM NaCl, 0.1% SDS, 1% Triton X, BioShop Inc and 0.5% sodium deoxycholate, Sigma-Aldrich) containing protease inhibitor cocktail (cOmplete ULTRA tablets Mini; Roche) and phosphatase inhibitor cocktail (Calbiochem). Each lysate was transferred to Eppendorf tubes and further lysed by passing five times through a 25 gauge needle/syringe. After each sample was centrifuged at 12,000 rpm for 5 minutes at 4°C, the supernatant was collected, and cell pellet was discarded. Protein concentration was obtained using BCA protein assay kit (Thermo Scientific), and loading samples were prepared containing equal µg of protein. The samples were heated at 60°C for 10 minutes, and then loaded onto an SDS-PAGE gel. After protein transfer, the appropriately cut sections of the PVDF membrane (Bio-Rad) were incubated with primary antibody solutions at 4°C overnight. The membranes were then incubated in the appropriate horse-radish peroxidase (HRP)-linked secondary antibody solutions for 1h and immunoblots were developed using enhanced chemiluminescence (Western Lighting Plus ECL; Perkin and Amersham HyperfilmTM ECL; GE Health Care). Densitometric quantification of Western blot bands was conducted using Bio-Rad Quantity One software.

The following primary antibodies were used: peIF2α (ser51), LC3B and caspase 3 (1:1000; Cell Signaling; Beverly, MA), p62 (1:1000; BD Transduction Laboratories), and caspase 12 (1:1000; Sigma-Aldrich). The following secondary antibodies were used: anti-rabbit, anti-mouse and anti-rat (1:10,000; Cell Signaling; Beverly, MA). βActin (1:1000; Cell Signaling; Beverly, MA) was used as a loading control.

2.5. Endogenous LC3 Immunofluorescence Microscopy

Immunofluorescence of LC3 tagged with Alexa Fluor 488 goat anti-rabbit secondary antibody (Invitrogen) was used to visualize endogenous LC3 puncta, using confocal microscopy. The puncta exhibited green fluorescence, indicative of the induction of autophagy and formation of autophagosomes. Briefly, L6 wt myoblasts were grown on cover slips in 6 or 12 well plates and treated as required. They were then washed with PBS three times, fixed with 4% paraformaldehyde for 20 min, and washed with PBS again. The cells were quenched first with 1% glycine in PBS for 1 min, then in 0.1% glycine in PBS for 10 min. After washing again three times with PBS, 0.1% Triton X 100 in PBS was added for 3 min, and then the cells were washed with PBS again three times. Blocking took place for 30min in 3% BSA in PBS, after which the cells were incubated overnight at 4°C with 1:500 primary LC3B antibody in 3% BSA in PBS. The next day the cells were washed three times with PBS, incubated with 1:1000 secondary antibody in 3% BSA in PBS for 1h at room temperature in the dark and washed three times with PBS again. The slides were then mounted on slides using Vecta Shield mounting medium for fluorescence with DAPI, and analyzed using confocal microscopy.

2.6. Magic Red Cathepsin B Assay for Lysosomal Activity

The activity of proteolytic lysosomal enzyme cathepsin B, may be taken as an indicator of autolysosomal activity in the later stage of autophagy. The Magic Red Cathepsin B Assay Kit (ImmunoChemistry Technologies) employs the cresyl violet (CV) fluorogenic substrate CV-(Arg-Arg)2 or CV-(RR)2. When the fluorophore is di-substituted with two R-R dipeptide cathepsin B targeting sequences, it is non-fluorescent, but the active cathepsin B lysosomal enzyme will catalyze the hydrolysis of the two R-R target sequences, which when cleaved from the Magic Red molecule, will convert it to the red fluorescent form.

Briefly, L6 wt myoblasts were grown on cover slips in 6 or 12 well plates and treated as required. They were then washed with PBS three times, fixed with 4% paraformaldehyde for 20 min, and washed with PBS again. The cells were quenched first with 1% glycine in PBS for 1 min, then in 0.1% glycine in PBS for 10 min. After washing again three times with PBS, 0.1% Triton X 100 in PBS was added for 3 min to permeabilize cells, and then the cells were washed with PBS again three times. Blocking took place for 30min in 3% BSA, after which the Magic Red reagent was added directly to the blocking solution. According to the manufacturer's protocol, 40ul of 26x diluted Magic Red per 1ml of blocking solution was added for 30 min. The cells were washed with PBS three times and the cover slips mounted on slides using Vecta Shield mounting medium for fluorescence with DAPI. The fluorescence signal (ex 540-590 nm, em >610nm) was then detected with confocal fluorescence microscopy.

2.7. Inhibition of Autophagy using ATG5K130R Dominant Negative Mutant

To elucidate the potential relationship between the processes of autophagy and ER stress, the dominant negative mutant L6 stable cell line ATG5K130R was created. The target sequence RFPATG5-K130R from the vector pmCherry-ATG5-K130R (Addgene) was subcloned into the retroviral cloning vector pQCXIP. The viral vector was then transfected into HEK-derived packaging cell line, EcoPack 2-293 (Clontech), expressing the MMLV Gag, Pol and Env proteins. The culture medium containing the virus was collected 48h post transfection. 100 ul of the collected supernatant, or viral soup, was directly applied to L6 cells in presence of polybrene (4ug/ml) in 10 cm culture dish on the next day after being seeded. Cells were incubated with the virus for 24h in the incubator, and the medium was replaced with fresh growth medium containing the selection antibiotic, puromycin (2ug/ml) (Sigma Aldrich). The pool of cells resistant to the antibiotic was selected and maintained. The ATG5K130R dominant negative mutant is defective in conjugating to Atg12 on the lysine (K) residue, as lysine has been replaced with arginine. This inhibits LC3 incorporation into the early autophagosome, thus

inhibiting autophagy by inhibiting autophagic vacuole formation [119, 120]. Empty vector (EV) cells were used as the corresponding control.

2.8. Caspase 3/7 Green Detection Reagent Assay

CellEvent Caspase-3/7 Green Detection Reagent (Life Technologies) was used to visualize apoptotic cells under a confocal microscope, by identifying those cells that showed a bright green fluorescence signal in their nuclei. The reagent is a four amino acid peptide (DEVD) conjugated to a nucleic a cid binding dye with an absorption/emission maxima of ~502/530 nm. When caspase 3/7 is activated in apoptosis, cleavage of the DEVD peptide occurs which allows the dye to bind to DNA and produce a bright, fluorogenic response. L6 wt myoblasts were grown on cover slips in 6 or 12 well plates and were treated as required. Caspase 3/7 Green Detection Reagent was added in the last 30 minutes of the treatment at 8µM, following which the medium was gently aspirated and the cells were gently rinsed with PBS. Fixation was conducted with 4% paraformaldehyde for 20min, and gently rinsed again with PBS. The cover slips were then mounted on slides using Vecta Shield Mounting Medium containing DAPI and analyzed using confocal microscopy. Quantification of the images was done by calculating the mean percentage of apoptotic cells exhibiting a nuclear green fluorescence signal.

2.9. MTT Assay

Cell viability was determined using 3-(4,5-dimethylthiazol-2-yl)-2, 5-diphenyltetrazolium bromide (MTT) assay. L6 myoblasts were seeded, grown and treated in a clear 96 well plate. Approximately 2 hours before the end of the treatments, the cells were incubated with MTT solution (5 mg/mL in PBS; Sigma-Aldrich) at 37°C. During this time the yellow MTT was reduced in the mitochondria of living cells to an insoluble formazan that precipitated as purple crystals. The media was then gently aspirated and the purple formazan crystals were dissolved using

DMSO. Using a spectrometer, the absorbance was measured at 550nm. The intensity of the purple color directly related to the amount of viable cells present.

2.10. Statistical Analysis

Values are given as mean + SEM, unless indicated otherwise. Statistical analysis was conducted using GraphPad Prism version 3 software. Normality of data was tested using Kolmogorov-Smirnov and Shapiro-Wilk tests. If the data set was found to have normal distribution, parametric tests were used. Specifically, one-way ANOVA with Tukey's *post hoc* test was used to compare three or more groups, and one-tailed unpaired t-test was used to compare two groups. If the data was not normal, non-parametric tests were used. Specifically, Kruskal-Wallis with Dunn's multiple comparison *post hoc* test was used to compare three or more groups, and one-tailed Mann-Whitney U test was used to compare two groups. $P<0.05$ was considered statistically significant.

Chapter 3: Effect of Palmitate on ER Stress, Autophagy and Apoptosis and Regulation by Adiponectin

3.1. Effect of Palmitate on ER Stress and Autophagy

3.1.1. Introduction

It is well known that excessive amounts of saturated fatty acids promotes lipotoxicity in non-adipose tissues, which greatly increases the risk for developing serious health problems such as insulin resistance, dyslipidemia, obesity and cardiovascular diseases [121]. It has therefore become important to better understand the cellular mechanisms and processes that are involved in mediating the harmful consequences of lipotoxicity.

To this end, much research in the field has demonstrated a close relationship between lipotoxicity and ER stress, with the proposal that ER stress may represent an early component of lipotoxicty [44, 121]. As indicated in Chapter 1, Section 1.3.1.2, excessive lipids may disrupt proper ER functioning. Elevated palmitate levels in primary rat hepatocytes and H4IIEC3 hepatic cells compromised the ER's ability to maintain calcium stores, and instead promoted the net redistribution of intracellular calcium from the ER to the mitochondria[122]. This increased citric acid cycle flux, mitochondrial glutamine metabolism, and production of reactive oxygen species, ultimately leading to cellular dysfunction and apoptosis [122]. Palmitate has also been observed to lead to protein accumulation[44], perhaps through its impairment of ER-to-Golgi protein trafficking which was visualized via use of GFP-tagged, temperature-sensitive reporter protein VSVG in MIN6 cells[43]. In control cells, under the permissive temperature of 32°C, VSVG moved from colocalizing with ER marker calnexin to colocalizing with Golgi marker GOLGA2 within 20 minutes. This transition was severely impaired by palmitate pretreatment

[43]. A more direct mechanism for palmitate's effects on ER function was found by Borradaile et al [123] who reported that palmitate disrupted ER membrane structure and integrity by becoming incorporated into saturated phospholipid and triglyceride species in microsomal membranes of Chinese hamster ovary cells. This membrane remodeling accompanied prominent dilatation of the ER and redistribution of protein-folding chaperones to the cytosol [123]. As discussed in Chapter 1, Section 1.3.1.2. the induction of ER stress by palmitate has been shown to upregulate UPR markers across several cell types i.e. in H9c2 cardiomyocytes [44], HepG2 liver cells [45] and L6 skeletal muscle myotubes [47]. In insulin-sensitive tissues, the activation of ER stress has been linked to insulin resistance, as it has been shown that the IRE1/JNK pathway may lead to a decrease in insulin signaling through phosphorylation of IRS1 [124] and a decrease in phosphorylation of Akt [45, 47].

The effect of obesity and lipotoxicity on autophagy has also come under investigation, with some studies showing that excess lipid accumulation upregulates autophagy and some others demonstrating that it inhibits autophagy. For example, autophagy has been understood to be a protective mechanism that is stimulated to combat lipotoxicity in several models. It degrades excess lipids via lipophagy in liver cells thereby regulating lipid metabolism and protecting against hepatic steatosis [58], and it protects against palmitate-induced beta cell death in INS1 cells [125]. However on the other hand, an inhibition of autophagic flux has been reported in response to conditions of obesity, which may itself contribute to further metabolic complications. Masini et al [126] states that both the pancreas of diabetics orpancreatic beta cells treated with fatty acids exhibited impaired autophagic turnover. This was characterized by abnormal accumulation of autophagosomes and reduced gene expression of lysosomal proteins cathepsins B and D, and LAMP2, which ultimately may contribute to beta cell death and exacerbate type 2 diabetes. Gukovsky et al [54] similarly noted the inhibition of autophagic flux in acute pancreatitis, which has been known to be caused by obesity. They stated that

accumulation of large autophagic vacuoles was observed in acinar cells, and corresponded to increased levels of LC3II and p62. The authors go on to describe how impairment of autophagy may contribute to the upregulation of inflammation, such as through the activation of NF-*κ*B pathway and the production of ROS required for NLR3P inflammasome activation[54]. Taken together, these data seem to suggest an overall protective role for autophagy, though if it is specifically upregulated or downregulated by lipid accumulation may be unclear and appears to depend on the cell type and specific physiological conditions.

The goals of this study were to first elucidate whether palmitate exposure, my model for lipotoxicity, increases or decreases ER stress and autophagy in L6 rat skeletal muscle cells. It is of interest to investigate this as the regulation of these processes by lipotoxicity may have repercussions on important endpoints such as insulin signaling/glucose metabolism and apoptosis. To study changes in the processes of ER stress and autophagy induced by palmitate, I have used well-established methods such as immunoblotting for UPR and autophagic protein markers, in addition to setting up protocols used for the first time in our laboratory such as ThT assay for assessing protein accumulation, GRP78mcherry microscopy that utilizes a reporter construct to visualize enhanced expression of the ER chaperone GRP78, and Magic Red Cathepsin B assay for assessing lysosomal activity, which may provide an indication of autolysosomal function. I used tunicamycin as a positive control for inducing ER stress as it causes accumulation of unfolded glycoproteins in the ER, leading to ER stress. It does this through blockage of the initial step of glycoprotein biosynthesis in the ER, as it is an inhibitor of the UDP-N-acetylglucosamine-dolichol phosphate N-acetylglucosamine-1-phosphate transferase (GPT) [38].

3.1.2. Results

3.1.2.1. Palmitate induces ER stress, as evidenced by increased cellular protein aggregation, increase in GRP78mcherry expression and upregulation of the UPR

The accumulation of proteins in the cell, an important hallmark of ER stress was assessed with ThT Assay via both confocal microscopy and spectrometry. Palmitate was found to increase protein aggregation as visualized in Figure 2.1A where 24h Pal shows an apparent increase in green fluorescence of ThT dye compared to the control condition. Analysis by spectrometry demonstrated a significant increase of ThT fluorescence in palmitate treatment compared to the control condition (Figure 3.1B). Tunicamycin, was used as a positive control to induce ER stress and also appeared to show marked protein aggregation in Figure 3.1A and a significant increase in fluorescence in Figure 3.1B, thereby substantiating the validity of the assay. The actual induction of ER stress by palmitate was evidenced by an increase in the expression of GRP78 chaperone protein that is known to induce the UPR when it is recruited for protein folding and becomes uncoupled from the three ER transmembrane proteins PERK, IRE1 and ATF6 [40]. Figure 3.2 demonstrates greater red fluorescence of the GRP78mcherry reporter construct in 24h Pal compared to control, and the upregulation of GRP78 was further increased with prolonged exposure of fatty acid at 48h Pal (Figure 3.2B). Tunicamycin similarly demonstrated an increase in GRP78mcherry expression. Direct evidence for the upregulation of the UPR in response to palmitate was provided in Figure 3.3 which illustrates that palmitate demonstrates a trend towards upregulating the UPR marker peIF2α, as assessed by Western blot. The difference in peIF2α expression between palmitate and control was significant at the 24h time point.

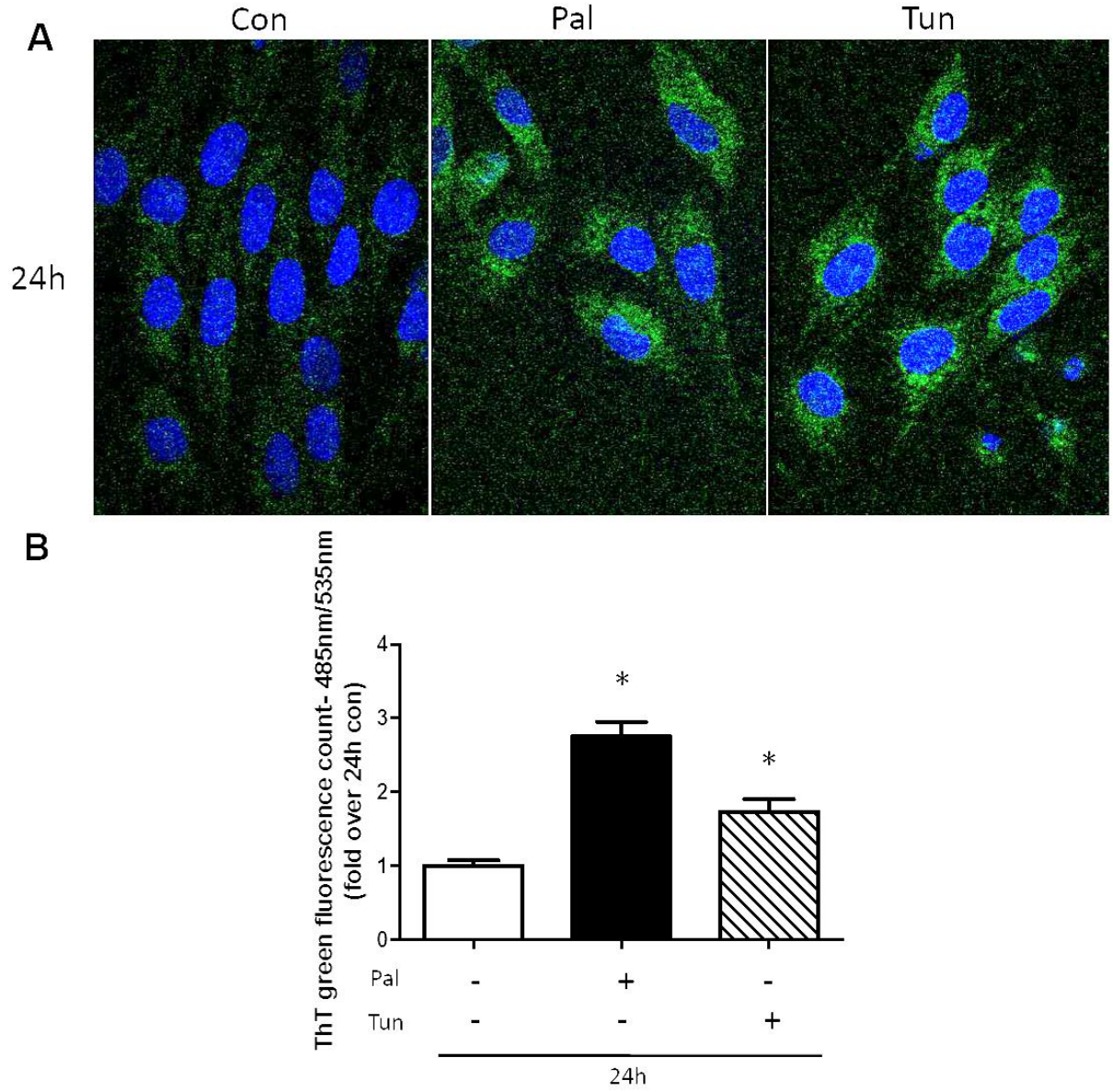

Figure 3.1. Palmitate induces ER stress by increasing cellular protein aggregation, as assessed by ThT Assay.
(A) Representative image for ThT microscopy in L6 wt myoblasts | 24h | n=4 | An apparent increase in protein aggregation is visualized in 24h Pal compared to 24h Con. The positive control for ER stress, 24h Tun, appears to show marked protein aggregation.
(B) Quantification graph from ThT spectrometry in L6 wt myotubes | 24h | n=6 for Con and Pal; n=5 for Tun | Protein aggregation is significantly upregulated by 24h Pal and 24h Tun as compared to 24h Con, as denoted by * ($p<0.05$) | Statistical analysis done by one-way ANOVA with Dunnett's multiple comparison post-hoc test. Normal distribution was verified by Shapiro-Wilk and Kolmogorov-Smirnov tests.

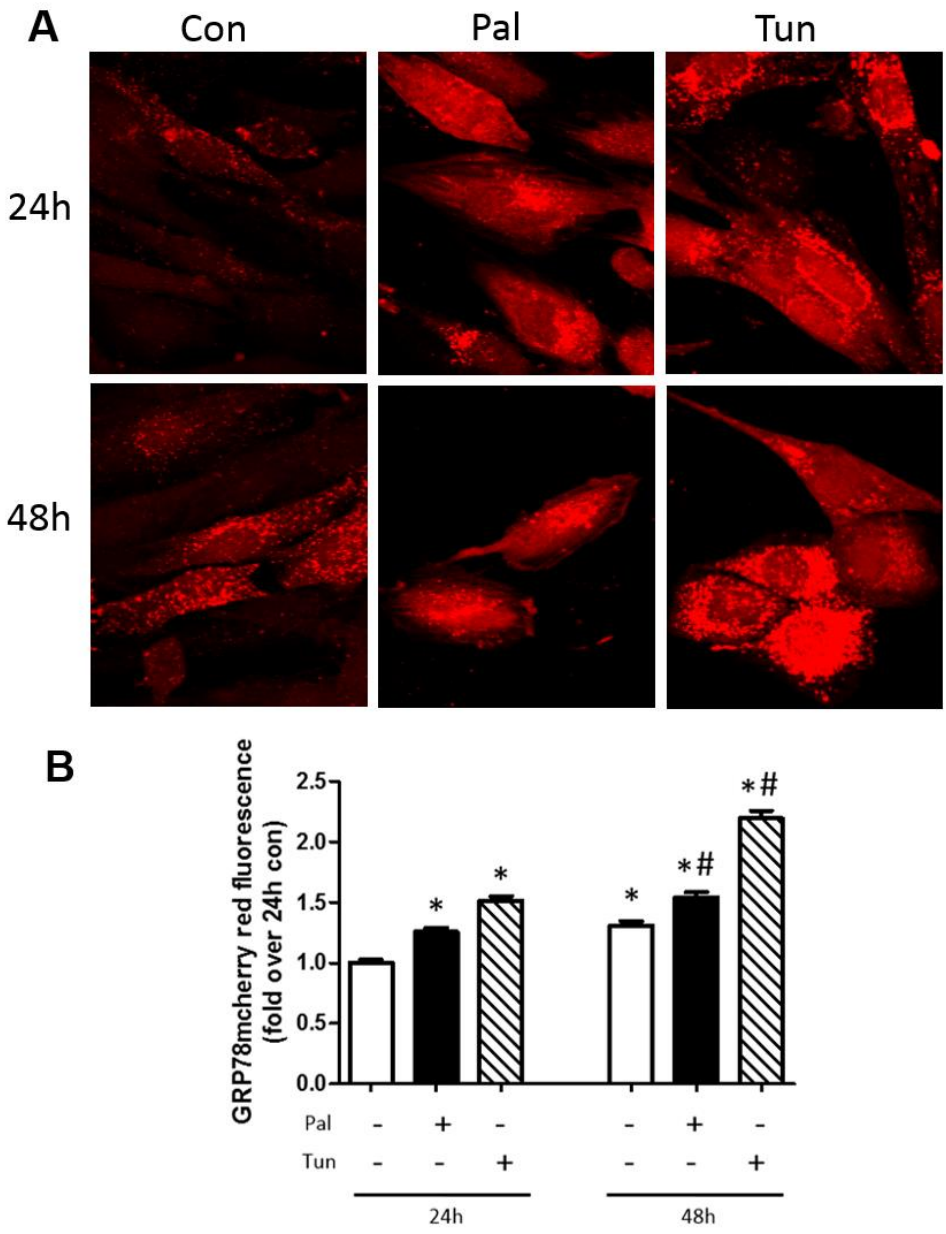

Figure 3.2. An increase in GRP78mcherry expression provides evidence for induction of ER stress by palmitate.
(A) Representative image for microscopy of L6 GRP78mcherry myoblasts.
(B) Quantification graph of L6 GRP78mcherry microscopy using Image J software. Each column represents the mean of 30-50 cells | 24h, 48h | n=3 | Significantly greater red fluorescence of GRP78mcherry reporter construct is observed in 24h Pal and 24h Tun compared to 24h Con, and 48h Pal and 48h Tun compared to 48h Con, indicating an increase in ER stress induction by palmitate and tunicamycin at these time points, as denoted by * ($p<0.05$). ER stress induction is significantly increased with prolonged exposure to palmitate and tunicamycin, as 48h Pal is significantly greater than 24h Pal, and 48h Tun is significantly greater than 24h Tun, as indicated by # ($p<0.05$). 48h Con shows significantly greater red fluorescence than 24h Con, as denoted by * ($p<0.05$) | Statistical analysis done by Kruskal-Wallis test with Dunn's multiple comparison post-hoc test.

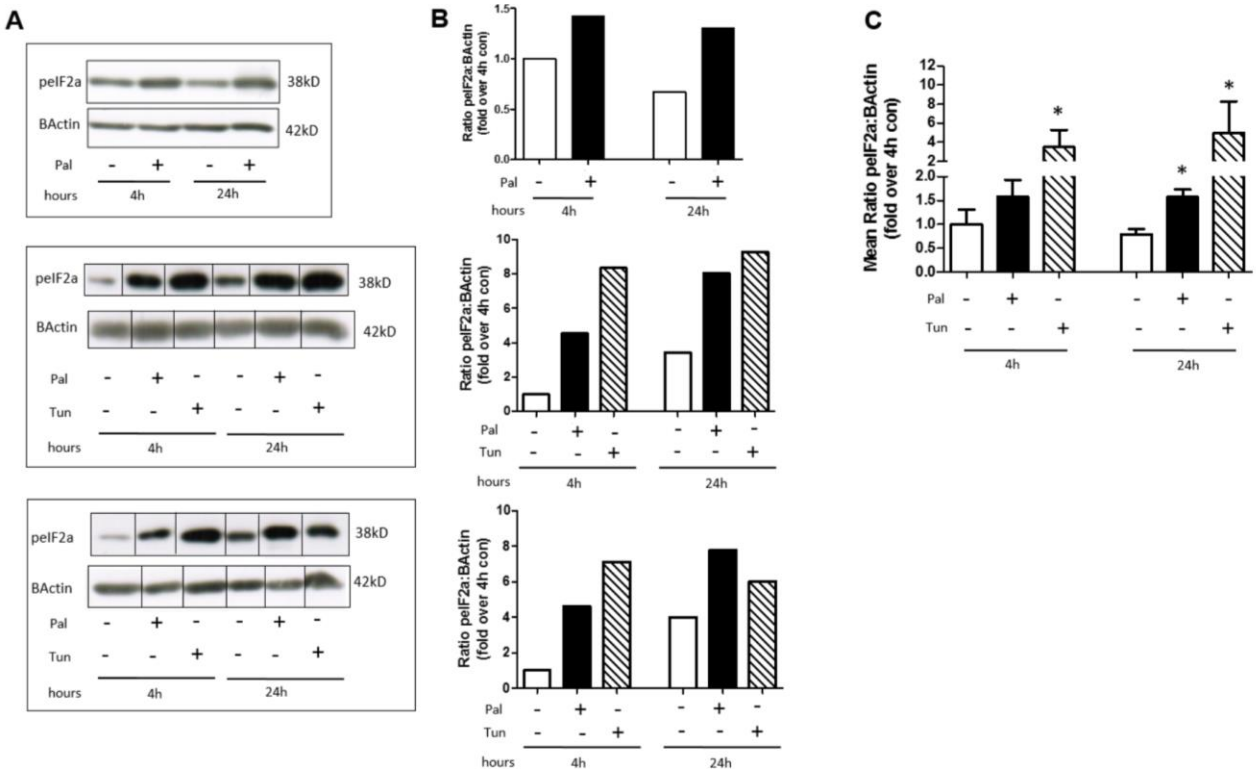

Figure 3.3. Palmitate demonstrates a trend towards upregulating UPR marker peIF2α, as assessed by Western blot
(A) Representative Western blot images, from individual experiments, for time points 4h, 24h.
(B) Corresponding Western blot quantification graphs for individual experiments shown in (A)
(C) Cumulative graph of Western blot quantification | n=6 for 4h and 24h Con and Pal; n=3 for 4h, 24h Tun | 24h Pal and 24h Tun demonstrate significantly greater peIF2α than 24h Con, as denoted by * ($p<0.05$). 4h Tun demonstrates significantly greater peIF2α than 4h Con, as denoted by * ($p<0.05$). Statistical analyses done by Mann-Whitney U test.

3.1.2.2. Palmitate appears to increase autophagic flux, as evidenced by apparent increased autophagosome formation and lysosome activity

In my model of lipotoxicity in L6 rat skeletal muscle cells, palmitate exposure seemed to increase autophagosome formation, as assessed by endogenous LC3 immunofluorescence microscopy in Figure 3.4. An apparent increase in the amount of green LC3 puncta was visible in palmitate treatments over the time course 1h-24h compared to control cells. This may correspond to an increase in autophagosome formation, as fluorescently tagged LC3 becomes lipidated to its LC3II form and incorporated into the autophagosomal membrane, thereby giving rise to visually discernable puncta. Evidence for the progression of autophagy from its beginning autophagosome stage to its later degradative autolysosome stage was given by Magic Red Cathepsin B assay microscopy (Figure 3.5) which showed significantly greater red fluorescence indicating greater activity of lysosomal cathepsin B enzyme in 4h Pal and 24h Pal compared to corresponding controls. This increase was not evident at 48h however, an observation which will be discussed subsequently in chapter 4, section 4.4. Further support for increased autophagic flux induced by palmitate was provided by Western blotting for autophagy proteins LC3II and p62. Figure 3.6 demonstrates that compared to corresponding timed controls, palmitate may demonstrate an overall trend towards increasing LC3II and decreasing p62, consistent with the characteristic increased autophagosome formation and degradation of p62 discussed in Chapter 1, Section 1.3.2.1.

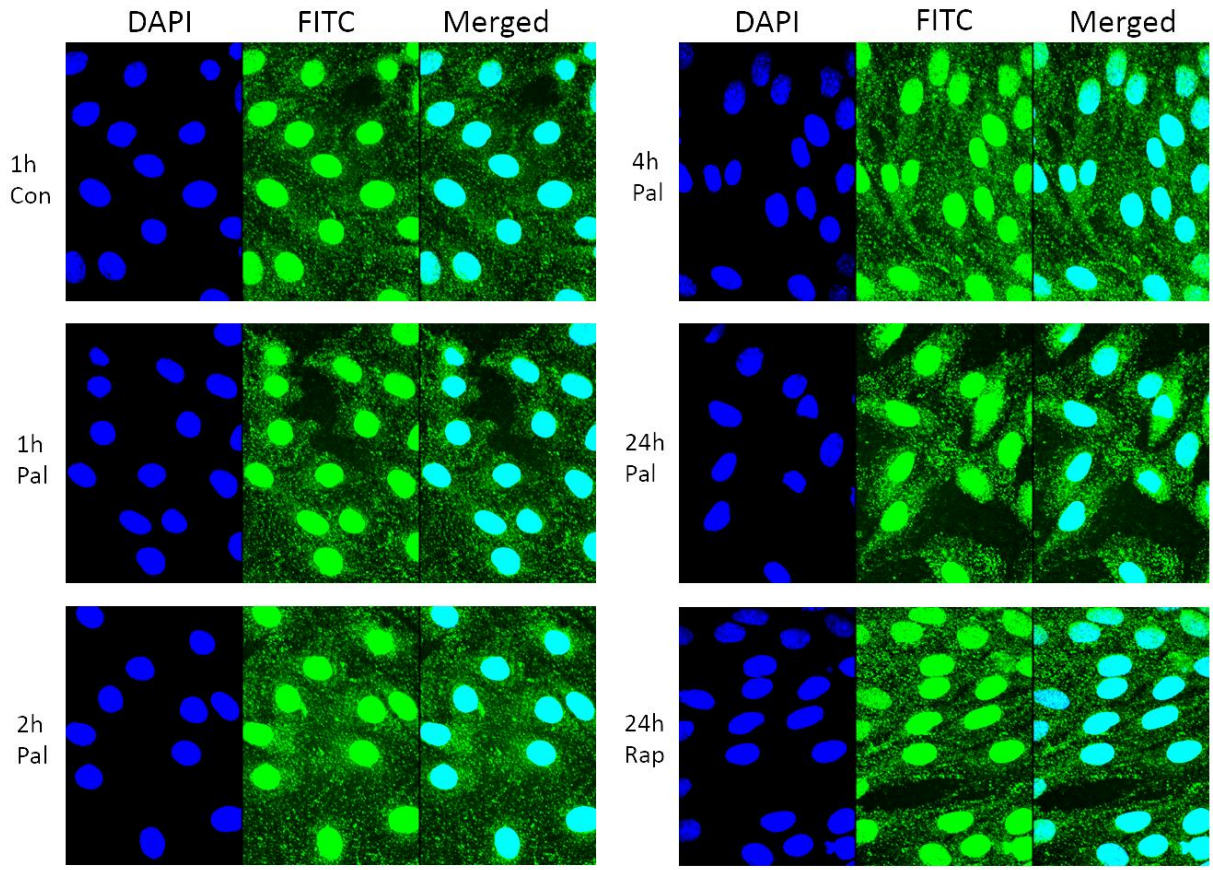

Figure 3.4. Palmitate appears to increase autophagosome formation, as assessed by endogenous LC3 puncta immunofluorescence (IF) microscopy. Representative IF images for time course 1h-24h | n=2 | Amount of LC3 puncta appears to be increased in palmitate treatments compared to control.

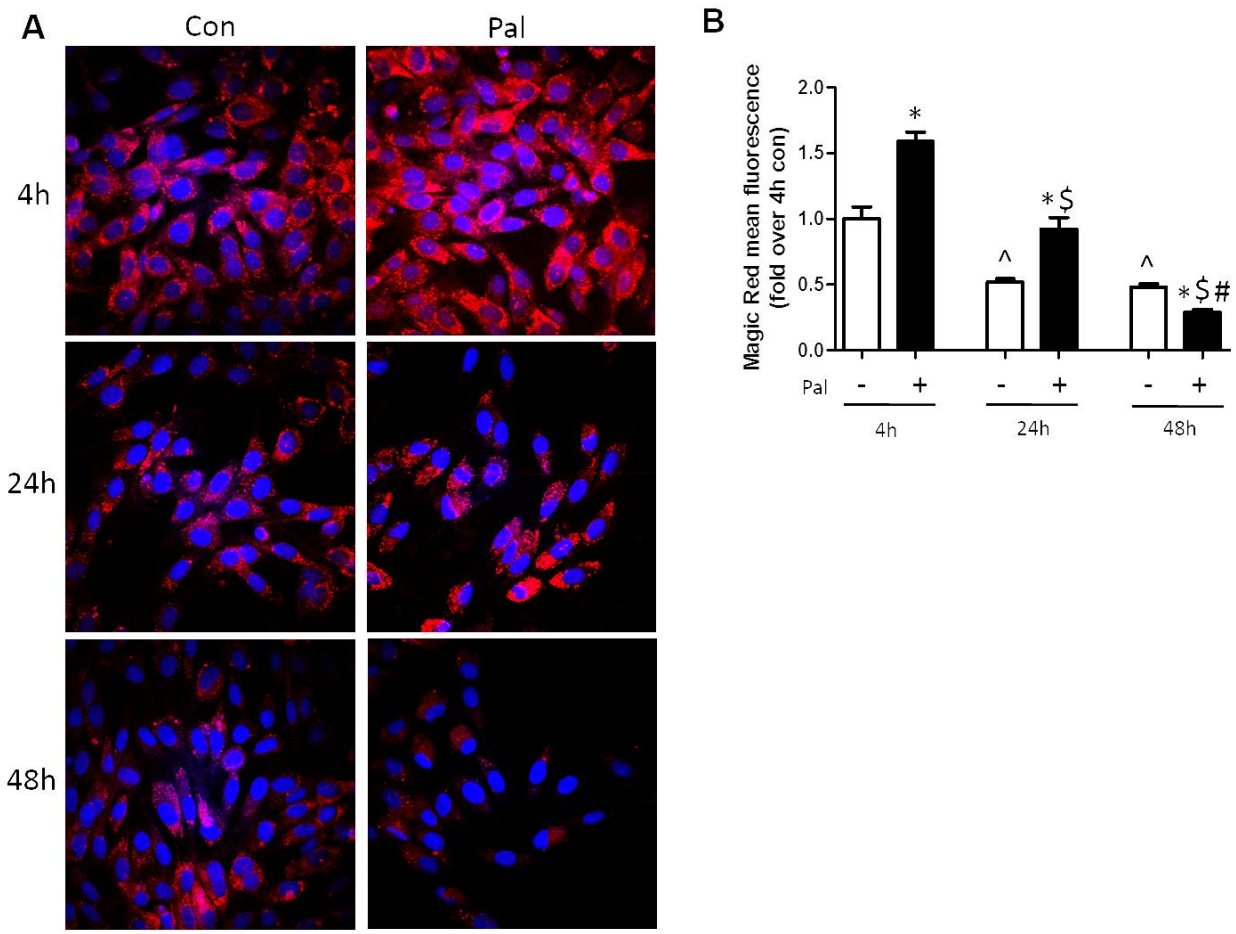

Figure 3.5. Palmitate may increase lysosome activity, as assessed by Magic Red Cathepsin B Assay microscopy.
(A) Representative images for time points 4h, 24h and 48h | n=3 for 4h; n=6 for 24h; n=1 for 48h
(B) Corresponding quantification graph of individual experiment shown in (A), done using Image J software. Each column represents the mean of ~50 cells | n=1 | 4h Pal and 24h Pal show significantly greater red fluorescence indicating active lysosomal cathepsin B enzyme, as compared to their respective controls 4h Con and 24h Con, denoted by * ($p<0.05$). Conversely, 48h Pal shows significantly less red fluorescence than 48h Con, denoted by * ($p<0.05$). With increased duration of exposure to palmitate, red fluorescence significantly decreases, as 48h Pal and 24h Pal show significantly less fluorescence than 4h Pal, denoted by $ ($p<0.05$), and 48h Pal shows significantly less fluorescence than 24h Pal, denoted by # ($p<0.05$). 24h Con and 48h Con show significantly less fluorescence than 4h Con, denoted by ^ ($p<0.05$). Statistical analyses done by Kruskal-Wallis test with Dunn's multiple comparison post hoc test.

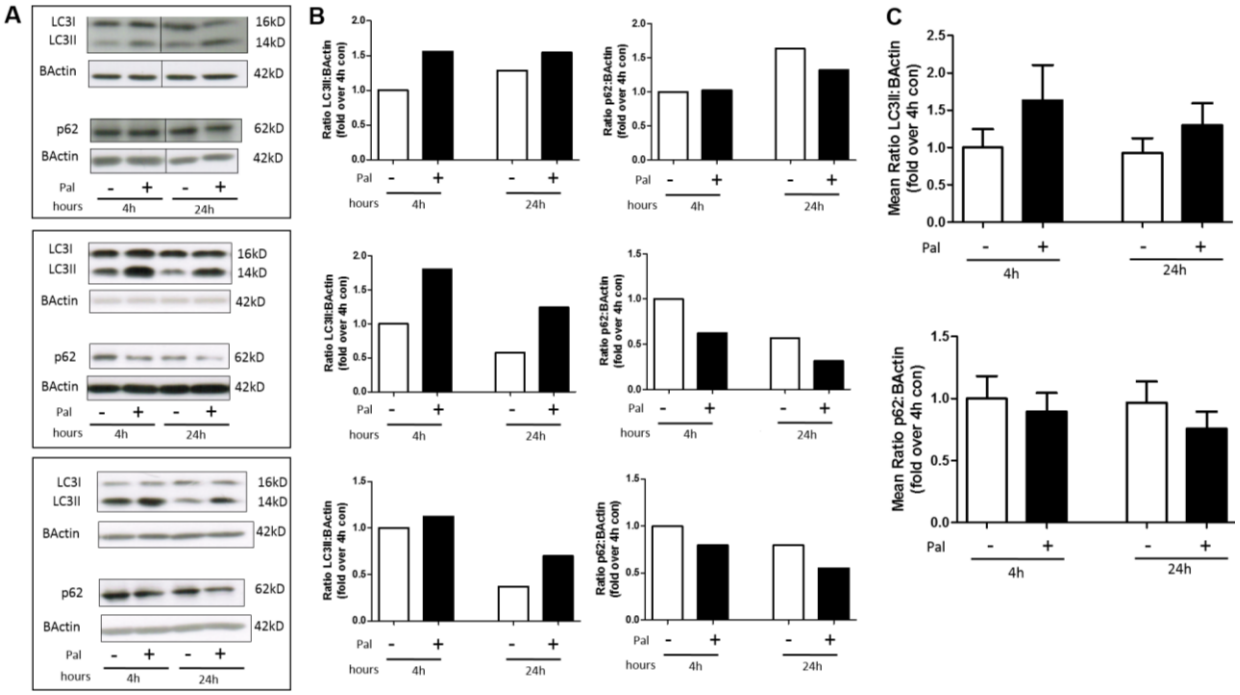

Figure 3.6. Palmitate demonstrates a trend towards increasing autophagic flux, as assessed by Western blot for LC3II and p62.
(A) Representative Western blot images, from individual experiments, for time points 4h, 24h.
(B) Corresponding Western blot quantification graphs for individual experiments shown in (A)
(C) Cumulative graph of Western blot quantification | n=8 for 4h; n=9 for 24h | Compared to corresponding timed controls, Pal may demonstrate an overall trend towards greater LC3II and lesser p62.

3.2. ER Stress May Induce Autophagy as a Rescue Mechanism

3.2.1. Introduction

As discussed in Chapter 1, Section 1.4.1, though the UPR is recognized as the primary well-established response of the cell to manage ER stress induced by protein overload [39], several studies have reported that autophagy too may be recruited as a rescue mechanism to ultimately attenuate ER stress, via its ability to degrade accumulated proteins and thereby reduce the protein overload on the cell [44, 74, 127]. Furthermore, an interesting study by Bernales et al [128] reported a potential role for ER-phagy, a sub-type of autophagy, in removing unfolded proteins from the ER. The authors observed that when ER stress was induced in wild type yeast cells by dithiothreitol (DTT), the expected ER expansion was accompanied by the formation of autophagosome-like structures, which were packed with membrane cisternae derived from ER. However, these ER-containing autophagosomes (ERAs) were not generated in cells genetically modified to express $Hac1^{i}$ (the yeast ortholog of XBP1), that is primarily involved in initiating transcriptional programs directed towards protein folding, maturation and degradation. This suggested that ERA formation required the actual presence of unfolded proteins, something that would be ameliorated in the *hac1Δ* cells. The authors therefore proposed that in response to ER stress induced by protein overload, an expanded ER could facilitate ER-phagy as a protective mechanism, which sequestered potentially toxic unfolded proteins or aggregates into distinct regions of the ER, and packaged them into ERAs for eventual degradation[128].

As an adaptive response to ER stress, autophagy has been shown to increase cell viability, by steering the cell away from ER stress-induced apoptosis. Studies in support of this conclusion have shown that when autophagy is pharmacologically inhibited with 3-

methyladenine (3-MA), glomerular podocytes and breast cancer cells stimulated to undergo ER stress with tunicamycin or thapsigargin demonstrated increased cell death [127, 129]. The role of autophagy in attenuating ER stress-induced apoptosis will be discussed in more detail in subsequent chapters; here I will principally focus on elucidating the link between the activation of autophagy in response to ER stress.

As discussed in Chapter 1, Section 1.4.1, there is much evidence to show that ER stress directly stimulates the initial stage of autophagy, the formation of autophagosomes. Yorimitsu et al [76] demonstrated that tunicamycin-induced ER stress stimulated the formation of the pre-autophagosomal structure in yeast atg11Δ cells that otherwise are inherently defective in this. Morever, several studies have shown that stimulation of ER stress with triggers such as thapsigargin, tunicamycin or poluglutamine 72 (PolyQ72) aggregates led to conversion of LC3I to LC3II [39, 75, 127, 129].

UPR pathways and proteins have also been implicated in the activation of autophagy following ER stress. As described in Chapter 1, Section 1.4.1, IRE1-deficient MEF cells or cells treated with JNK inhibitor SP600125, exhibited inhibition of autophagic GFP-LC3 puncta formation, demonstrating that the IRE-JNK pathway is involved in facilitating autophagy [39]. Similarly, C2C5 cells with genetically impaired PERK or eIF2α displayed reduced conversion of LC3I to LC3II [75]. Moreover, in HepG2 cells ATF4-siRNA suppressed ATF4 protein and mRNA expression and inhibited NaF- or tunicamycin- induced autophagy [130].

The goals of this study were to investigate whether ER stress induces autophagy in my model of L6 rat skeletal muscle cells, and to elucidate the link between the peIF2α branch of the UPR and autophagic activity. Salubrinal, a dephosphorylation inhibitor of eIF2α that prolongs peIF2α downstream signaling [131] has been used to investigate this. In addition, I studied the

effect of impairing autophagy on ER stress using molecular and pharmacological approaches. An ATG5K130Rdominant negative mutant, that was defective in conjugating to Atg12 on the lysine (K) residue, was used to inhibit autophagosome formation through inhibition of LC3 incorporation into the early autophagosome [119]. Next, a late phase autophagy inhibitor, chloroquine, was used to inhibit fusion of autophagosomes with lysosomes and lysosomal protein degradation, by increasing the pH of autophagic vacuoles and inhibiting lysosomal enzymes that required an acidic pH to function [49]. Previously described methods such as Western blotting, ThT assay, Magic Red cathepsin B assay and GRP78mcherry assay were also employed in this study.

3.2.2. Results

3.2.2.1. Tunicamycin, an established inducer of ER stress, appears to increase autophagic flux as evidenced by Western blotting for autophagic proteins and apparent increase in lysosomal activity

I first verified the effect of tunicamycin in stimulating ER stress and upregulating the UPR through Western blotting for UPR marker peIF2α. It was found that compared to corresponding controls, tunicamycin appeared to show greater peIF2α at both 4h and 24h, as would be expected (Figure 3.7). Next, it was found that tunicamycin also appeared to upregulate LC3II compared to controls at 4h and 24h, while perhaps decreasing p62 (Figure 3.8). In addition, as observed in Figure 3.9, tunicamycin appeared to increase lysosomal activity at 4h compared to its corresponding control, assessed by Magic Red Cathepsin B assay microscopy which demonstrated an increase in red fluorescence, indicative of active cathepsin B enzyme. Taken together, these results may provide support for the line of thinking that ER stress may induce autophagy.

It was noted however in Figure 3.3, that at 24h, tunicamycin does not appear to elicit increased lysosomal cathepsin B activity compared to the control. This may indicate that perhaps tunicamycin's effect to increase lysosomal activity is most prominent only in the short term; the reasons as to why this might be the case will be discussed in Chapter 4, Section 4.4.

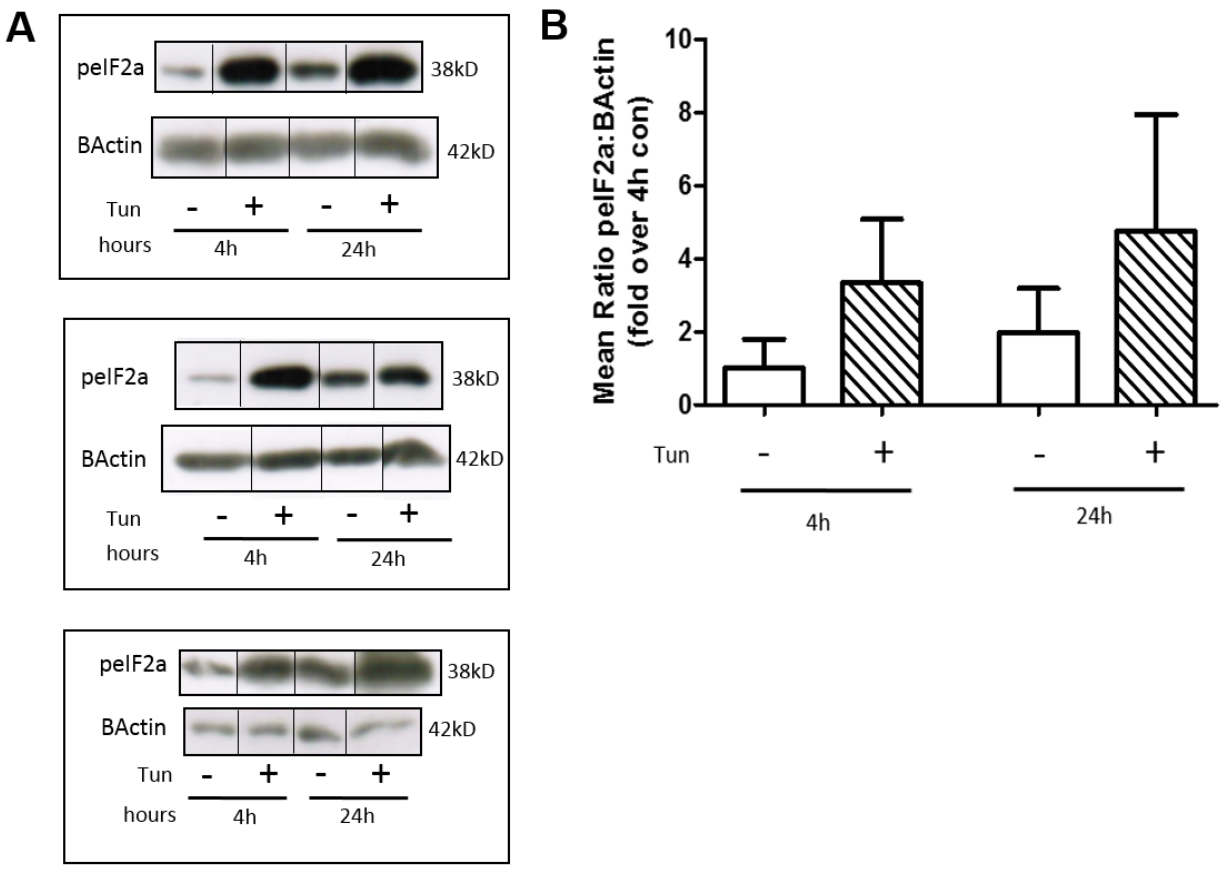

Figure 3.7. Tunicamycin demonstrates a trend towards upregulating UPR marker peIF2α, as assessed by Western blot.
(A) Western blot images, from individual experiments, for time points 4h, 24h
(B) Cumulative graph of Western blot quantification | n=3 | Compared to corresponding timed control, Tun appears to show greater peIF2α.

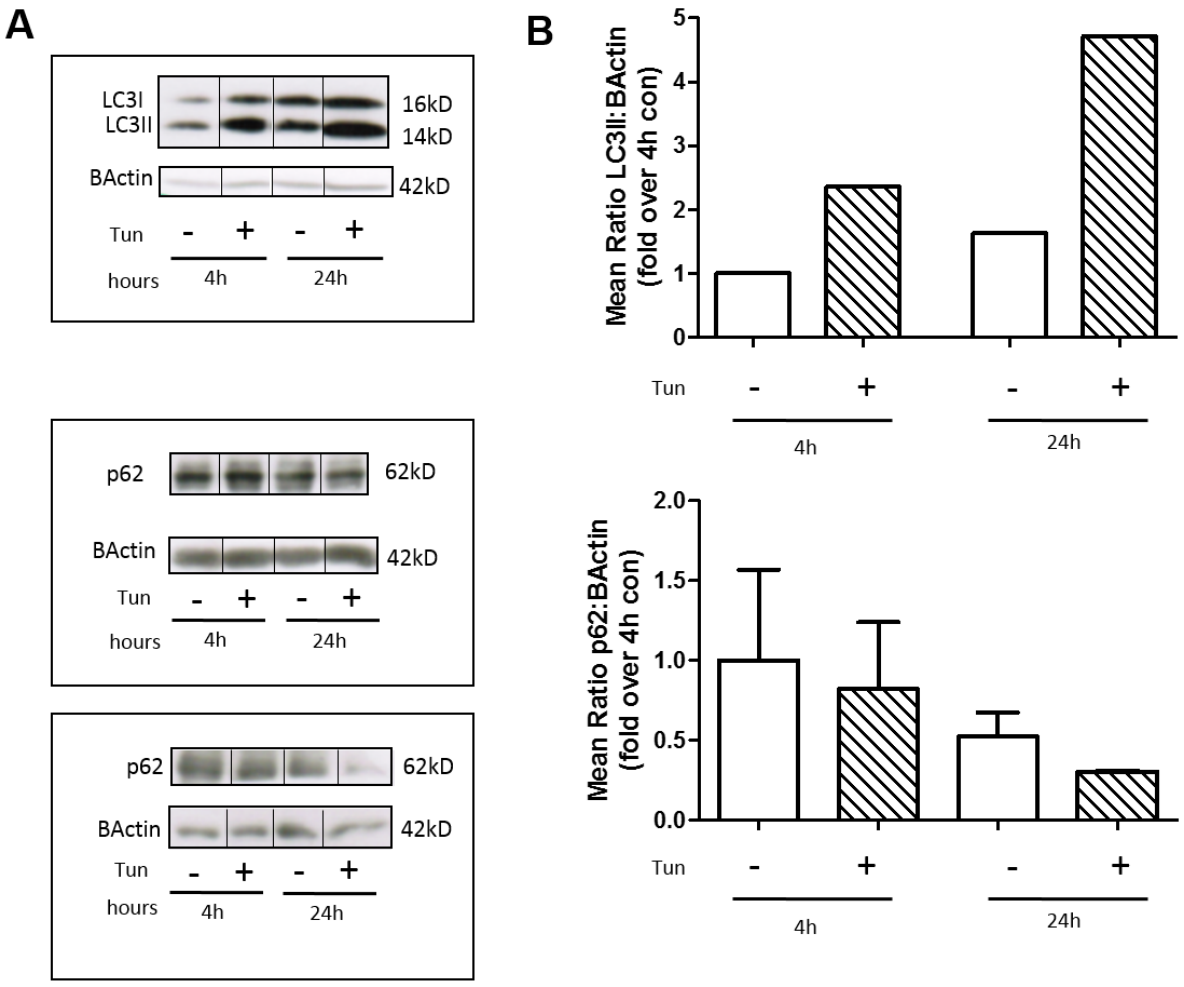

Figure 3.8. Tunicamycin, an inducer of ER stress, demonstrates a trend towards increasing autophagic flux, as assessed by Western blot for LC3II and p62.
(A) Western blot images for time points 4h, 24h
(B) Cumulative graph of Western blot quantification | n=1 for LC3II; n=2 for p62 | Compared to corresponding timed controls, Tun may appear to demonstrate a trend towards increasing LC3II and decreasing p62.

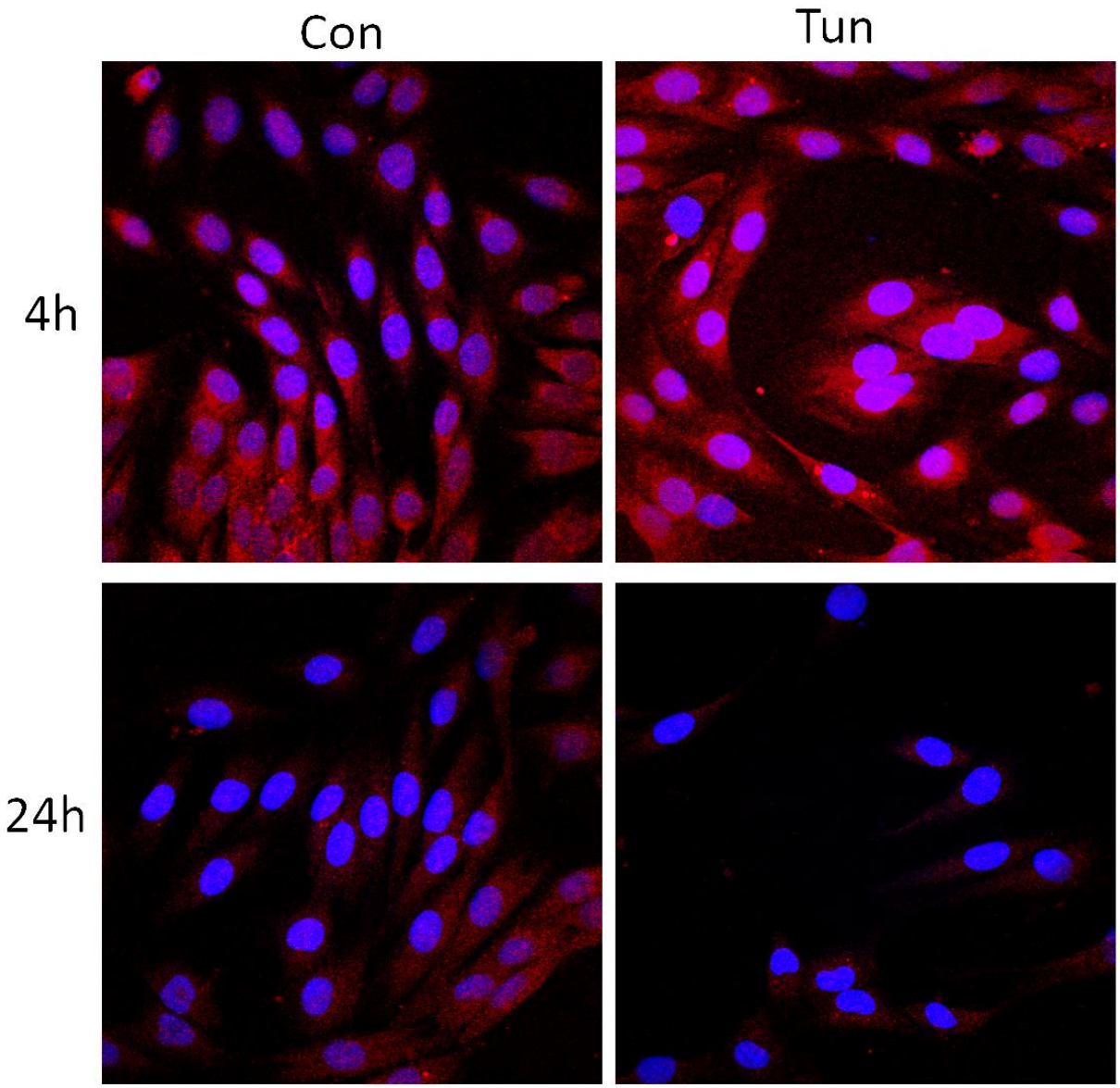

Figure 3.9. Tunicamycin, an inducer of ER stress, appears to increase lysosomal activity, at 4h but not 24h, as assessed by Magic Red Cathepsin B Assay microscopy. Representative images for 4h, 24h | n=1 for 4h; n=3 for 24h | 4h Tun appears to show more overall red fluorescence, indicative of cathepsin B lysosomal activity than 4h con. However at 24h, Tun does not elicit such a response. This may indicate that perhaps Tun's effect to increase lysosomal activity occurs more so in the short term, and dwindles in the long term.

3.2.2.2. Sustaining UPR activity and preventing dephosphorylation of eIF2α with ER stress inhibitor salubrinal, appears to increase lysosomal activity, as assessed by Magic Red Cathepsin B assay microscopy

Further evidence for the sequential link between ER stress and autophagy was provided by the Magic Red Cathepsin B Assay observations exhibited in Figure 3.10. It may be seen that pretreatment with salubrinal in both control and palmitate conditions appears to increase the red fluorescence, indicative of cathepsin B lysosomal activity, at both 4h and 24h. Therefore, keeping the UPR active by keeping the peIF2α signaling pathway active with the use of salubrinal could perhaps also upregulate the autophagic pathway.

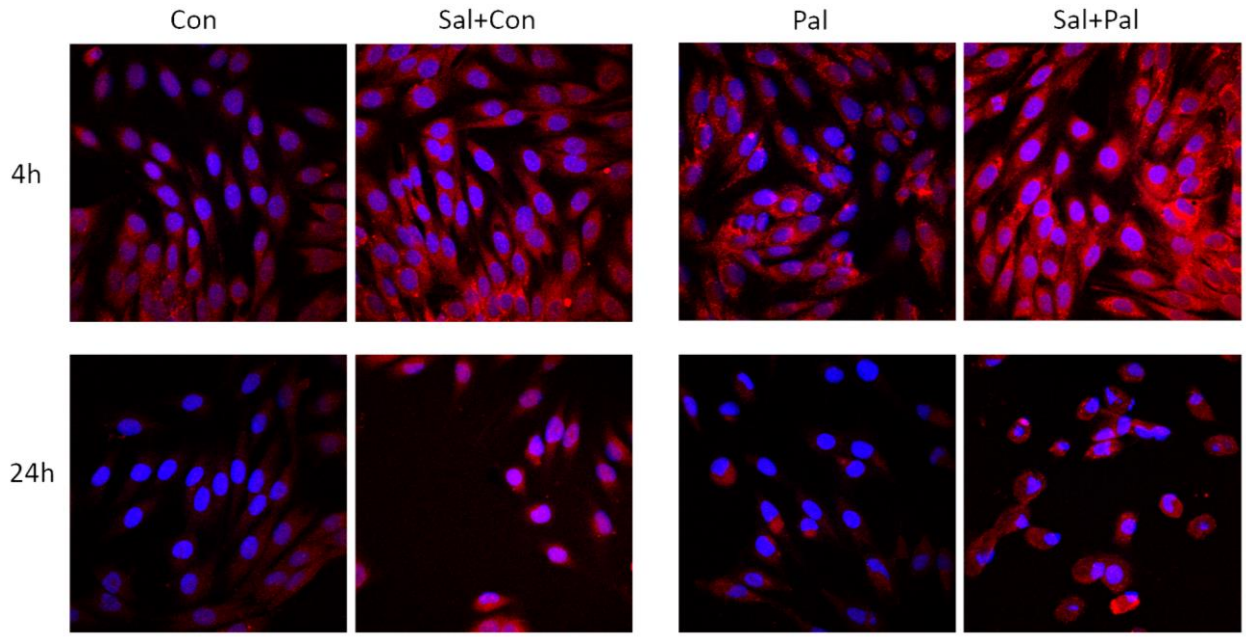

Figure 3.10. Sustaining UPR activity by preventing dephosphorylation of eIF2α with ER stress inhibitor salubrinal, may increase lysosomal activity, as assessed by Magic Red Cathepsin B Assay microscopy. Representative images for 4h, 24h | n=1 for 4h; n=4 for 24h | Pretreatment with salubrinal in the control or palmitate conditions appears to increase the overall red fluorescence, indicative of cathepsin B lysosomal activity, at both 4h and 24h. Therefore, this may provide evidence that keeping UPR active by keeping peIF2α pathway active could also upregulate autophagy rescue mechanism. | Note: The images for control conditions are the same between Figures 3.10 and 3.9 as both figures show the same representative experiment, where the experimental treatments were conducted at the same time. Experimental treatments tunicamycin and salubrinal are shown separately for the purpose of clarifying discussion.

3.2.2.3. Inhibiting autophagy using ATG5K130R dominant negative cell line or pharmacological inhibitor, chloroquine appears to increase ER stress, as evidenced by apparent increases in protein aggregation and UPR stimulation

The expected impairment in autophagic flux exhibited by ATG5K130R dominant negative myoblasts was first verified by Western blotting for autophagy proteins LC3II and p62. As observed in Figure 3.11A, compared to EV, the control, palmitate and tunicamycin conditions in ATG5K130R cells appeared to show less LC3II. According to Figure 3.11B, ATG5K130R control and palmitate conditions exhibited significantly less LC3II than EV control and palmitate conditions, at both 4h and 24h. Overall, ATG5K groups appeared to demonstrate a trend towards increased p62, compared to EV groups. These findings correspond to a blockage in autophagic flux; specifically reduced incorporation of LC3 into the autophagosomal membrane and accumulation of undegraded p62.

The consequences of impaired autophagy on ER stress were then elucidated by various ER stress assays previously described. The ThT microscopy assay shown in Figure 3.12 depicted apparent increases in overall protein aggregation in ATG5K130R cells compared to EV cells. This perhaps indicates that impairment in the autophagic degradative pathway leads to increased protein accumulation. Additionally, Figure 3.13 Western blot illustrates that compared to EV, the control and palmitate conditions in ATG5K130R cells exhibited significantly increased peIF2α, providing evidence that an impairment in autophagy may exacerbate ER stress and upregulate the UPR. Finally, Figure 3.14 shows that pharmacological inhibition of autophagy with chloroquine, may similarly upregulate ER stress, as significantly greater red fluorescence of GRP78mcherry reporter construct was observed in the control condition pretreated with chloroquine as compared to the control, and in the palmitate condition pretreated with chloroquine compared to palmitate. Taken together, these results may indicate that autophagy

does indeed help to alleviate the burden of ER stress, such that when it is compromised, ER stress is aggravated.

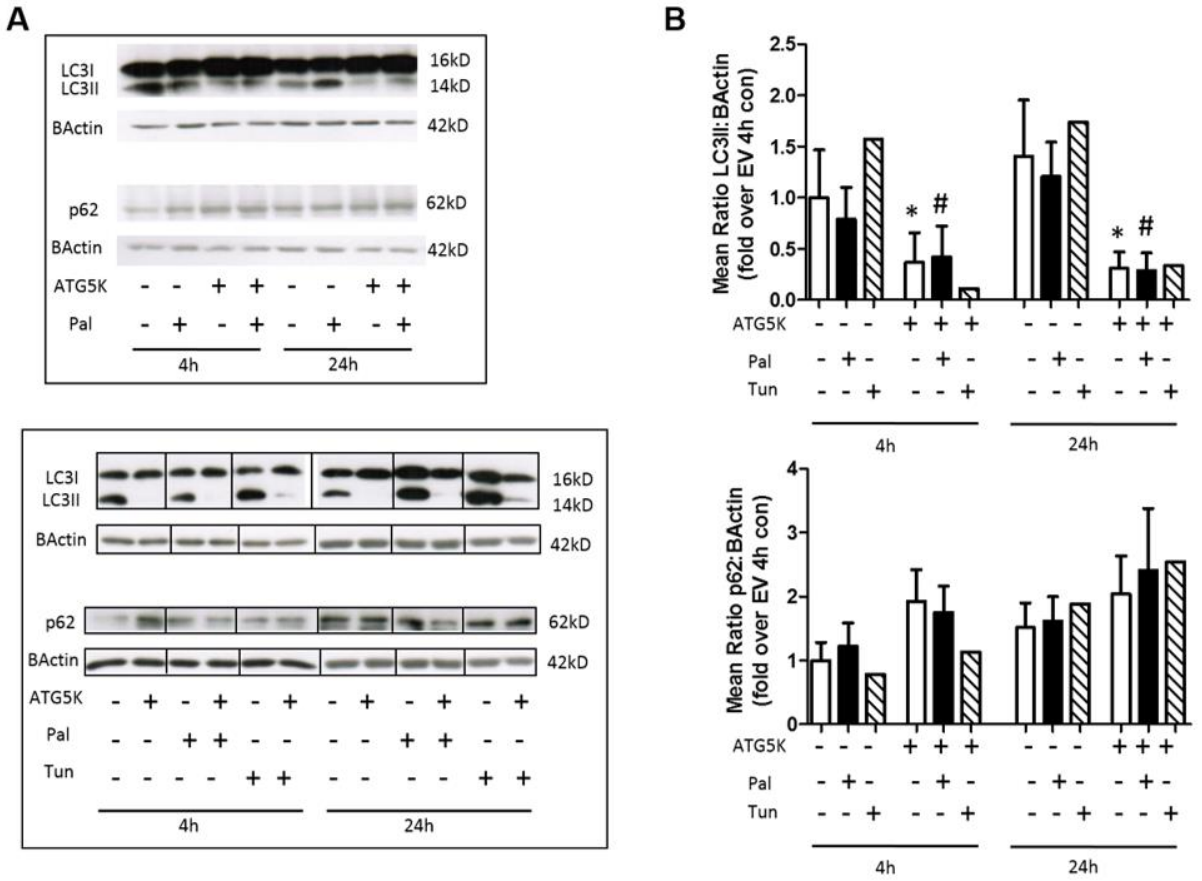

Figure 3.11. ATG5K130R myoblasts appear to demonstrate impaired autophagy, as assessed by Western blot for LC3II and p62. (A) Representative Western blot images for time points 4h, 24h (B) Summary graph of Western blot quantification | n=7 for con and Pal; n=1 for Tun | ATG5K 4h and 24h Con exhibit significantly less LC3II than EV 4h and 24h Con respectively, as denoted by * ($p<0.05$). ATG5K 4h and 24h Pal exhibit significantly less LC3II than EV 4h and 24h Pal respectively, as denoted by # ($p<0.05$). Statistical analyses done by Mann-Whitney U test. | Overall, ATG5K groups appear to demonstrate a trend towards increased p62, compared to EV groups. | This may correspond to reduced incorporation of LC3 into the autophagosomal membrane and accumulation of undegraded p62.

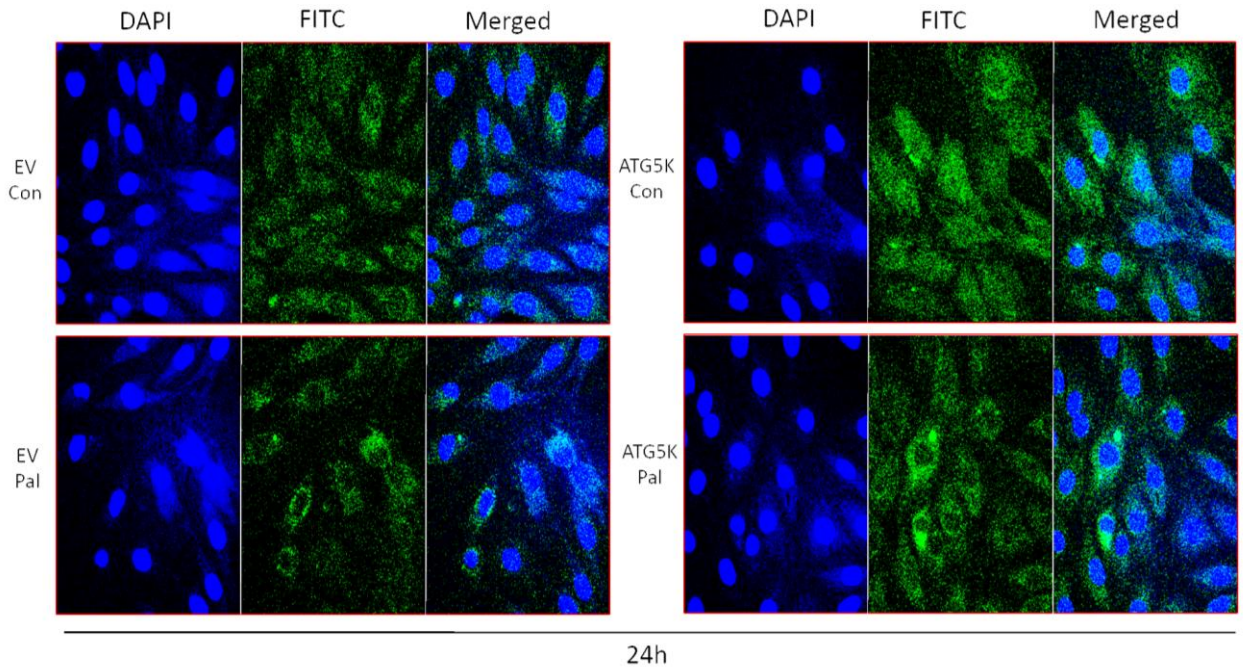

Figure 3.12. ATG5K130R cells appear to demonstrate increased protein aggregation, as assessed by ThT microscopy assay. Representative images for ThT Microscopy | 24h | n=1 | An apparent increase in protein aggregation may be visualized overall in ATG5K cells compared to EV cells, perhaps indicating that impairment in autophagic degradative pathway may lead to increased protein accumulation.

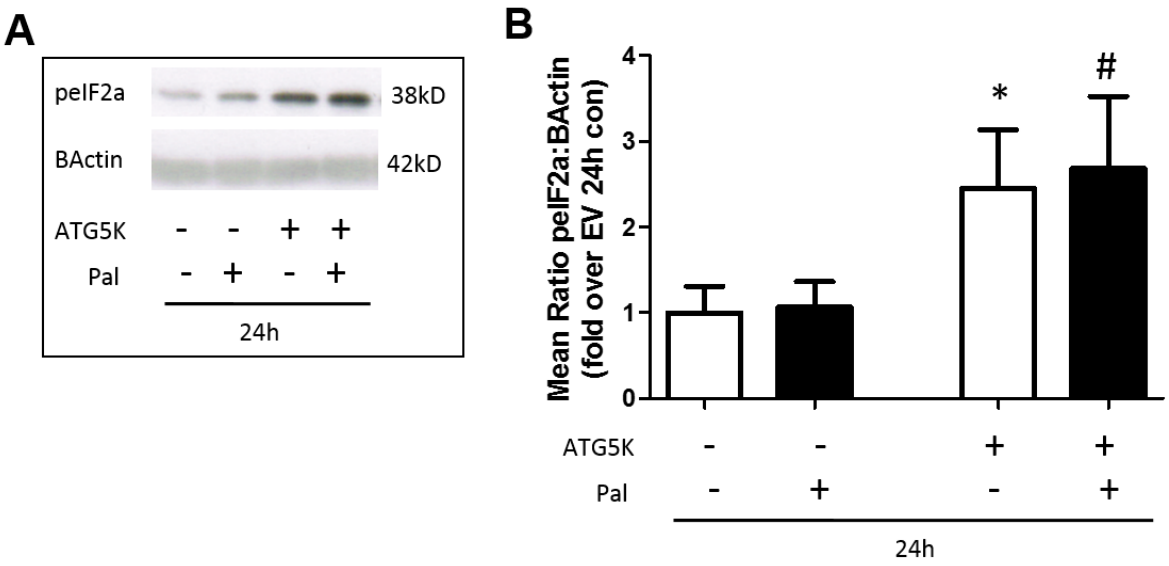

Figure 3.13. ATG5K130R myoblasts demonstrate increased expression of UPR marker, peIF2α, as assessed by Western blot.
(A) Representative Western blot image for time point 24h
(B) Cumulative graph of Western blot quantification | n=6 | Compared to EV groups, ATG5K groups exhibit greater peIF2α, which may indicate greater ER stress, perhaps as a result of the autophagy rescue mechanism being impaired. | ATG5K 24h Con demonstrates significantly more peIF2α than EV 24h Con, denoted by * ($p<0.05$). ATG5K 24h Pal demonstrates significantly more peIF2α than EV 24h Pal, denoted by # ($p<0.05$). Statistical analyses done by Mann-Whitney U test.

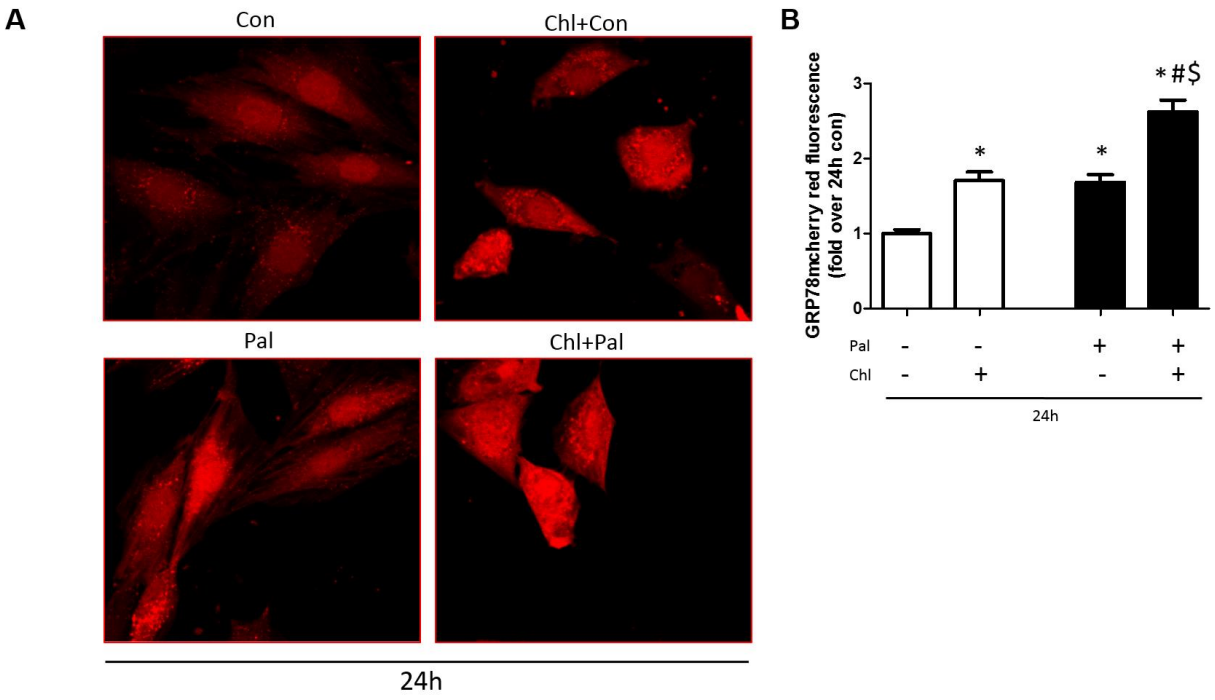

Figure 3.14. Inhibiting autophagy with chloroquine increases GRP78mcherry expression and induction of ER stress
(A) Representative images for GRP78mcherry microscopy
(B) Quantification graph of GRP78mcherry microscopy using Image J software. Each column represents the mean of 30-50 cells | 24h | n=2 | 24h palmitate significantly increases overall red fluorescence of GRP78mcherry reporter construct compared to 24h control, denoted by * ($p<0.05$). Pretreatment of control condition with chloroquine significantly increases GRP78mcherry fluorescence compared to control, denoted by * ($p<0.05$). Pretreatment of palmitate condition with chloroquine significantly increases GRP78mcherry fluorescence compared to control denoted by * ($p<0.05$), compared to palmitate denoted by # ($p<0.05$) and compared to control condition pretreated with Chl denoted by $ ($p<0.05$). | Statistical analysis done by Kruskal-Wallis test with Dunn's multiple comparison post-hoc test.

3.3. Prolonged, Excessive or Uninhibited ER Stress Induces Apoptosis

3.3.1. Introduction

As discussed in Chapter 1, Sections 1.4.1 and 1.4.3.4, and Chapter 3, autophagy may be induced in the cell to help alleviate ER stress by degrading excessive proteins, and through this action it may help circumvent ER stress-induced apoptosis [44, 127]. Many studies have been conducted to demonstrate autophagy's cytoprotective role in this regard. The stimulation of autophagy using rapamycin has been found to decrease ER stress-induced apoptosis in C2C5 cells [75], H9c2 cells [44], HeLa cells [39] and diabetic Akita mice [96]. Meanwhile, loss of function of autophagy in ER stress conditions has contributed to uninhibited ER stress and increased apoptosis. For instance, ATG5-deficient MEF cells exposed to tunicamycin [39], or bafilomycin-treated H9c2 cells stressed with palmitate [44], exhibited increased apoptosis. Lastly the suggestion that autophagy may be activated as a protective mechanism downstream of the UPR's pPERK/peIF2α signaling pathway may be supported by work which showed that suppression of the transcription factor ATF4 by ATF4-siRNA in HepG2 cells, completely inhibited the autophagy induced by NaF or tunicamycin [130]. Taken together, these studies point to autophagy as being a protective mechanism that may be recruited to alleviate ER stress-induced apoptosis. However it is important to understand that if the intensity or duration of ER stress surpasses the cell's ability to cope via the UPR or autophagy, then apoptotic programmes are likely to take over and move the cell towards ER stress-induced cell death [35, 51].

The ER has been found to induce apoptosis via several pathways. Upon prolonged ER stress, the UPR protein IRE1α recruits TNF receptor-associated factor 2 (TRAF2), which in turn

recruits and activates ASK, a component of the c-Jun N-terminal kinase (JNK) pathway. JNK is translocated to the mitochondrial membrane and stimulates intrinsic apoptosis through the phosphorylation of Bim, a BH3-only Bcl-2 protein, which then leads to Bax-dependent cytochrome *c* release and activation of caspase 9 initiator caspase [132], which then cleaves and activates effector/executioner caspases, caspase 3 and caspase 7 [51]. Among the executioner caspases, caspase 3 is considered the most important [62]. It can be activated by any of the initiator caspases i.e. caspase 8, caspase 9 or caspase 10, and in apoptotic cells, cleaved caspase 3 cleaves the inhibitor of the endonuclease CAD (ICAD) to release CAD, which then degrades chromosomal DNA and causes chromatin condensation. In addition, caspase 3 also induces cytoskeletal reorganization and disintegration of the cell into apoptotic bodies [62]. The other branches of the UPR have also been implicated in ER stress-induced intrinsic apoptosis. As indicated in Chapter 1, Section 1.4.2, CHOP which is part of the pPERK/peIF2α pathway promotes the transcription of proapoptotic Bim which helps facilitate MOMP [74], while ATF6 signaling upregulates CHOP during prolonged ER stress, and can therefore also contribute to apoptosis [81].

Another important ER stress-mediated apoptotic pathway occurs through the activation of caspase 12, which predominantly localizes in the ER [75, 133, 134]. Nakagawa et al [133] has shown that caspase 12 is specifically activated in apoptosis caused by ER stress-inducing stimuli, but not in apoptosis caused by membrane- or mitochondrial-targeted signals. In particular, procaspase 12 failed to be activated by apoptosis caused by serum deprivation in PC12 cells, or by apoptosis caused by cyclohexamide, TNF or anti-Fas in W4 cells. However treatment of PC12 cells or embryonic fibroblast cells with ER stressors such as brefeldin A which inhibits ER to Golgi transport, tunicamycin which inhibits *N*-glycosylation in ER, thapsigargin and calcium ionophore A23187 which disrupt intracellular calcium homeostasis, successfully induced cleavage of procaspase 12 [133]. Hitomi et al [135] have also shown that

activated caspase 12 can activate cytoplasmic caspase 3 during ER stress, as both caspase 3 activation and cleavage of procaspase 3 were significantly increased in SK-N-SH cells that stably expressed caspase 12, compared to empty vector cells, when treated with tunicamycin [135].

The goals of this study have been to investigate the effect of tunicamycin and palmitate on apoptosis through caspase activation in L6 rat skeletal muscle cells, and to examine the effect on apoptosis of inhibiting autophagy via chloroquine, as well as inhibiting ER stress through sustaining the peIF2α UPR pathway with salubrinal. To do so, I have used various assays for studying apoptosis such as Western blotting for apoptotic protein markers, MTT cell viability assay and a fluorescence microscopy assay for determining caspase activity. An additional goal of this study was to interpret results in the context of the previous studies described in Chapters 2 and 3 and to elucidate potential links and cross talk between ER stress, autophagy and apoptosis caused by palmitate and tunicamycin in this model of L6 rat skeletal muscle cells.

3.3.2. Results

3.3.2.1. Tunicamycin and palmitate, both stimulators of ER stress, appear to induce apoptosis by activating caspase activity, as evidenced by Western blotting

In my model of L6 skeletal muscle cells, Western blotting indicated that tunicamycin appeared to increase ER-resident caspase 12 at 24h compared to control (Figure 3.15), providing evidence that it may induce an ER-specific apoptosis pathway. It was additionally found that both tunicamycin and palmitate, appeared to increase expression of another apoptotic marker, cleaved caspase 3, compared to control (Figure 3.16). Expression of cleaved caspase 3 may demonstrate a trend towards being greater at the longer time point of 24h than at 4h (Figure 3.16).

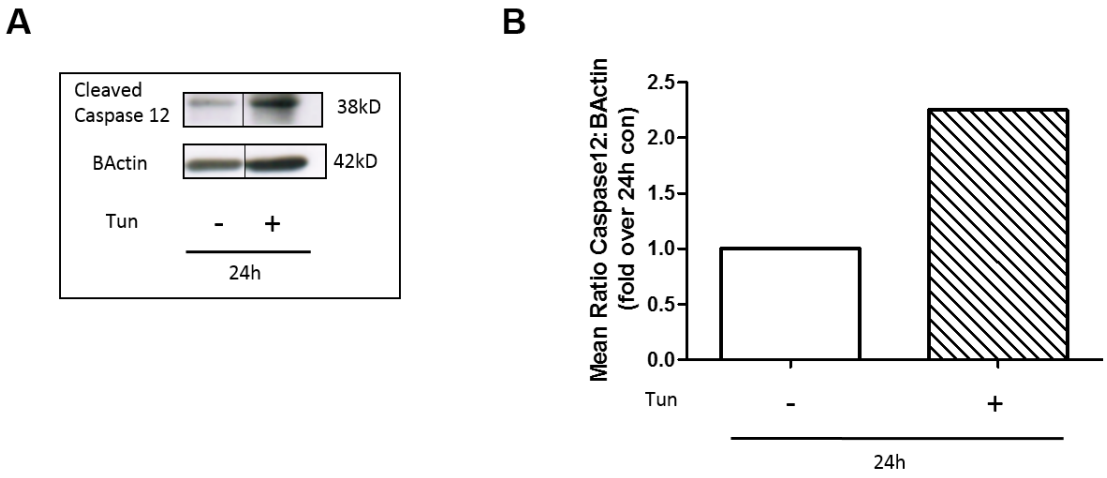

Figure 3.15. Tunicamycin, an inducer of ER stress, may increase caspase 12, as assessed by Western blot.
(A) Western blot image for time point 24h
(B) Graph of Western blot quantification | n=1 | Compared to the control, Tun appears to show greater caspase 12.

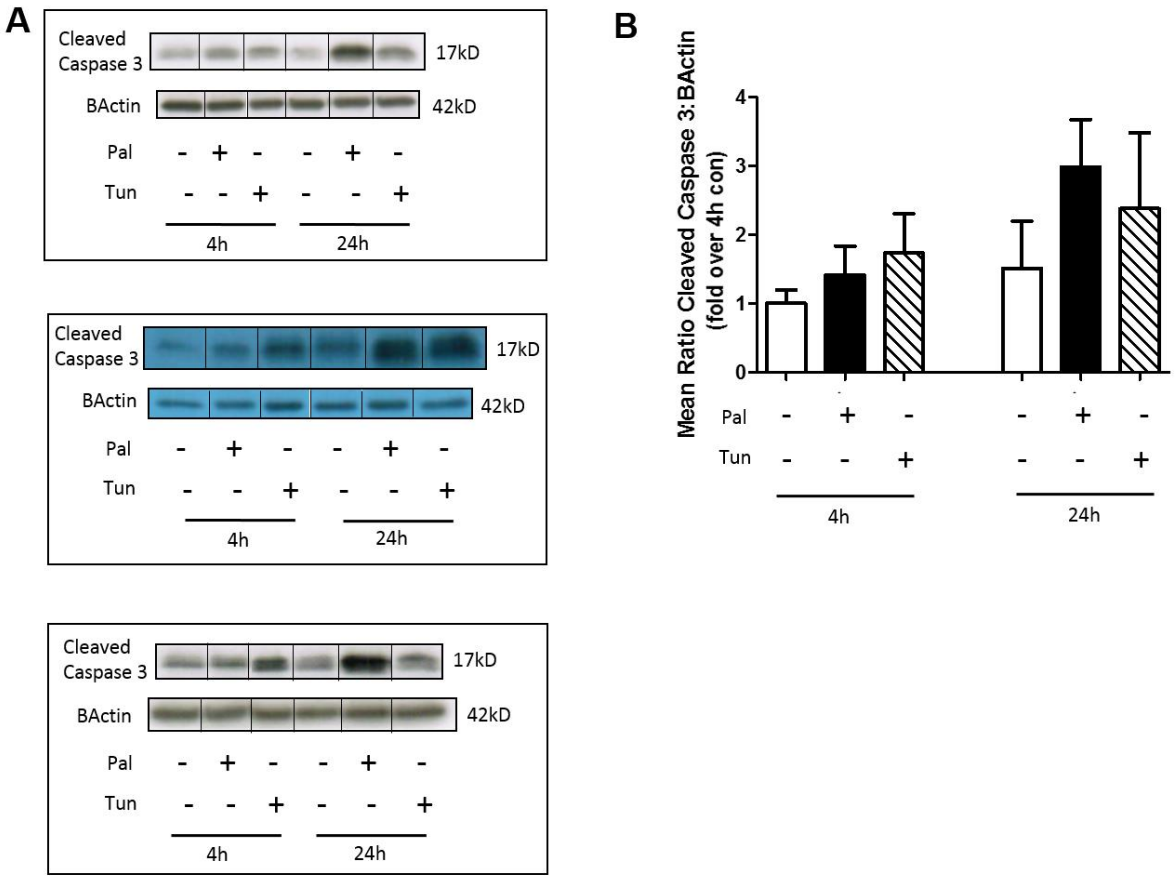

Figure 3.16. Palmitate and tunicamycin, both stimulators of ER stress, demonstrate a trend towards increasing cleaved caspase 3, as assessed by Western blot in L6 wt myotubes.
(A) Western blot images, from individual experiments, for time points 4h, 24h in L6 wt myotubes.
(B) Cumulative graph of Western blot quantification in L6 wt myotubes | n=3 | Compared to the corresponding timed controls, both Pal and Tun may appear to induce apoptosis, as evidenced by apparent increases in cleaved caspase 3. Expression of cleaved caspase 3 may be greater at the longer time point of 24h compared to 4h.

3.3.2.2. Apoptosis induced by palmitate may be exacerbated by inhibiting autophagy with chloroquine, and may be ameliorated by inhibiting ER stress through sustaining peIF2α UPR pathway with salubrinal, as evidenced by caspase activity and MTT cell viability assay

Consistent with Figure 3.16, Western blotting in Figure 3.17 demonstrates that with a 24h treatment, both palmitate and tunicamycin appeared to increase cleaved caspase 3 levels compared to control. However, in addition, Figure 3.17 illustrates that inhibiting autophagy with chloroquine in both control and palmitate conditions may increase cleaved caspase 3 further. Furthermore inhibiting ER stress with salubrinal in the palmitate treatment may decrease cleaved caspase 3 compared to palmitate. This latter difference appears to be most apparent in the upper Western blot image in Figure 3.17A, which is quantified in the upper graph of Figure 3.17B.

L6 wt myoblasts analyzed with caspase 3/7 green detection reagent microscopy appeared to demonstrate similar trends. As evidenced in Figure 3.18, 24h Pal significantly increased the quantity of apoptotic cells i.e. those cells showing green nuclear fluorescence compared to control. Though statistically not significant, representative microscopy images shown in Figure 3.18.A may provide further evidence that inhibiting autophagy with chloroquine in palmitate-treated cells may increase apoptosis further, while inhibiting ER stress with salubrinal in palmitate treatment may decrease apoptosis compared to palmitate. As expected, cells treated with H2O2 as a positive control, showed significantly more apoptosis than the control condition.

Lastly an MTT cell viability assay yielded similar observations. Figure 3.19 illustrates that 24h Pal significantly decreased cell viability compared to control, while inhibiting ER stress with salubrinal in the palmitate treatment significantly increased cell viability compared to palmitate alone. Though not statistically significant, the inhibition of autophagy with chloroquine in the

palmitate treatment appeared to demonstrate a trend towards reducing cell viability further than palmitate. H2O2-treated cells elicited significantly less cell viability than any of the other conditions.

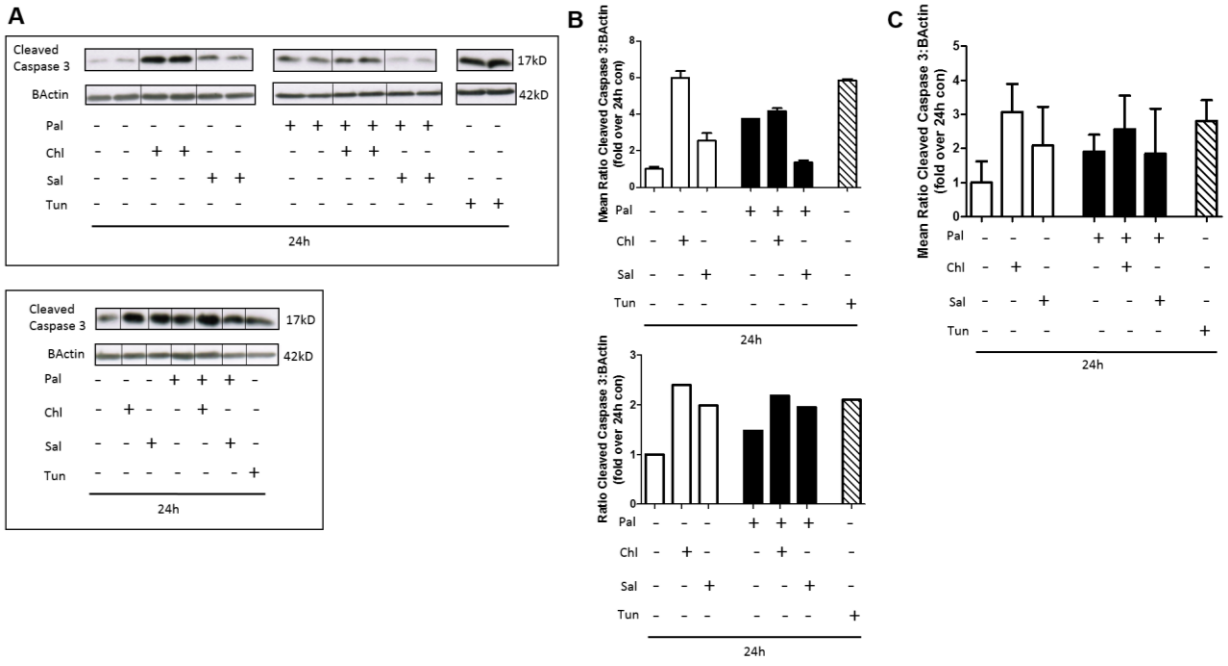

Figure 3.17. Apoptosis in L6 wt myoblasts as assessed by cleaved caspase 3 Western blot
(A) Western blot images, from individual experiments, for time point 24h
(B) Corresponding Western blot quantification graphs for individual experiments shown in (A). In upper graph, data columns illustrate mean±SEM of the duplicates for each condition.
(C) Cumulative graph of Western blot quantification | n=2 | Pal and Tun seem to increase cleaved caspase 3 compared to control. Inhibiting autophagy with Chl in both control and Pal conditions seems to increase cleaved caspase 3 further, while inhibiting ER stress with Sal in Pal treatment appears to decrease cleaved caspase 3 compared to Pal, at least in the upper graph of (B).

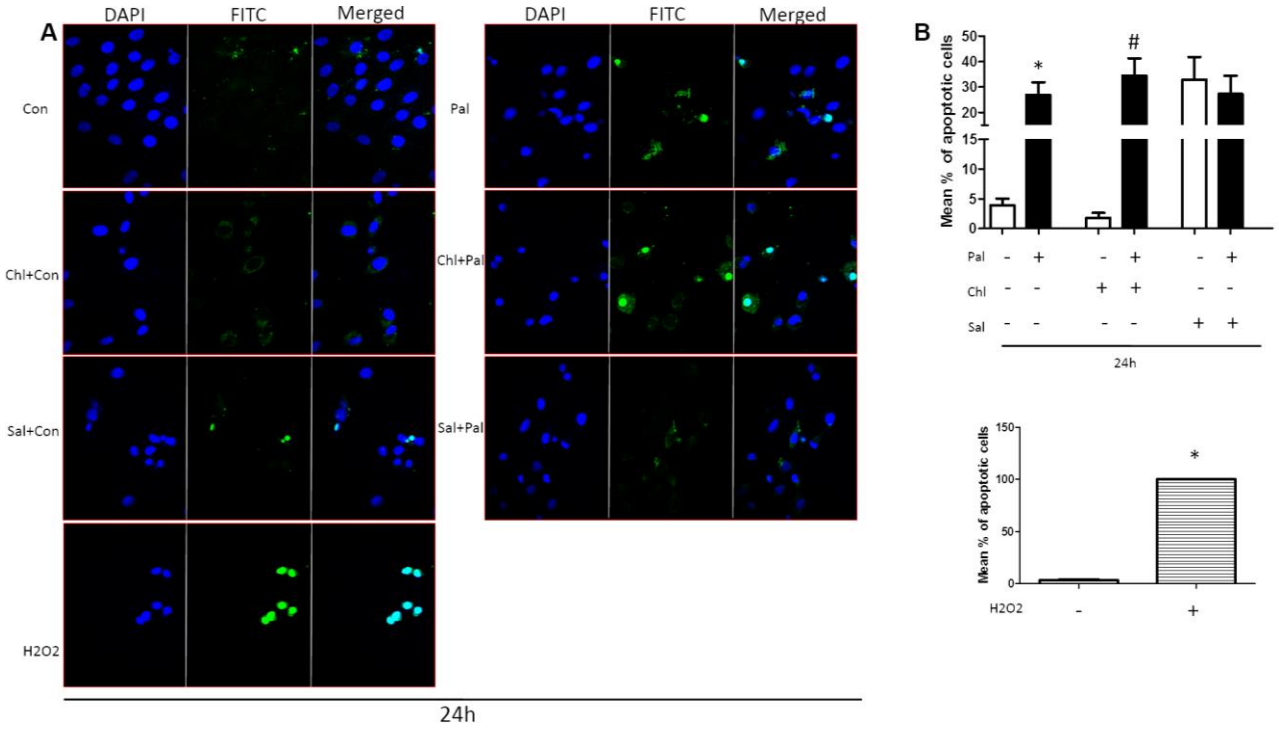

Figure 3.18. Apoptotic cells, as assessed by Caspase 3/7 Green Detection Reagent Microscopy
(A) Representative microscopy images at 24h time point
(B) Quantification of images done by calculating the mean percentage of apoptotic cells exhibiting a nuclear green fluorescence signal | n=3 for con, Pal, Chl+con, Chl+Pal, Sal+con, Sal+Pal; n=2 for H2O2 | 24h Pal significantly increases the quantity of apoptotic cells i.e. those cells showing green nuclear fluorescence compared to 24h Con, as denoted by * ($p<0.05$). Palmitate condition pretreated with chloroquine significantly increases quantity of apoptotic cells compared to control condition pretreated with chloroquine, as denoted by # ($p<0.05$). Statistical analysis done by Kruskal-Wallis test with Dunn's multiple comparison post-hoc test. | Though statistically not significant in the graph, a trend might be demonstrated and visualized in the representative microscopy images that inhibiting autophagy with Chl in Pal treatment seems to increase apoptosis further than Pal, while inhibiting ER stress with Sal in Pal treatment appears to decrease apoptosis compared to Pal. | H2O2 causes significantly more apoptosis than control, as denoted by * ($p<0.05$), analyzed by Mann-Whitney U test.

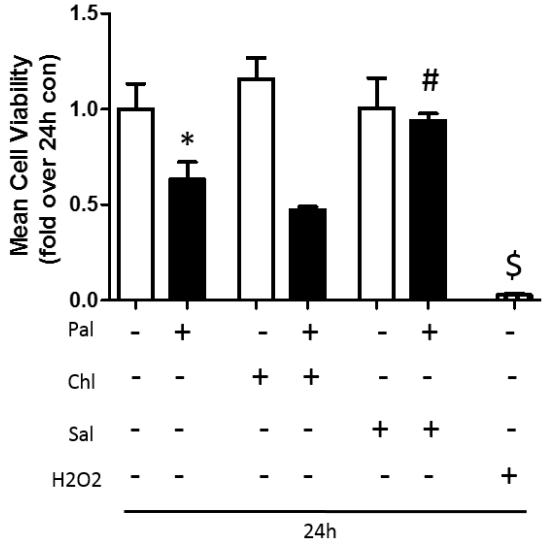

Figure 3.19. Cell viability as assessed by MTT Assay in L6 wt myoblasts | n=4 for con, Pal, H2O2; n=3 for Chl+con, Chl+Pal, Sal+con, Sal+Pal | 24 Pal demonstrates significantly less cell viability than 24h Con, denoted by * ($p<0.05$). Salubrinal pretreatment prior to palmitate significantly increases cell viability, as compared to palmitate, denoted by # ($p<0.05$). H2O2, the positive control for cell death, demonstrates significantly less cell viability than any of the other conditions, denoted by $ ($p<0.05$). Statistical analyses done by Mann-Whitney U test. Though not statistically significant, inhibiting autophagy with chloroquine in palmitate treatment appears to demonstrate a trend towards reducing cell viability further than palmitate.

3.4. Adiponectin Regulates ER stress, Autophagy and Apoptosis

3.4.1. Introduction

As discussed in Chapter 1, Section 1.5, although adiponectin usually circulates in the blood of healthy individuals at high concentrations of between 3-30µg/ml, thereby accounting for approximately 0.01% of total serum proteins [110, 136], its expression and serum levels have been found to be decreased in conditions of obesity [136], type 2 diabetes [99], dyslipidemia [100], cardiovascular disease [101], hypertension [102], cancer [103] and non-alcoholic steatohepatitis [104]. Given the importance that its deficiency has in the pathogenesis of such disorders, much research in the field has focused on upregulating adiponectin action, and has found that it mediates several beneficial effects through its antidiabetic, anti-inflammatory, antiatherogenic, and cardioprotective properties [136]. Now new insights are being gained into how adiponectin may mediate its protective outcomes via regulating the cellular processes of ER stress, autophagy, oxidative stress and apoptosis, and this research will be discussed here.

Liu et al [110] demonstrated that treating high-fat diet (HFD) fed-adiponectin knockout (AdKO) mice with adiponectin attenuated skeletal muscle insulin resistance by stimulating autophagy and antioxidant potential. Increased levels of autophagic proteins LC3II, Beclin 1 and ULK1 were observed, along with a decrease in p62, which indicated upregulation of autophagic flux. In addition, oxidative stress induced by HFD was corrected by adiponectin, while temporal analysis of glucose tolerance and insulin sensitivity using hyperinsulinemic-euglycemic clamp and muscle IRS and Akt phosphorylation demonstrated that AdKO mice with adiponectin replenishment exhibited less HFD-induced insulin resistance than AdKO control mice.

Adiponectin-stimulated autophagy was also found by Nepal et al [137] to have a protective role in reducing apoptosis induced by ethanol in liver cells. In that study in primary rat hepatocytes and HepG2 cells, ethanol suppressed the expression of Atg5, necessary for autophagosome elongation. Adiponectin treatment was demonstrated to restore this and was additionally found to increase p62 degradation in HepG2 cells, which the authors interpreted to indicate completion of autophagic flux. Secondly, siRNA targeting Atg5 was found to significantly inhibit the protective effect that adiponectin had in rescuing HepG2 cells from apoptosis caused by ethanol, as assessed by MTS assay and analysis of caspase 3 activation. Hence autophagy induced by adiponectin was found to protect cells from cytotoxicity.

Amelioration of apoptosis by adiponectin has additionally been demonstrated to occur by downregulation of ER stress. For example, the apoptosis induced by hyperglycemia in human glomerular podocytes was found to be decreased by 10% when adiponectin was administered. This reduction in cell death was accompanied by a downregulation of mRNA and protein expressions of key ER stress-related proteins GRP78, CHOP and caspase 12 [138]. Similarly in Wistar rats exposed to chronic intermittent hypoxia (CIH), cardiac left ventricular dysfunction and myocardial apoptosis were found to be rescued by adiponectin (Ad) treatment as assessed by echocardiograph and TUNEL analysis respectively. Protein expression levels of cleaved caspase 3, cleaved caspase 9 and cleaved caspase 12 were also decreased in the CIH+Ad group. These results correlated with decreased expression of GRP78, CHOP and reactive oxygen species (ROS), thereby indicating that adiponectin protected against cardiac dysfunction and apoptosis by inhibiting ROS-dependent ER stress [139].

Therefore, it is evident that a rapidly growing body of literature has begun to characterize the role of adiponectin in regulating autophagy, ER stress and apoptosis. The goals of this study

were to examine the hypothesis that adiponectin upregulates autophagy, and downregulates ER stress and apoptosis, and to determine the relationships between regulation of these processes by adiponectin in my model of L6 rat skeletal muscle cells.

3.4.2. Results

3.4.2.1. Adiponectin appears to increase autophagy, as evidenced by apparent increased autophagosome formation and lysosome activity

Figure 3.20 shows that fAd appears to increase the expression of LC3II, a key autophagosome marker, compared to control at both 1h and 2h. However, p62 levels appear approximately the same across all conditions. Figure 3.21 demonstrates that in independent experiments for time points 4h and 24h, the addition of fAd in the control condition as well as in the palmitate treatment, appears to increase lysosomal activity compared to the non-fAd control and the non-fAd palmitate, as evidenced by apparent increased red fluorescence of active cathepsin B enzyme. These results collectively indicate that adiponectin may stimulate autophagic flux by increasing autophagosome formation and lysosome activity.

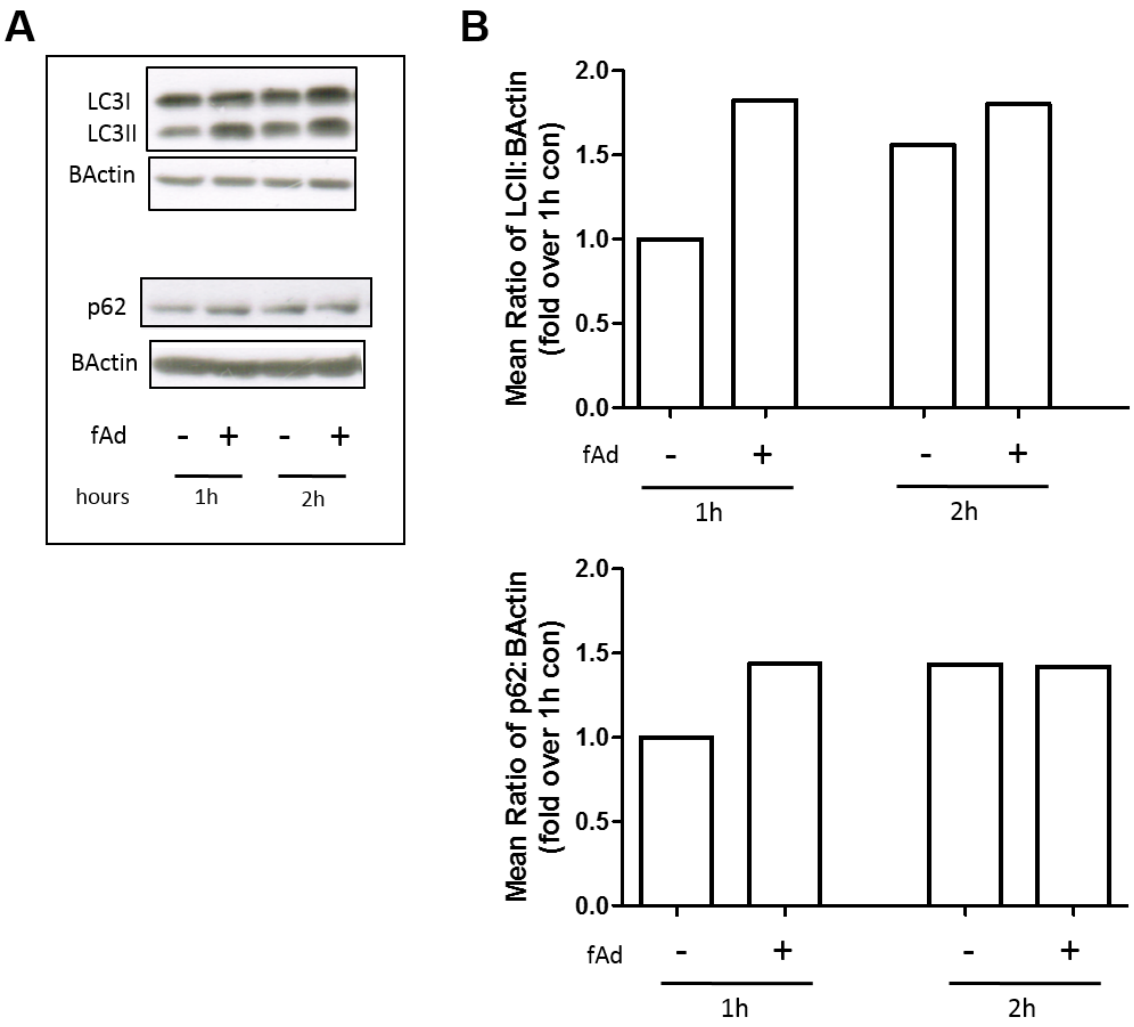

Figure 3.20. Analysis of autophagic flux markers, LC3II and p62 by Western blot
(A) Western blot image for L6 wt myoblasts for time points 1h, 2h
(B) Quantification graph of Western blot shown in (A) | n=1 | fAd appears to increase LC3II compared to control, which corresponds to an increase in autophagosome formation.

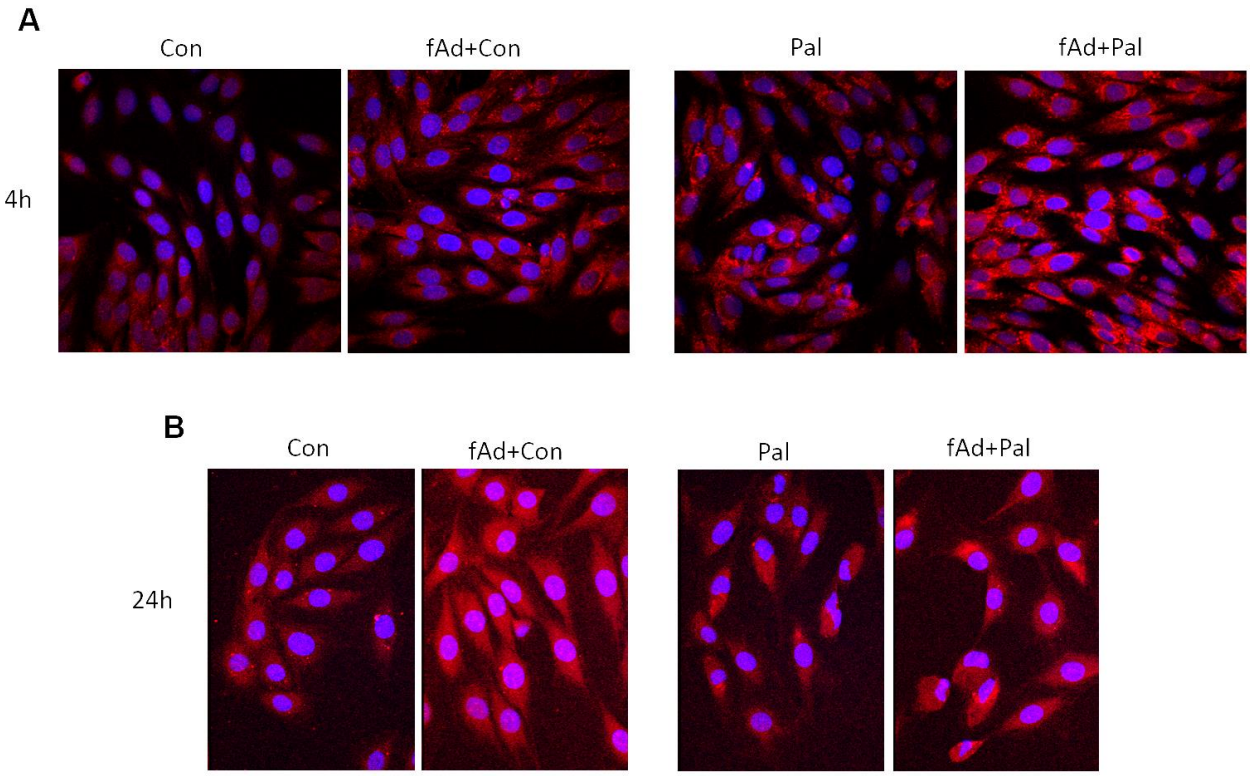

Figure 3.21. Adiponectin appears to stimulate autophagy as evidenced by Magic Red Cathepsin B Assay microscopy
(A) Microscopy images for time point 4h | n=1 | fAd pretreatment prior to both 4h Con and 4h Pal appears to increase lysosomal activity compared to 4h Con and 4h Pal
(B) Representative images for time point 24h | n=4 | fAd pretreatment prior to both 24h Con and 24h Pal appears to increase lysosomal activity compared to 24h Con and 24h Pal.

3.4.2.2. Adiponectin appears to reduce ER stress induced by palmitate, as evidenced by apparent decreased cellular protein aggregation and GRP78mcherry expression

Figure 3.22A demonstrates that fAd pretreatment prior to 24h Pal appears to reduce the amount of protein aggregation visualized via ThT assay compared to 24h Pal. In keeping with results from Chapter 2, spectrometry analysis of ThT fluorescence (Figure 3.22B) illustrates that 24h Pal significantly increases protein aggregation compared to control. It is observed that 24h fAd also significantly increases protein aggregation compared to control. When fAd is added as a pretreatment to 24h Pal, it appears to blunt the protein aggregation caused by palmitate. Furthermore, Figure 3.23 shows that fAd pretreatment prior to 24h Pal significantly decreases the red fluorescence of the GRP78mcherry reporter construct compared to 24h Pal. Collectively, these results may indicate that fAd may reduce ER stress.

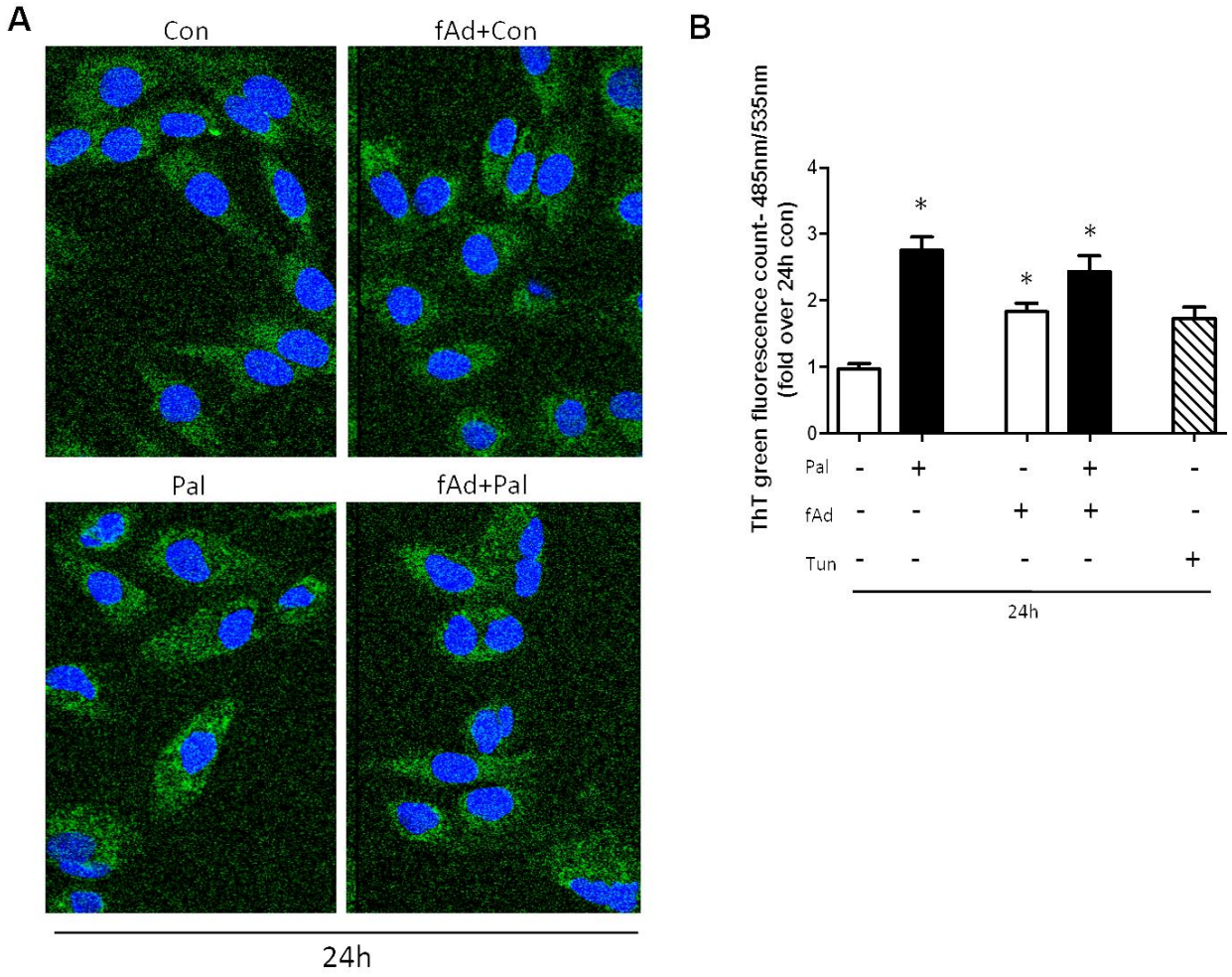

Figure 3.22. Adiponectin may demonstrate a trend towards reducing protein aggregation caused by palmitate's induction of ER stress, as assessed by ThT Assay
(A) Representative image for ThT Microscopy in L6 wt myoblasts | 24h | n=1 | fAd pretreatment prior to 24h palmitate may be seen to demonstrate a trend towards reducing green fluorescence of ThT, indicating protein aggregation, compared to 24h palmitate
(B) ThT Spectrometry graph from L6 wt myotubes | 24h | n=6 for con, Pal; n=4 for fAd, fAd+Pal; n=5 for Tun | 24h palmitate significantly increases protein aggregation compared to control, denoted by * ($p<0.05$). fAd pretreatment prior to both control and palmitate significantly increases protein aggregation compared to control, denoted by * ($p<0,05$). Though not statistically significant, a trend towards a slight decrease in protein aggregation may be observed between the palmitate condition and palmitate pretreated with fAd. Statistical analysis done by one-way ANOVA with Tukey's post hoc test. Normal distribution verified by Kolmogorov-Smirnov and Shapiro Wilk tests.

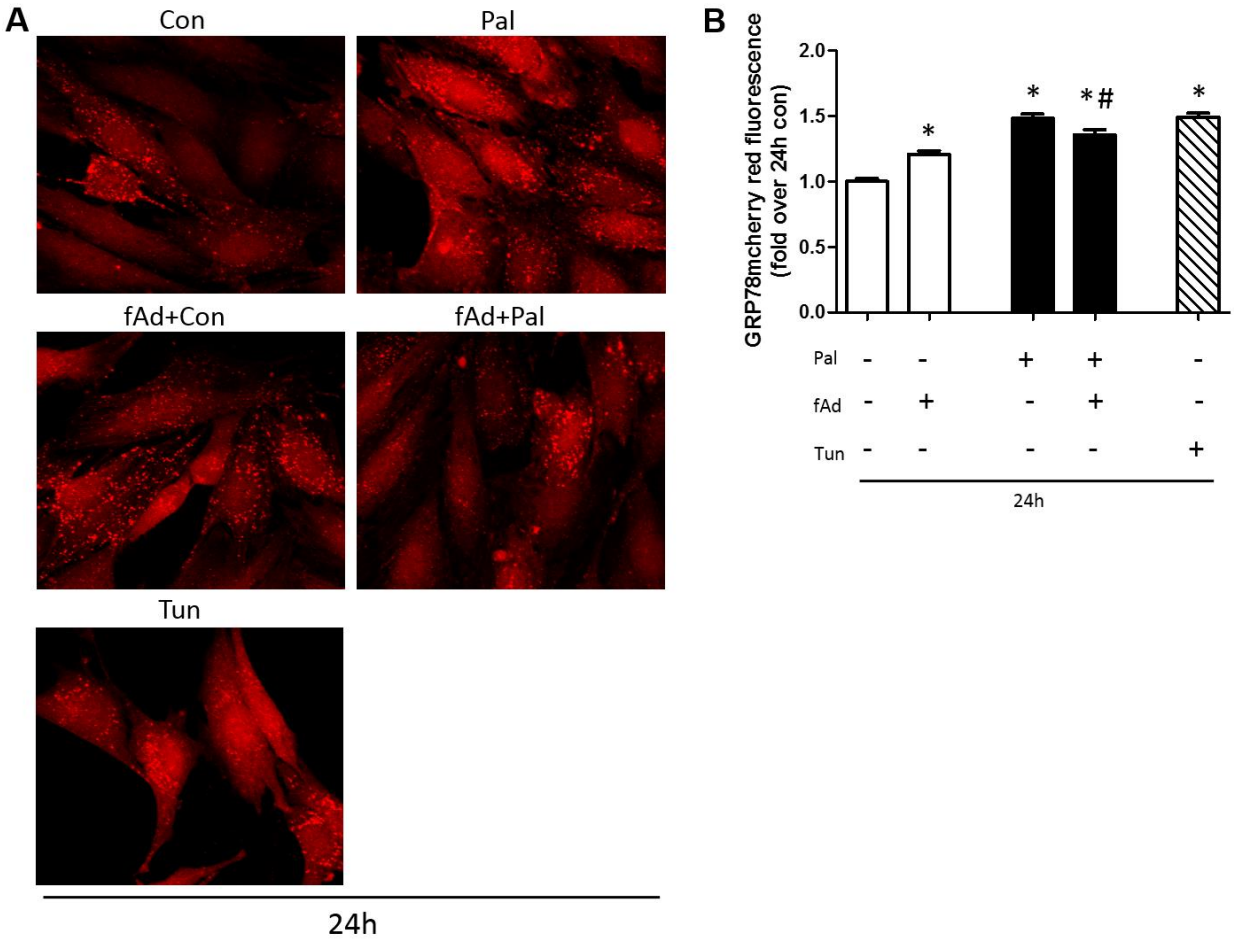

Figure 3.23. Adiponectin reduces GRP78mcherry expression in palmitate condition, providing evidence that it may reduce the ER stress induced by palmitate
(A) Representative image for GRP78mcherry microscopy
(B) Quantification graph of GRP78mcherry microscopy using Image J software. Each column represents the mean of 30-50 cells | 24h | n=3 | 24h palmitate and 24h tunicamycin significantly increase overall red fluorescence of GRP78mcherry reporter construct compared to 24h control, denoted by * ($p<0.05$). fAd pretreatment prior to both control and palmitate significantly increases overall red fluorescence compared to 24h control, denoted by * ($p<0.05$). fAd pretreatment prior to palmitate significantly decreases red fluorescence compared to palmitate, as denoted by # ($p<0.05$). | Statistical analysis done by Kruskal-Wallis test with Dunn's multiple comparison post-hoc test.

3.4.2.3. Adiponectin reduces apoptosis induced by palmitate, as assessed by Caspase 3/7 Green Detection Reagent Microscopy

It can be observed in Figure 3.24, that while 24h Pal significantly increases the mean percentage of apoptotic cells compared to the control ($p<0.05$), fAd pretreatment prior to 24h Pal significantly decreases the quantity of apoptotic cells compared to 24h Pal.

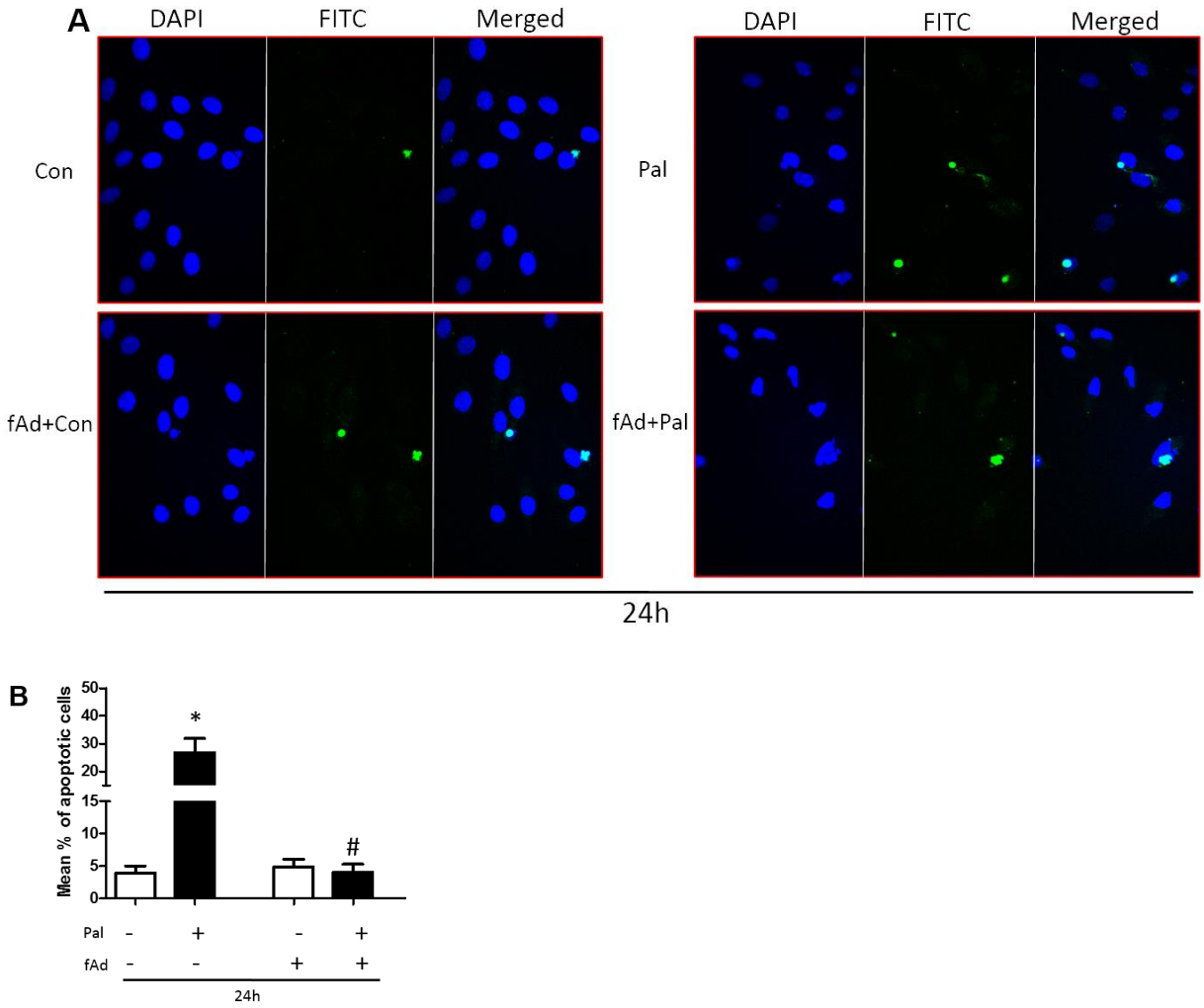

Figure 3.24. Adiponectin reduces apoptosis caused by palmitate, as assessed by Caspase 3/7 Green Detection Reagent Microscopy
(A) Representative microscopy images
(B) Quantification of images done by calculating the mean percentage of apoptotic cells exhibiting a nuclear green fluorescence signal | 24h | n=3 | Pal significantly increases quantity of apoptotic cells compared to control, denoted by * ($p<0.05$). fAd pretreatment prior to Pal significantly decreases the quantity of apoptotic cells, compared to Pal, denoted by # ($p<0.05$). Statistical analyses done by Mann-Whitney U test.

Chapter 4: Discussion

4.1. Effect of Palmitate on ER Stress and Autophagy

The direct link between obesity-induced lipotoxicity and ER stress has been well described [140], with several articles showing that saturated fatty acids like palmitate cause protein accumulation [43] and upregulation of UPR protein markers [44, 45, 47]. My studies also support these findings, as palmitate treatment was seen to significantly increase protein aggregation and GRP78 chaperone expression, while also significantly increasing the UPR protein peIF2α at the 24h time point. ThT analysis of protein aggregation, used initially in studies of Alzheimer's disease where the dye provided visualization of B-sheets [141], was first described as a new tool for investigating ER stress induced by thapsigargin in Beriault & Werstuck [36]. Here I have shown that it may be used effectively to study and quantify ER stress induced by saturated fatty acids like palmitate in skeletal muscle cells.

As discussed earlier in Section 2.1, there has been some conjecture in the field regarding whether conditions of high-fat, obesity and lipotoxicity stimulates [58, 125] or inhibits [126] autophagic flux. My studies appear to support the former assertion, as apparent increases in LC3II expression, along with an increase in lysosomal activity are evident in palmitate conditions. In addition, though quantitative analysis for the LC3 immunofluorescence assay is required, the images may visually show an increase in autophagosome formation, evidenced by an increase in green puncta in palmitate conditions. Indeed, autophagy has been shown to become activated in response to moderate lipid overload in the cell where it specifically targets lipids for degradation through lipophagy [58], or it has also been shown to be activated in response to fatty-acid induced-protein overload to help rid the cell of excess proteins [44]. It may

be noted from the LC3 immunofluorescence images that nuclei appeared green, and this was found not be an artifact of microscopy imaging caused by potential bleed through of DAPI and simultaneous excitation of both blue and green wavelengths, as an additional experiment was performed that demonstrated that even when DAPI staining was absent, the nuclei still fluoresced green. This might indicate a true presence of LC3 in nuclei, as corroborated by Martinez-Lopez & Singh [142] who propose the role of autophagic structures as nuclear scaffolds for MAPK phosphorylation.

4.2. ER Stress May Induce Autophagy as a Rescue Mechanism

The sequential link between ER stress and autophagy proposed previously in the literature [76], appeared to be confirmed in this study using L6 skeletal muscle cells. First, ER stress induced by tunicamycin was found to correspond to an apparent upregulation of LC3II and an apparent decrease in p62 by Western blotting. Furthermore, after 4h, an apparent increase in lysosomal activity was indicated by cathepsin B enzyme activity. The increase in autophagic stimulation observed after ER stress is well supported in the field as studies utilizing ER stressors thapsigargin, tunicamycin and polyglutamine 72 (PolyQ72) aggregates have shown increased conversion of LC3I to LC3II[39, 75, 127, 129]. Additionally, ER stress induced by hypoxia-ischemia in neonatal rats showed increased expression in brain tissue of not only LC3 II, but also Beclin 1, another protein involved in autophagosome assembly. Enhancing autophagy in these animals with rapamycin significantly reduced ER stress proteins GRP78 and CHOP, thereby indicating that autophagy may act to alleviate ER stress [143].

I also found that pretreatment with salubrinal in both control and palmitate conditions appeared to increase cathepsin B lysosomal activity. These findings indicate that autophagy

may be upregulated as a part of UPR downstream adaptive signaling, specifically by sustained phosphorylation of eIF2α and prolonged activation of its pathway by salubrinal. This is in keeping with reports such as Kouroku et al [75] that demonstrated that the PERK/eIF2α pathway has an imperative role in the induction of autophagy. In C2C5 cells, stimulated to undergo ER stress by PolyQ, eIF2α phosphorylation was demonstrated to upregulate Atg12 mRNA and protein, which was necessary for Atg5-Atg12-Atg16 complex-dependent LC3I to LC3II conversion. In addition, when the PERK/peIF2α pathway was inhibited, by either an eIF2α A/A mutation which replaced a phosphorylatable Ser51 with Ala51, or by using a dominant-negative PERK, PolyQ72-induced LC3 conversion was inhibited [75].

Lastly, exacerbation of ER stress upon impairment of autophagy was demonstrated in this study and provided further evidence for the protective role that autophagy plays in ameliorating ER stress. There was greater apparent accumulation of protein aggregates, as indicated by ThT Assay, and significantly greater peIF2α expression, as indicated by Western blotting, in ATG5K130R compared to EV cells. In control and palmitate conditions pretreated with chloroquine, significantly greater expression of GRP78mcherry reporter construct was observed than in control or palmitate alone. These results all indicated that with an impairment in the autophagic pathway, either induced in the early stage with defective ATG5K130R protein or in the later stage with chloroquine, ER stress may have become aggravated. Undegraded proteins appeared to accumulate more in the absence of the autophagic degradative outlet and the UPR was found to be upregulated. These findings are in line with studies such as Kouroku et al [75] which similarly found that Atg5 deficiency increased the number of C2C5 cells showing polyQ72 aggregates. Carloni et al [143] reported that the decrease in expression of GRP78 observed when hypoxic-ischemic neonatal rats were treated with rapamycin, an autophagy inducer, was completely reversed when they were exposed to 3-MA, an autophagy inhibitor.

4.3. Prolonged, Excessive, or Uninhibited ER Stress Induces Apoptosis

In this study of L6 rat skeletal muscle cells, my data suggested that apoptosis caused by tunicamycin occurred, at least in part, specifically through ER stress. This is based on results showing that tunicamycin appeared to increase expression of the ER-resident caspase 12 by Western blot. Caspase 12 has been shown to be activated only in apoptosis caused by ER stress-inducing stimuli such as tunicamycin, and loss of caspase 12 has been shown to inhibit ER stress-mediated apoptosis [133]. Tunicamycin effectively induces ER stress, as it blocks *N*-glycosylation, thereby leading to accumulation of unfolded glycoproteins in the ER [38], and it has previously been shown to induce caspase 12 activation in several cell types and models [133, 144, 145], therefore supporting my findings here.

Additionally, both tunicamycin and palmitate were found in this study to apparently increase the expression of cleaved caspase 3, an executioner caspase. Furthermore, palmitate significantly increased the mean percentage of apoptotic cells, assessed by microscopy using caspase 3/7 green detection reagent assay. This is in keeping with results from various reports that have shown similar upregulation of caspase 3 by tunicamycin and palmitate [44, 146]. It is of interest that some research in the field has indicated that caspase 3 might be activated by caspase 12 in response to ER stress. As discussed previously, Hitomi et al [135] has demonstrated that when treated with tunicamycin, cleavage of procaspase 3 was significantly increased in SK-N-SH cells that stably expressed caspase 12 compared to empty vector cells [135]. In addition, Morishima et al [147] has shown that in C2C12 cells, recombinant caspase 12 cleaves and activates procaspase 9, since mutation of specific Asp residues in the proscaspase 9 polypeptide significantly reduced cleavage by caspase 12. Active caspase 9 is then noted to catalyze the cleavage of procaspase 3 [147]. Hence, it is possible that the caspase 3 apoptotic

signaling apparently induced by palmitate and tunicamycin in the current model of L6 rat skeletal muscle cells may originate from ER stress-mediated caspase 12 apoptotic signaling.

When autophagy was inhibited with chloroquine in combination with palmitate treatment, cleaved caspase 3 expression appeared to be increased. The quantity of apoptotic cells visualized by localization of green fluorescence in nuclei also showed an apparent increase, and cell viability assessed by MTT assay showed an apparent decrease. This may be because with the impairment in the autophagic pathway induced by chloroquine, ER stress caused by palmitate as evidenced from results in Chapter 2, may be too much for the cell to cope with. The inhibition of autophagic flux would reduce the amount of proteins that could be degraded and would instead exacerbate ER stress, therefore inducing ER-stress mediated apoptosis. This suggestion is supported by studies like Xu et al [148] which demonstrated that while cisplatin treatment in HeLa cells normally induced degradation of ubiquitinated proteins by autophagy, thus reducing ER stress-induced apoptosis and the mitochondrial pathway of apoptosis, inhibition of autophagy with 3-MA or chloroquine upregulated the quantity of intracellular misfolded proteins, thereby increasing apoptosis [148]. An additional reason why inhibiting autophagy in palmitate treatment, might enhance apoptosis, might have to do with the downregulation in mitophagy that would follow. As discussed in Chapter 1, Section 1.4.3.1, cellular stressors may damage mitochondria and induce MOMP, releasing various proapoptotic factors into the cytoplasm. However the output of these proapoptotic factors might be decreased through mitophagy, a sub-type of autophagy that selectively targets damaged mitochondria for degradation [84, 85]. Since palmitate has been known to damage mitochondria in various ways such as by direct effects such as dissipating the mitochondrial transmembrane potential and causing the release of soluble apoptotic factors [149], by causing mitochondrial reactive oxygen species generation [47], and by converting to ceramide and inhibiting mitochondrial respiratory

chain complexes I and III [67], the inhibition of mitophagy by any autophagic inhibitor may indeed increase apoptosis.

The inhibition of ER stress through the maintenance of the activity of the peIF2α pathway of the UPR with salubrinal, appeared to decrease apoptosis as evidenced by caspase 3 Western blot, caspase 3/7 microscopy images and MTT cell viability assay. This might be because, as indicated in Chapter 3, section 3.4, the continued phosphorylation of eIF2α facilitated by salubrinal, may enable the continued activation of cytoprotective autophagy. This is possible because the activated peIF2α pathway upregulates Atg12 mRNA and protein, which plays a role in Atg5-Atg12-Atg16 complex-dependent LC3I to LC3II conversion, a central step in the induction of autophagy [75].

Collective consideration of the results of Chapters 2, 3 and 4 may elucidate a key trend – that prolonged exposure to palmitate or tunicamycin induces ER stress, and in the absence of an adequate autophagic protective mechanism, apoptotic signaling might be induced. As evidenced in Chapter 2 findings, a longer exposure of 48h to palmitate and tunicamycin significantly increased GRP78mcherry expression compared to 24h, and in addition, the expression of peIF2α by Western blotting appeared to increase over time i.e. from 4h to 24h exposure to palmitate. While ER stress seemed to increase over time, autophagy only appeared to be upregulated in the relative short term. As illustrated in Chapter 2, cathepsin B activity, indicative of lysosomal activity, was significantly enhanced at 4h and 24h Pal, but not 48h Pal, compared to corresponding controls. This enzyme activity also decreased with prolonged exposure to palmitate, showing significant reductions from 4h to 24h to 48h. With tunicamycin treatment, at 4h, the cathepsin B activity appeared greater compared to control, while 24h Tun did not elicit much difference from its control. With regards to apoptosis, it appeared that greater expression of cleaved caspase 3 induced by palmitate and tunicamycin, occurred at the longer

exposure time of 24h than at 4h. These results appear to indicate that autophagy may act acutely to rescue ER stress, but with prolonged ER stress, autophagy may not be able to cope anymore and apoptosis may take over. As noted in Chapter 1, Section 1.4.3.2, once apoptosis is underway, its caspase activity may in fact inactivate the autophagic pathway through digestion of essential autophagy proteins [91]. Several examples in the literature support this line of thinking. Gonzalez-Rodriguez et al [150] has shown that treatment of Huh7 human hepatic cells with palmitate for 8h activated both the UPR and autophagic flux, but a longer treatment for 24h induced ER stress and cell death, while inhibiting autophagic flux. Similarly, in HepG2 cells treated with thapsigargin to induce ER stress and rapamycin to induce autophagy, it was found that with a shorter exposure to thapsigargin for 2h, autophagy was adaptively upregulated to decrease stress levels, and increase cell viability. This was evidenced by an increase in LC3I to LC3II conversion. However with a longer 24h exposure to thapsigargin, autophagy became inhibited, as evidenced by an increase in p62, while apoptosis was upregulated, as evidenced by induction of PARP cleavage and reduction in procaspase 3 [151].

4.4. Adiponectin Regulates ER Stress, Autophagy and Apoptosis

As supported by the literature described previously, that demonstrates that adiponectin increases autophagic flux [110, 137], the results of this study illustrated that L6 wt myoblasts treated with adiponectin, appeared to have increased LC3II expression compared to control cells at both 1h and 2h. In addition, adiponectin in both control and palmitate conditions for 4h and 24h, appeared to increase lysosomal activity as evidenced by apparent increased lysosomal protease cathepsin B activity. Liu et al [110] provides specific corroboration for these trends, as in cultured L6 myoblasts, increased LC3II expression and increased lysosomal enzyme activity were found to be facilitated by adiponectin in an AMPK-dependent manner.

Adiponectin's apparent effect in decreasing ER stress induced by palmitate, evidenced by apparent reduced protein aggregation and significant reduced GRP78 expression, is supported by studies [138, 139] that show similar decreases in GRP78 expression as well as decreases in more downstream markers of ER stress-induced apoptosis, namely CHOP and caspase 12, after adiponectin intervention. In addition, adiponectin's role in attenuating ER stress was further extended by Guo et al [152] who showed that it conferred resistance to ER stress and cardiomyocyte injury induced by ischemia/reperfusion in rats by modulating ER Ca^{2+}-ATPase (SERCA) activity via activation of PI3K/Akt signaling [152]. The same study also found that adiponectin reduced expression of GRP78, CHOP and caspase 12, which had been upregulated by hypoxia/reoxygenation and thapsigargin [152]. However it was also observed that adiponectin added to the control condition increased protein aggregation. Such an effect of adiponectin has been previously unreported in the literature and the significance of such a finding remains unknown.

The protective effect of adiponectin in guarding against apoptosis was demonstrated by the significant reduction in quantity of cells exhibiting caspase 3/7 activity in the palmitate condition pretreated with adiponectin, compared to palmitate alone. Several studies have shown that adiponectin may mediate its cytoprotective effect by upregulating autophagy and decreasing oxidative and ER stress [137, 138, 139, 117, 152]. In addition, an interesting study by Lin et al [153] demonstrated further insights into how adiponectin's stimulation of autophagy might mediate its cytoprotective effects. Liver cells of AdKO mice and primary hepatocytes, stressed with acetaminophen overdose, demonstrated aggravated mitochondrial dysfunction and damage, oxidative stress and necrosis. However administration of adiponectin was found to stimulate autophagosome formation in an AMPK-dependent manner, which led to the increased degradation of damaged mitochondria via mitophagy. Accumulation of ROS was also reduced, as were other indicators of mitochondrial damage such as serum mtDNA levels,

phosphorylation of mitochondrial JNK, and dysfunction of mitochondrial respiratory chain complexes [153].

Therefore, in my study it may be concluded that adiponectin pretreatment prior to palmitate, may mediate beneficial effects by upregulating autophagy. Such an outcome would be adaptive as autophagy may rescue palmitate-induced ER stress and protein accumulation as demonstrated in Chapter 3, and therefore ameliorate ER stress-induced apoptosis as was discussed in Chapter 4. As suggested by the literature described previously, adiponectin may bring about these results by decreasing expression of ER stress-related proteins GRP78, CHOP and caspase 12 [138, 139, 152], in addition to potentially stimulating removal of damaged mitochondria through mitophagy [153] and downregulating activation of caspase 3 [139]. Indeed the current study showed an apparent increase in autophagy, accompanied by apparent decreases in GRP78 expression and activity of caspase 3/7. In addition to boosting the n number of the current preliminary data, analysis of CHOP, caspase 12 and mitophagy markers could be conducted in future experiments to further investigate these mechanisms.

Chapter 5: Summary

5.1. Overview of Results

The research presented in this project may extend our understanding of the effects of palmitate-induced lipotoxicity in L6 rat skeletal muscle cells. Though some of the data requires a higher number of experiments to confer statistical significance, there are noticeable trends that emerge from combined consideration of the various experiments and assays conducted so far which build a case for the conclusions made. In particular, I have elucidated the mechanisms involved in the cross talk between ER stress, autophagy and apoptosis (Figure 5.1). I have shown that palmitate induces excessive protein accumulation in the cell, thereby causing ER stress and activation of the UPR. Autophagy may be recruited as a compensatory mechanism downstream of phosphorylation of PERK/eIF2α in the UPR, to help the cell cope with the stress induced by protein overload through its degradative pathway. However when stress levels exceed the adaptive capabilities of the cell, apoptotic signaling may overwhelm the system and inhibit protective outputs such as autophagy, leading the cell to its demise. Additionally, adiponectin may play a facilitatory role in ameliorating these processes, as I have shown that it may increase autophagic flux and contribute to beneficial cellular cytoprotective effects of reducing ER stress and apoptosis.

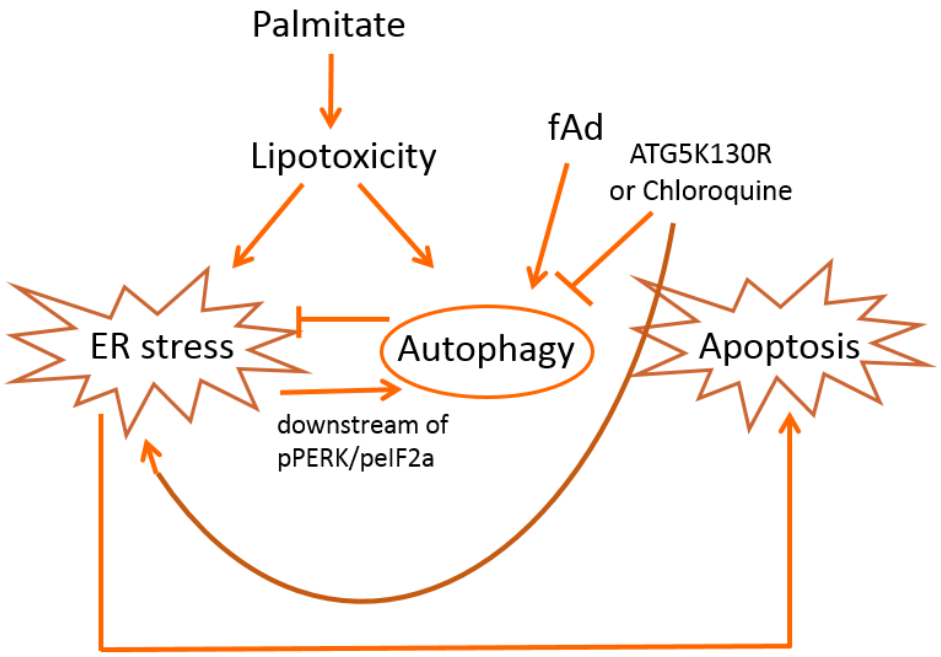

Figure 5.1. Effect of palmitate-induced lipotoxicity on ER stress, autophagy and apoptosis and regulation by adiponectin in L6 skeletal muscle cells. Palmitate induces ER stress and activation of the UPR. Autophagy may be recruited as a compensatory mechanism downstream of phosphorylation of PERK/eIF2α in the UPR, to inhibit EFpeR stress. However if autophagy is inhibited through the use of molecular or pharmacological approaches, such as using ATG5K130R dominant negative mutant or chemical inhibitor chloroquine, and/or ER stress exceeds the adaptive capabilities of the cell, apoptotic signaling may be induced. Adiponectin may stimulate autophagy and therefore ameliorate the processes of ER stress and apoptosis.

5.2. Future Directions

Lipotoxicity in skeletal muscle has long been established to contribute to the development of insulin resistance and impairment of glucose metabolism that is characteristic in metabolic disorders such as type 2 diabetes and obesity [23, 154], and recent studies have now been exploring the role of lipotoxicity-induced ER stress [47, 155], autophagy [110] and apoptosis [71] in mediating these metabolic effects. Hence I would be most interested in furthering the scope of my project to verify the effect of palmitate and adiponectin intervention on insulin-signaling and glucose uptake, which previous studies have shown are inhibited in conditions of obesity [12, 22, 23]. I would perform Western blots for key proteins involved in intracellular insulin signaling such as IR (insulin receptor), phospho IRS (Y612; phosphorylation of insulin receptor substrate) and phospho Akt (S473 and T308) [23, 110]. Glucose uptake and GLUT4 translocation would be measured as described in Fang et al [117].

Another important cellular process, oxidative stress with its contingent production of free radicals and impaired antioxidant defence [156], has been implicated in the pathogenesis of skeletal muscle insulin resistance and mitochondrial dysfunction induced by lipotoxicity [157], and adiponectin has been shown to regulate this [110]. Investigating the effects of palmitate and adiponectin in L6 rat skeletal muscle cells on the levels of major anti-oxidative enzymes such as superoxide dismutase, catalase and glutathione peroxidase, using assays established in our lab and described in Liu et al [110], would provide a valuable perspective on the progression of metabolic dysfunction observed in diabetes and obesity. It would also be of interest to study the cross talk between oxidative stress, ER stress, autophagy and apoptosis in a lipotoxic skeletal muscle model, to further insights provided by other studies in the field that have linked these processes [158, 159]. To do this, I would again use methods that have been recently developed in our lab. As tunicamycin and palmitate have been shown in my studies to elicit apparent

increases in ER stress, autophagy and apoptosis, I would check if these increases might be accompanied by increased oxidative stress as detected by CellROX Deep Red reagent and CellROX Green reagent (Life Technologies) that are fluorogenic, cell-permeant dyes which exhibit enhanced fluorescence upon oxidation by reactive oxygen species. In addition, the use of inhibitors, chloroquine for autophagy and N-acetyl-cysteine for oxidative stress, would show whether the inhibition of one process has any effects on the upregulation or downregulation of the other processes, and thereby help discern mechanistic relationships between them.

As it is established that lipotoxicity mediates harmful effects to the cell through ER stress and oxidative stress, which damage mitochondria and thereby induce apoptosis, the study of mitophagy, the selective degradation of damaged mitochondria by autophagy, has come to be recognized as an important protective mechanism for the cell [84, 85]. Mitophagy increases adaptive turnover of aberrant mitochondria, reduces abnormal mitochondrial functioning and inhibits the release of proapoptotic factors such as AIF, EndoG, SMAC and cytochrome *c* into the cytoplasm [84, 85, 158]. Hence verifying whether mitophagy specifically is upregulated in L6 skeletal muscle cells by palmitate and adiponectin, rather than simply generic macroautophagy, would help to further flesh out the findings of this project. To this end, I would conduct Western blotting for key proteins necessary for mitophagy, such as Pink1 and Parkin, which are involved in priming damaged mitochondria for selective autophagic recognition, transmission electron microscopy (TEM) analysis to visualize the stages of mitophagy such as the early stage which would be recognizable by the double membraned autophagosomal structure containing mitochondria detectable by their characteristic cristae, and fluorescence microscopy in which colocalization could be observed between mitochondria discernable by MitoTracker and autophagosomes discernable by GFP-LC3 [160].

In addition to the courses of study outlined above that could be pursued to broaden the scope of this project, other specific assays that have been recently established in our lab, could be conducted to gain further insight into the current observations that have been made in this thesis report. Microscopy work could be extended in the following ways: transmission electron microscopy (TEM) analysisis still regarded as a gold standard in studying autophagy and would enable visualization of autophagosomes during autophagy. TEM can also detect additional features of the cell architecture, such as extension and swelling of the rough endoplasmic reticulum during ER stress [44]. Specific analysis of autolysosomes could be achieved using a compound consisting of fluorescent BODIPY dye conjugated to bovine serum albumin (DQ-BSA) that is self-quenched, but when engulfed by the cell and proteolysed by lysosomal proteases, becomes dequenched and releases brightly fluorescent protein fragments. The use of DQ-BSA in conjunction with immunofluorescence of p62, a characteristic autophagic marker described previously, would enable detection of the actively degradative autolysosome, through demonstration of the convergence between an autophagic compartment and functional lysosome[161]. Autophagic flux could be examined in more depth using the L6 skeletal muscle cell line stably overexpressing RFP/GFP-LC3. In this approach, GFP but not RFP, would be sensitive to quenching by the acidic environment of the autophagolysosome. Completion of autophagic flux can therefore be established when merged images exhibit maintained red and decreased green fluorescence [110].

Moreover, to further solidify the statements I have made from the data presented in this thesis, the following additions to the existing experiments may be made. To provide support that ER stress may induce autophagy as a rescue mechanism to help the cell cope with increased protein load, I could use rapamycin to upregulate autophagy and check whether it decreases protein aggregation via ThT assay, decreases GRP78mcherry expression and decreases peIF2α expression in Western blot. In addition, using salubrinal in the endogenous LC3

immunofluorescence assay should show increased green LC3 puncta, indicative of increased autophagosome formation. This would corroborate my thinking that maintaining the activity of the UPR's peIF2α signaling pathway leads to upregulation of autophagy induction, as well as the statement that autophagy may be upregulated as a part of UPR downstream adaptive signaling, specifically as part of the pPERK/peIF2α pathway. Though I have demonstrated that tunicamycin and palmitate both appear to increase caspase 3 activation, and that tunicamycin appears to increase caspase 12 activation, my next step would be check if palmitate also increases caspase 12 activation. In addition, I would examine whether tunicamycin and palmitate both increase the level of CHOP expression. These combined results would provide further information as to whether tunicamycin and palmitate induce apoptosis specifically through ER stress. Lastly, to verify the cytoprotective effect of autophagy and its ability to circumvent ER stress-induced apoptosis, ATG5K130R cells, defective for autophagy could be treated with tunicamycin and palmitate and should show increased caspase 12 and caspase 3 expression, increased quantity of apoptotic cells in the caspase 3/7 green detection reagent assay, and decreased cell viability in the MTT assay, as compared to EV control cells.

5.3. Concluding Remarks

In conclusion, my thesis project has elucidated the effects of palmitate-induced lipotoxicity on important cellular mechanisms ER stress, autophagy and apoptosis in L6 skeletal muscle cells. I have demonstrated how these processes may interact in conditions of cellular stress and how they might be regulated by adiponectin. However, as discussed in detail previously, there is much more that can be explored to broaden the scope of this project and to gather further evidence to support the insights made.

REFERENCES

1. Padwal, R.S., *Obesity, diabetes, and the metabolic syndrome: the global scourge.* Can J Cardiol, 2014. **30**(5): p. 467-72.
2. World Health Organization. Office of Health Communications and Public Relations., *Obesity and overweight*. WHO fact sheet2006, Geneva: World Health Organization. 3 p.
3. Luo, W., et al., *The burden of adult obesity in Canada.* Chronic Dis Can, 2007. **27**(4): p. 135-44.
4. Twells, L.K., et al., *Current and predicted prevalence of obesity in Canada: a trend analysis.* CMAJ Open, 2014. **2**(1): p. E18-26.
5. Lavallard, V.J., et al., *Autophagy, signaling and obesity.* Pharmacol Res, 2012. **66**(6): p. 513-25.
6. Ouchi, N., et al., *Adipokines in inflammation and metabolic disease.* Nat Rev Immunol, 2011. **11**(2): p. 85-97.
7. Hummasti, S. and G.S. Hotamisligil, *Endoplasmic reticulum stress and inflammation in obesity and diabetes.* Circ Res, 2010. **107**(5): p. 579-91.
8. Bonen, A., et al., *Triacylglycerol accumulation in human obesity and type 2 diabetes is associated with increased rates of skeletal muscle fatty acid transport and increased sarcolemmal FAT/CD36.* FASEB J, 2004. **18**(10): p. 1144-6.
9. Goodpaster, B.H., et al., *Intramuscular lipid content is increased in obesity and decreased by weight loss.* Metabolism, 2000. **49**(4): p. 467-72.
10. Goodpaster, B.H. and D. Wolf, *Skeletal muscle lipid accumulation in obesity, insulin resistance, and type 2 diabetes.* Pediatr Diabetes, 2004. **5**(4): p. 219-26.
11. Akhmedov, D. and R. Berdeaux, *The effects of obesity on skeletal muscle regeneration.* Front Physiol, 2013. **4**: p. 371.
12. Nawrocki, A.R. and P.E. Scherer, *The delicate balance between fat and muscle: adipokines in metabolic disease and musculoskeletal inflammation.* Curr Opin Pharmacol, 2004. **4**(3): p. 281-9.
13. Tamilarasan, K.P., et al., *Skeletal muscle damage and impaired regeneration due to LPL-mediated lipotoxicity.* Cell Death Dis, 2012. **3**: p. e354.
14. Thiebaud, D., et al., *The effect of graded doses of insulin on total glucose uptake, glucose oxidation, and glucose storage in man.* Diabetes, 1982. **31**(11): p. 957-63.
15. DeFronzo, R.A., et al., *Synergistic interaction between exercise and insulin on peripheral glucose uptake.* J Clin Invest, 1981. **68**(6): p. 1468-74.
16. DeFronzo, R.A. and D. Tripathy, *Skeletal muscle insulin resistance is the primary defect in type 2 diabetes.* Diabetes Care, 2009. **32 Suppl 2**: p. S157-63.
17. Maurya, C.K., et al., *4-Hydroxyisoleucine ameliorates fatty acid-induced insulin resistance and inflammatory response in skeletal muscle cells.* Mol Cell Endocrinol, 2014. **395**(1-2): p. 51-60.
18. Van Obberghen, E., et al., *Surfing the insulin signaling web.* Eur J Clin Invest, 2001. **31**(11): p. 966-77.
19. Lizcano, J.A., DR, *The insulin signaling pathway.* Curr Biol, 2002. **12**: p. 236-238.
20. O'Neill, H.M., *AMPK and Exercise: Glucose Uptake and Insulin Sensitivity.* Diabetes Metab J, 2013. **37**(1): p. 1-21.
21. Lelliott, C. and A.J. Vidal-Puig, *Lipotoxicity, an imbalance between lipogenesis de novo and fatty acid oxidation.* Int J Obes Relat Metab Disord, 2004. **28 Suppl 4**: p. S22-8.
22. Eckardt, K., A. Taube, and J. Eckel, *Obesity-associated insulin resistance in skeletal muscle: role of lipid accumulation and physical inactivity.* Rev Endocr Metab Disord, 2011. **12**(3): p. 163-72.
23. Martins, A.R., et al., *Mechanisms underlying skeletal muscle insulin resistance induced by fatty acids: importance of the mitochondrial function.* Lipids Health Dis, 2012. **11**: p. 30.
24. Xu, A., et al., *The fat-derived hormone adiponectin alleviates alcoholic and nonalcoholic fatty liver diseases in mice.* J Clin Invest, 2003. **112**(1): p. 91-100.

25. Fukushima, M., et al., *Adiponectin gene therapy of streptozotocin-induced diabetic mice using hydrodynamic injection.* J Gene Med, 2007. **9**(11): p. 976-85.
26. Fruebis, J., et al., *Proteolytic cleavage product of 30-kDa adipocyte complement-related protein increases fatty acid oxidation in muscle and causes weight loss in mice.* Proc Natl Acad Sci U S A, 2001. **98**(4): p. 2005-10.
27. Sishi, B., et al., *Diet-induced obesity alters signalling pathways and induces atrophy and apoptosis in skeletal muscle in a prediabetic rat model.* Exp Physiol, 2011. **96**(2): p. 179-93.
28. Woo, M., et al., *Early life nutrition modulates muscle stem cell number: implications for muscle mass and repair.* Stem Cells Dev, 2011. **20**(10): p. 1763-9.
29. Samuel, V.T., K.F. Petersen, and G.I. Shulman, *Lipid-induced insulin resistance: unravelling the mechanism.* Lancet, 2010. **375**(9733): p. 2267-77.
30. Paturi, S., et al., *Impaired overload-induced hypertrophy in obese Zucker rat slow-twitch skeletal muscle.* J Appl Physiol (1985), 2010. **108**(1): p. 7-13.
31. Sitnick, M., S.C. Bodine, and J.C. Rutledge, *Chronic high fat feeding attenuates load-induced hypertrophy in mice.* J Physiol, 2009. **587**(Pt 23): p. 5753-65.
32. Ghavami, S., et al., *Autophagy and apoptosis dysfunction in neurodegenerative disorders.* Prog Neurobiol, 2014. **112**: p. 24-49.
33. Shaw, J. and L.A. Kirshenbaum, *Molecular regulation of autophagy and apoptosis during ischemic and non-ischemic cardiomyopathy.* Autophagy, 2008. **4**(4): p. 427-34.
34. Marciniak, S.J. and D. Ron, *Endoplasmic reticulum stress signaling in disease.* Physiol Rev, 2006. **86**(4): p. 1133-49.
35. Lin, J.H., P. Walter, and T.S. Yen, *Endoplasmic reticulum stress in disease pathogenesis.* Annu Rev Pathol, 2008. **3**: p. 399-425.
36. Beriault, D.R. and G.H. Werstuck, *Detection and quantification of endoplasmic reticulum stress in living cells using the fluorescent compound, Thioflavin T.* Biochim Biophys Acta, 2013. **1833**(10): p. 2293-301.
37. Panzhinskiy, E., J. Ren, and S. Nair, *Protein tyrosine phosphatase 1B and insulin resistance: role of endoplasmic reticulum stress/reactive oxygen species/nuclear factor kappa B axis.* PLoS One, 2013. **8**(10): p. e77228.
38. Oslowski, C.M. and F. Urano, *Measuring ER stress and the unfolded protein response using mammalian tissue culture system.* Methods Enzymol, 2011. **490**: p. 71-92.
39. Ogata, M., et al., *Autophagy is activated for cell survival after endoplasmic reticulum stress.* Mol Cell Biol, 2006. **26**(24): p. 9220-31.
40. Basseri, S. and R.C. Austin, *Endoplasmic reticulum stress and lipid metabolism: mechanisms and therapeutic potential.* Biochem Res Int, 2012. **2012**: p. 841362.
41. Montane, J., L. Cadavez, and A. Novials, *Stress and the inflammatory process: a major cause of pancreatic cell death in type 2 diabetes.* Diabetes Metab Syndr Obes, 2014. **7**: p. 25-34.
42. Hara, T., et al., *Calcium efflux from the endoplasmic reticulum leads to beta-cell death.* Endocrinology, 2014. **155**(3): p. 758-68.
43. Preston, A.M., et al., *Reduced endoplasmic reticulum (ER)-to-Golgi protein trafficking contributes to ER stress in lipotoxic mouse beta cells by promoting protein overload.* Diabetologia, 2009. **52**(11): p. 2369-73.
44. Park, M., et al., *Palmitate induces ER stress and autophagy in H9c2 cells: implications for apoptosis and adiponectin resistance.* J Cell Physiol, 2014.
45. Cho, H.K., J.Y. Lee, and Y.H. Kwon, *Induction of endoplasmic reticulum stress by palmitate may contribute to insulin-resistance in HepG2 cell lines.* Faseb Journal, 2007. **21**(6): p. A1054-A1054.

46. Deldicque, L., et al., *The unfolded protein response is activated in skeletal muscle by high-fat feeding: potential role in the downregulation of protein synthesis.* Am J Physiol Endocrinol Metab, 2010. **299**(5): p. E695-705.
47. Yuzefovych, L.V., et al., *Mitochondrial DNA damage via augmented oxidative stress regulates endoplasmic reticulum stress and autophagy: crosstalk, links and signaling.* PLoS One, 2013. **8**(12): p. e83349.
48. Mizushima, N., *Autophagy: process and function.* Genes Dev, 2007. **21**(22): p. 2861-73.
49. Shintani, T. and D.J. Klionsky, *Autophagy in health and disease: a double-edged sword.* Science, 2004. **306**(5698): p. 990-5.
50. Maiuri, M.C., et al., *Self-eating and self-killing: crosstalk between autophagy and apoptosis.* Nat Rev Mol Cell Biol, 2007. **8**(9): p. 741-52.
51. Marino, G., et al., *Self-consumption: the interplay of autophagy and apoptosis.* Nat Rev Mol Cell Biol, 2014. **15**(2): p. 81-94.
52. Mari, M., S.A. Tooze, and F. Reggiori, *The puzzling origin of the autophagosomal membrane.* F1000 Biol Rep, 2011. **3**: p. 25.
53. Sandri, M., *Autophagy in skeletal muscle.* FEBS Lett, 2010. **584**(7): p. 1411-6.
54. Gukovsky, I., et al., *Inflammation, autophagy, and obesity: common features in the pathogenesis of pancreatitis and pancreatic cancer.* Gastroenterology, 2013. **144**(6): p. 1199-209 e4.
55. Moscat, J. and M.T. Diaz-Meco, *p62: a versatile multitasker takes on cancer.* Trends Biochem Sci, 2012. **37**(6): p. 230-6.
56. Green, D.R., L. Galluzzi, and G. Kroemer, *Mitochondria and the autophagy-inflammation-cell death axis in organismal aging.* Science, 2011. **333**(6046): p. 1109-12.
57. Kim, K.H., et al., *Autophagy deficiency leads to protection from obesity and insulin resistance by inducing Fgf21 as a mitokine.* Nat Med, 2013. **19**(1): p. 83-92.
58. Singh, R., et al., *Autophagy regulates lipid metabolism.* Nature, 2009. **458**(7242): p. 1131-5.
59. Ebato, C., et al., *Autophagy is important in islet homeostasis and compensatory increase of beta cell mass in response to high-fat diet.* Cell Metab, 2008. **8**(4): p. 325-32.
60. Galluzzi, L., et al., *Guidelines for the use and interpretation of assays for monitoring cell death in higher eukaryotes.* Cell Death Differ, 2009. **16**(8): p. 1093-107.
61. Dupont-Versteegden, E.E., *Apoptosis in skeletal muscle and its relevance to atrophy.* World J Gastroenterol, 2006. **12**(46): p. 7463-6.
62. Elmore, S., *Apoptosis: a review of programmed cell death.* Toxicol Pathol, 2007. **35**(4): p. 495-516.
63. Tait, S.W. and D.R. Green, *Mitochondria and cell death: outer membrane permeabilization and beyond.* Nat Rev Mol Cell Biol, 2010. **11**(9): p. 621-32.
64. Liu, F.T., A.C. Newland, and L. Jia, *Bax conformational change is a crucial step for PUMA-mediated apoptosis in human leukemia.* Biochem Biophys Res Commun, 2003. **310**(3): p. 956-62.
65. Oda, E., et al., *Noxa, a BH3-only member of the Bcl-2 family and candidate mediator of p53-induced apoptosis.* Science, 2000. **288**(5468): p. 1053-8.
66. Unger, R.H. and L. Orci, *Lipoapoptosis: its mechanism and its diseases.* Biochim Biophys Acta, 2002. **1585**(2-3): p. 202-12.
67. Kusminski, C.M., et al., *Diabetes and apoptosis: lipotoxicity.* Apoptosis, 2009. **14**(12): p. 1484-95.
68. Shimabukuro, M., et al., *Fatty acid-induced beta cell apoptosis: a link between obesity and diabetes.* Proc Natl Acad Sci U S A, 1998. **95**(5): p. 2498-502.
69. Hickson-Bick, D.L., L.M. Buja, and J.B. McMillin, *Palmitate-mediated alterations in the fatty acid metabolism of rat neonatal cardiac myocytes.* J Mol Cell Cardiol, 2000. **32**(3): p. 511-9.
70. Tsugane, K., et al., *A possible role of nuclear ceramide and sphingosine in hepatocyte apoptosis in rat liver.* J Hepatol, 1999. **31**(1): p. 8-17.

71. Turpin, S.M., et al., *Apoptosis in skeletal muscle myotubes is induced by ceramides and is positively related to insulin resistance.* Am J Physiol Endocrinol Metab, 2006. **291**(6): p. E1341-50.
72. Chiu, H.C., et al., *A novel mouse model of lipotoxic cardiomyopathy.* J Clin Invest, 2001. **107**(7): p. 813-22.
73. Summers, S.A., et al., *Regulation of insulin-stimulated glucose transporter GLUT4 translocation and Akt kinase activity by ceramide.* Mol Cell Biol, 1998. **18**(9): p. 5457-64.
74. Verfaillie, T., et al., *Linking ER Stress to Autophagy: Potential Implications for Cancer Therapy.* Int J Cell Biol, 2010. **2010**: p. 930509.
75. Kouroku, Y., et al., *ER stress (PERK/eIF2αlpha phosphorylation) mediates the polyglutamine-induced LC3 conversion, an essential step for autophagy formation.* Cell Death Differ, 2007. **14**(2): p. 230-9.
76. Yorimitsu, T., et al., *Endoplasmic reticulum stress triggers autophagy.* J Biol Chem, 2006. **281**(40): p. 30299-304.
77. Rutkowski, D.T., et al., *Adaptation to ER stress is mediated by differential stabilities of pro-survival and pro-apoptotic mRNAs and proteins.* PLoS Biol, 2006. **4**(11): p. e374.
78. Brush, M.H., D.C. Weiser, and S. Shenolikar, *Growth arrest and DNA damage-inducible protein GADD34 targets protein phosphatase 1 alpha to the endoplasmic reticulum and promotes dephosphorylation of the alpha subunit of eukaryotic translation initiation factor 2.* Mol Cell Biol, 2003. **23**(4): p. 1292-303.
79. Marciniak, S.J., et al., *CHOP induces death by promoting protein synthesis and oxidation in the stressed endoplasmic reticulum.* Genes Dev, 2004. **18**(24): p. 3066-77.
80. Song, B., et al., *Chop deletion reduces oxidative stress, improves beta cell function, and promotes cell survival in multiple mouse models of diabetes.* J Clin Invest, 2008. **118**(10): p. 3378-89.
81. Logue, S.E., et al., *New directions in ER stress-induced cell death.* Apoptosis, 2013. **18**(5): p. 537-46.
82. Lin, J.H., et al., *Divergent effects of PERK and IRE1 signaling on cell viability.* PLoS One, 2009. **4**(1): p. e4170.
83. Lin, J.H., et al., *IRE1 signaling affects cell fate during the unfolded protein response.* Science, 2007. **318**(5852): p. 944-9.
84. Galluzzi, L., O. Kepp, and G. Kroemer, *Mitochondria: master regulators of danger signalling.* Nat Rev Mol Cell Biol, 2012. **13**(12): p. 780-8.
85. Youle, R.J. and D.P. Narendra, *Mechanisms of mitophagy.* Nat Rev Mol Cell Biol, 2011. **12**(1): p. 9-14.
86. Hou, W., et al., *Autophagic degradation of active caspase-8: a crosstalk mechanism between autophagy and apoptosis.* Autophagy, 2010. **6**(7): p. 891-900.
87. Shaid, S., et al., *Ubiquitination and selective autophagy.* Cell Death Differ, 2013. **20**(1): p. 21-30.
88. Oral, O., et al., *Cleavage of Atg3 protein by caspase-8 regulates autophagy during receptor-activated cell death.* Apoptosis, 2012. **17**(8): p. 810-20.
89. Wirawan, E., et al., *Caspase-mediated cleavage of Beclin-1 inactivates Beclin-1-induced autophagy and enhances apoptosis by promoting the release of proapoptotic factors from mitochondria.* Cell Death Dis, 2010. **1**: p. e18.
90. Luo, S. and D.C. Rubinsztein, *Apoptosis blocks Beclin 1-dependent autophagosome synthesis: an effect rescued by Bcl-xL.* Cell Death Differ, 2010. **17**(2): p. 268-77.
91. Pagliarini, V., et al., *Proteolysis of Ambra1 during apoptosis has a role in the inhibition of the autophagic pro-survival response.* Cell Death Differ, 2012. **19**(9): p. 1495-504.
92. Kroemer, G. and B. Levine, *Autophagic cell death: the story of a misnomer.* Nat Rev Mol Cell Biol, 2008. **9**(12): p. 1004-10.

93. Young, M.M., et al., *Autophagosomal membrane serves as platform for intracellular death-inducing signaling complex (iDISC)-mediated caspase-8 activation and apoptosis.* J Biol Chem, 2012. **287**(15): p. 12455-68.
94. Rubinstein, A.D., et al., *The autophagy protein Atg12 associates with antiapoptotic Bcl-2 family members to promote mitochondrial apoptosis.* Mol Cell, 2011. **44**(5): p. 698-709.
95. Kessel, D.H., M. Price, and J.J. Reiners, Jr., *ATG7 deficiency suppresses apoptosis and cell death induced by lysosomal photodamage.* Autophagy, 2012. **8**(9): p. 1333-41.
96. Bachar-Wikstrom, E., et al., *Stimulation of autophagy improves endoplasmic reticulum stress-induced diabetes.* Diabetes, 2013. **62**(4): p. 1227-37.
97. Fang, X. and G. Sweeney, *Mechanisms regulating energy metabolism by adiponectin in obesity and diabetes.* Biochem Soc Trans, 2006. **34**(Pt 5): p. 798-801.
98. Liu, Y. and G. Sweeney, *Adiponectin action in skeletal muscle.* Best Pract Res Clin Endocrinol Metab, 2014. **28**(1): p. 33-41.
99. Lindsay, R.S., et al., *Adiponectin and development of type 2 diabetes in the Pima Indian population.* Lancet, 2002. **360**(9326): p. 57-8.
100. Matsushita, K., et al., *Comparison of circulating adiponectin and proinflammatory markers regarding their association with metabolic syndrome in Japanese men.* Arterioscler Thromb Vasc Biol, 2006. **26**(4): p. 871-6.
101. Pischon, T., et al., *Plasma adiponectin levels and risk of myocardial infarction in men.* JAMA, 2004. **291**(14): p. 1730-7.
102. Adamczak, M., et al., *Decreased plasma adiponectin concentration in patients with essential hypertension.* Am J Hypertens, 2003. **16**(1): p. 72-5.
103. Paz-Filho, G.L., E.L.; Wong, M.L.; Licinio, J, *Associations between adipokines and obesity-related cancer.* Front Biosci, 2011. **16**: p. 1634-1650.
104. Belfort, R., et al., *A placebo-controlled trial of pioglitazone in subjects with nonalcoholic steatohepatitis.* N Engl J Med, 2006. **355**(22): p. 2297-307.
105. Yamauchi, T. and T. Kadowaki, *Adiponectin receptor as a key player in healthy longevity and obesity-related diseases.* Cell Metab, 2013. **17**(2): p. 185-96.
106. Trujillo, M.E. and P.E. Scherer, *Adiponectin--journey from an adipocyte secretory protein to biomarker of the metabolic syndrome.* J Intern Med, 2005. **257**(2): p. 167-75.
107. Kadowaki, T. and T. Yamauchi, *Adiponectin and adiponectin receptors.* Endocr Rev, 2005. **26**(3): p. 439-51.
108. Hara, K., T. Yamauchi, and T. Kadowaki, *Adiponectin: an adipokine linking adipocytes and type 2 diabetes in humans.* Curr Diab Rep, 2005. **5**(2): p. 136-40.
109. Yamauchi, T., et al., *The fat-derived hormone adiponectin reverses insulin resistance associated with both lipoatrophy and obesity.* Nat Med, 2001. **7**(8): p. 941-6.
110. Liu, Y., et al., *Adiponectin stimulates autophagy and reduces oxidative stress to enhance insulin sensitivity during high fat diet feeding in mice.* Diabetes, 2014.
111. Ceddia, R.B., et al., *Globular adiponectin increases GLUT4 translocation and glucose uptake but reduces glycogen synthesis in rat skeletal muscle cells.* Diabetologia, 2005. **48**(1): p. 132-9.
112. Hug, C., et al., *T-cadherin is a receptor for hexameric and high-molecular-weight forms of Acrp30/adiponectin.* Proc Natl Acad Sci U S A, 2004. **101**(28): p. 10308-13.
113. Mao, X., et al., *APPL1 binds to adiponectin receptors and mediates adiponectin signalling and function.* Nat Cell Biol, 2006. **8**(5): p. 516-23.
114. Boddu, N.T., S; Luo, S; Wei, JY; Ranganathan, G, *Is the lack of adiponectin associated with increased ER/SR stress and inflammation in the heart?* Adipocyte, 2014. **3**(1): p. 10-18.
115. Wei, C.D., et al., *Globular adiponectin protects H9c2 cells from palmitate-induced apoptosis via Akt and ERK1/2 signaling pathways.* Lipids Health Dis, 2012. **11**: p. 135.

116. Dadson, K., Y. Liu, and G. Sweeney, *Adiponectin action: a combination of endocrine and autocrine/paracrine effects.* Front Endocrinol (Lausanne), 2011. **2**: p. 62.
117. Fang, X., et al., *Hyperglycemia- and hyperinsulinemia-induced alteration of adiponectin receptor expression and adiponectin effects in L6 myoblasts.* J Mol Endocrinol, 2005. **35**(3): p. 465-76.
118. Schuiki, I., L. Zhang, and A. Volchuk, *Endoplasmic reticulum redox state is not perturbed by pharmacological or pathological endoplasmic reticulum stress in live pancreatic beta-cells.* PLoS One, 2012. **7**(11): p. e48626.
119. Hamacher-Brady, A., et al., *Response to myocardial ischemia/reperfusion injury involves Bnip3 and autophagy.* Cell Death Differ, 2007. **14**(1): p. 146-57.
120. Pyo, J.O., et al., *Essential roles of Atg5 and FADD in autophagic cell death: dissection of autophagic cell death into vacuole formation and cell death.* J Biol Chem, 2005. **280**(21): p. 20722-9.
121. Estadella, D., et al., *Lipotoxicity: effects of dietary saturated and transfatty acids.* Mediators Inflamm, 2013. **2013**: p. 137579.
122. Egnatchik, R.A., et al., *ER calcium release promotes mitochondrial dysfunction and hepatic cell lipotoxicity in response to palmitate overload.* Mol Metab, 2014. **3**(5): p. 544-53.
123. Borradaile, N.M., et al., *Disruption of endoplasmic reticulum structure and integrity in lipotoxic cell death.* J Lipid Res, 2006. **47**(12): p. 2726-37.
124. Flamment, M., et al., *New insights into ER stress-induced insulin resistance.* Trends Endocrinol Metab, 2012. **23**(8): p. 381-90.
125. Choi, S.E., et al., *Protective role of autophagy in palmitate-induced INS-1 beta-cell death.* Endocrinology, 2009. **150**(1): p. 126-34.
126. Masini, M., et al., *Autophagy in human type 2 diabetes pancreatic beta cells.* Diabetologia, 2009. **52**(6): p. 1083-6.
127. Cheng, X., et al., *Connecting endoplasmic reticulum stress to autophagy through IRE1/JNK/beclin-1 in breast cancer cells.* Int J Mol Med, 2014. **34**(3): p. 772-81.
128. Bernales, S., K.L. McDonald, and P. Walter, *Autophagy counterbalances endoplasmic reticulum expansion during the unfolded protein response.* PLoS Biol, 2006. **4**(12): p. e423.
129. Cheng, Y.C., et al., *Autophagy modulates endoplasmic reticulum stress-induced cell death in podocytes: A protective role.* Exp Biol Med (Maywood), 2014.
130. Matsumoto, H., et al., *Selection of autophagy or apoptosis in cells exposed to ER-stress depends on ATF4 expression pattern with or without CHOP expression.* Biol Open, 2013. **2**(10): p. 1084-90.
131. Wu, C.T., et al., *Salubrinal, an eIF2αlpha dephosphorylation inhibitor, enhances cisplatin-induced oxidative stress and nephrotoxicity in a mouse model.* Free Radic Biol Med, 2011. **51**(3): p. 671-80.
132. Momoi, T., *Caspases involved in ER stress-mediated cell death.* J Chem Neuroanat, 2004. **28**(1-2): p. 101-5.
133. Nakagawa, T., et al., *Caspase-12 mediates endoplasmic-reticulum-specific apoptosis and cytotoxicity by amyloid-beta.* Nature, 2000. **403**(6765): p. 98-103.
134. Szegezdi, E., et al., *Mediators of endoplasmic reticulum stress-induced apoptosis.* EMBO Rep, 2006. **7**(9): p. 880-5.
135. Hitomi, J., et al., *Apoptosis induced by endoplasmic reticulum stress depends on activation of caspase-3 via caspase-12.* Neurosci Lett, 2004. **357**(2): p. 127-30.
136. Nigro, E.S., O; Monaco, ML; Palmieri, A; Mazzarella, G; Costagliola, C; Bianco, A; Daniele, A, *New Insight into Adiponectin Role in Obesity and Obesity-Related Diseases.* Biomed Res Int, 2014.
137. Nepal, S., et al., *Modulation of Atg5 expression by globular adiponectin contributes to autophagy flux and suppression of ethanol-induced cell death in liver cells.* Food Chem Toxicol, 2014. **68**: p. 11-22.

138. Wang, Y., et al., *[Effects of adiponectin on endoplasmic reticulum stress-mediated apoptosis and cell cytoskeleton and its mechanism of podocytes cultured in high glucose].* Zhonghua Yi Xue Za Zhi, 2014. **94**(14): p. 1092-6.
139. Ding, W., et al., *Adiponectin protects rat myocardium against chronic intermittent hypoxia-induced injury via inhibition of endoplasmic reticulum stress.* PLoS One, 2014. **9**(4): p. e94545.
140. Hapala, I., E. Marza, and T. Ferreira, *Is fat so bad? Modulation of endoplasmic reticulum stress by lipid droplet formation.* Biol Cell, 2011. **103**(6): p. 271-85.
141. Naiki, H., et al., *Fluorometric determination of amyloid fibrils in vitro using the fluorescent dye, thioflavin T1.* Anal Biochem, 1989. **177**(2): p. 244-9.
142. Martinez-Lopez, N. and R. Singh, *ATGs: Scaffolds for MAPK/ERK signaling.* Autophagy, 2014. **10**(3): p. 535-7.
143. Carloni, S., et al., *Increased autophagy reduces endoplasmic reticulum stress after neonatal hypoxia-ischemia: role of protein synthesis and autophagic pathways.* Exp Neurol, 2014. **255**: p. 103-12.
144. He, L., et al., *ATM blocks tunicamycin-induced endoplasmic reticulum stress.* FEBS Lett, 2009. **583**(5): p. 903-8.
145. Fujita, E., et al., *Caspase-12 processing and fragment translocation into nuclei of tunicamycin-treated cells.* Cell Death Differ, 2002. **9**(10): p. 1108-14.
146. Quick, Q.A. and M.O. Faison, *CHOP and caspase 3 induction underlie glioblastoma cell death in response to endoplasmic reticulum stress.* Exp Ther Med, 2012. **3**(3): p. 487-492.
147. Morishima, N., et al., *An endoplasmic reticulum stress-specific caspase cascade in apoptosis. Cytochrome c-independent activation of caspase-9 by caspase-12.* J Biol Chem, 2002. **277**(37): p. 34287-94.
148. Xu, Y., et al., *Inhibition of autophagy enhances cisplatin cytotoxicity through endoplasmic reticulum stress in human cervical cancer cells.* Cancer Lett, 2012. **314**(2): p. 232-43.
149. de Pablo, M.A., et al., *Palmitate induces apoptosis via a direct effect on mitochondria.* Apoptosis, 1999. **4**(2): p. 81-7.
150. Gonzalez-Rodriguez, A., et al., *Impaired autophagic flux is associated with increased endoplasmic reticulum stress during the development of NAFLD.* Cell Death Dis, 2014. **5**: p. e1179.
151. Kapuy, O., P.K. Vinod, and G. Banhegyi, *mTOR inhibition increases cell viability via autophagy induction during endoplasmic reticulum stress - An experimental and modeling study.* FEBS Open Bio, 2014. **4**: p. 704-13.
152. Guo, J., et al., *Globular adiponectin attenuates myocardial ischemia/reperfusion injury by upregulating endoplasmic reticulum Ca(2)(+)-ATPase activity and inhibiting endoplasmic reticulum stress.* J Cardiovasc Pharmacol, 2013. **62**(2): p. 143-53.
153. Lin, Z., et al., *Adiponectin protects against acetaminophen-induced mitochondrial dysfunction and acute liver injury by promoting autophagy in mice.* J Hepatol, 2014. **61**(4): p. 825-31.
154. Brons, C. and A. Vaag, *Skeletal muscle lipotoxicity in insulin resistance and type 2 diabetes.* J Physiol, 2009. **587**(Pt 16): p. 3977-8.
155. Koh, H.J., et al., *Tribbles 3 mediates endoplasmic reticulum stress-induced insulin resistance in skeletal muscle.* Nat Commun, 2013. **4**: p. 1871.
156. Maritim, A.C., R.A. Sanders, and J.B. Watkins, 3rd, *Diabetes, oxidative stress, and antioxidants: a review.* J Biochem Mol Toxicol, 2003. **17**(1): p. 24-38.
157. Bonnard, C., et al., *Mitochondrial dysfunction results from oxidative stress in the skeletal muscle of diet-induced insulin-resistant mice.* J Clin Invest, 2008. **118**(2): p. 789-800.
158. Lee, J., S. Giordano, and J. Zhang, *Autophagy, mitochondria and oxidative stress: cross-talk and redox signalling.* Biochem J, 2012. **441**(2): p. 523-40.

159. Rieusset, J., *Mitochondria and endoplasmic reticulum: mitochondria-endoplasmic reticulum interplay in type 2 diabetes pathophysiology.* Int J Biochem Cell Biol, 2011. **43**(9): p. 1257-62.
160. Ding, W.X. and X.M. Yin, *Mitophagy: mechanisms, pathophysiological roles, and analysis.* Biol Chem, 2012. **393**(7): p. 547-64.
161. Vazquez, C.C., MI, *Chapter 6 Assays to Assess Autophagy Induction and Fusion of Autophagic Vacuoles with a Degradative Compartment, Using Monodansylcadaverine (MDC) and DQ-BSA.* Methods in Enzymology 2009. **452**: p. 85-95.

APPENDIX A: List of Contributions

Liu, Y., Palanivel, R., Rai, E., Park, M., Gabor, T.V., Scheid, M.P., Xu, A., Sweeney, G., *Adiponectin stimulates autophagy and reduces oxidative stress to enhance insulin sensitivity during high fat diet feeding in mice.* Diabetes, 2015. **64**(1): p. 36-48.

APPENDIX B: Permissions for use of adapted or reproduced figures from articles

Figure 1.1. Adapted from O'Neill [20]. Open Access article

O'Neill, H.M., *AMPK and Exercise: Glucose Uptake and Insulin Sensitivity.* Diabetes Metab J, 2013. **37**(1): p. 1-21.

Journal List › Diabetes Metab J › v.37(1); 2013 Feb › PMC3579147

dmj DIABETES & METABOLISM JOURNAL

This Article • About • For Contributors • e-Submission

http://e-dmj.org

Diabetes Metab J. 2013 Feb; 37(1): 1–21. PMCID: PMC3579147

Published online 2013 Feb 15. doi: 10.4093/dmj.2013.37.1.1

AMPK and Exercise: Glucose Uptake and Insulin Sensitivity

Hayley M. O'Neill

Author information ► Copyright and License information ▼

Copyright © 2013 Korean Diabetes Association

This is an Open Access article distributed under the terms of the Creative Commons Attribution Non-Commercial License (http://creativecommons.org/licenses/by-nc/3.0/) which permits unrestricted non-commercial use, distribution, and reproduction in any medium, provided the original work is properly cited.

Diabetes Metab J

Figure 1.2. Taken from Basseri and Austin [40]. Open Access article

Basseri, S. and R.C. Austin, *Endoplasmic reticulum stress and lipid metabolism: mechanisms and therapeutic potential.* Biochem Res Int, 2012. **2012**: p. 841362.

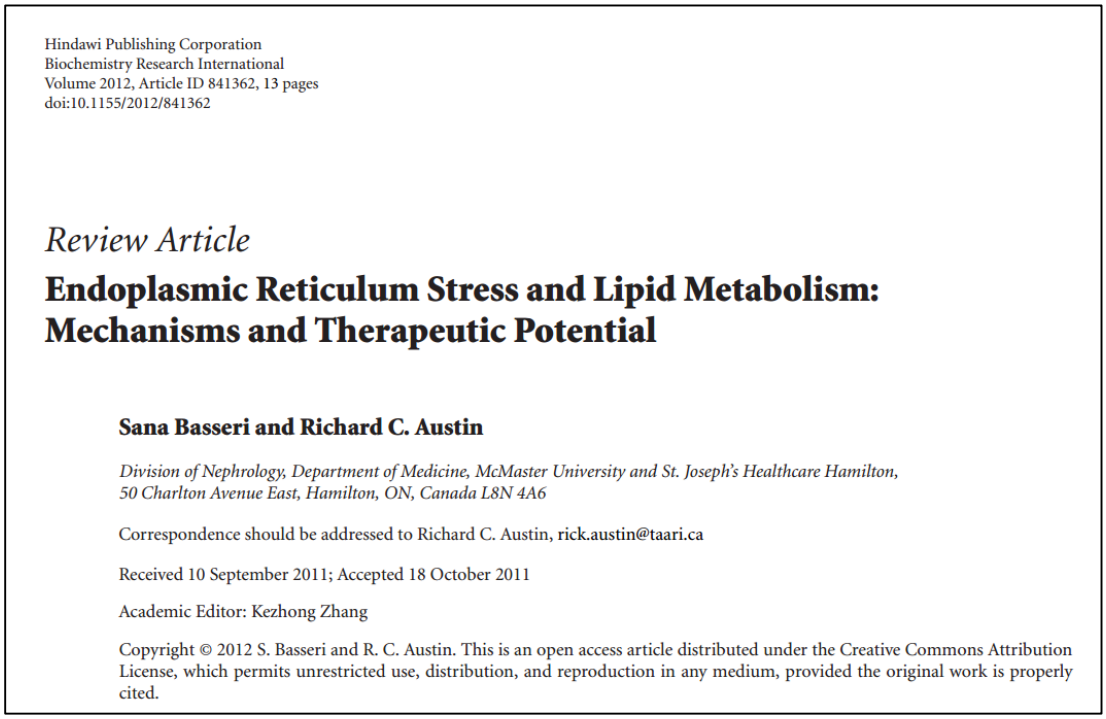

Hindawi Publishing Corporation
Biochemistry Research International
Volume 2012, Article ID 841362, 13 pages
doi:10.1155/2012/841362

Review Article

Endoplasmic Reticulum Stress and Lipid Metabolism: Mechanisms and Therapeutic Potential

Sana Basseri and Richard C. Austin

Division of Nephrology, Department of Medicine, McMaster University and St. Joseph's Healthcare Hamilton, 50 Charlton Avenue East, Hamilton, ON, Canada L8N 4A6

Correspondence should be addressed to Richard C. Austin, rick.austin@taari.ca

Received 10 September 2011; Accepted 18 October 2011

Academic Editor: Kezhong Zhang

Figures 1.3 and 1.4. Reprinted by permission from Macmillan Publishers Ltd: [Nat Rev Mol Cell Biol] (Marino et al [51]), copyright (2014). See below for License Agreement.

Marino, G., et al., *Self-consumption: the interplay of autophagy and apoptosis.* Nat Rev Mol Cell Biol, 2014. **15**(2): p. 81-94.

NATURE PUBLISHING GROUP LICENSE TERMS AND CONDITIONS

Mar 18, 2015

This is a License Agreement between Esther Rai ("You") and Nature Publishing Group ("Nature Publishing Group") provided by Copyright Clearance Center ("CCC"). The license consists of your order details, the terms and conditions provided by Nature Publishing Group, and the payment terms and conditions.

All payments must be made in full to CCC. For payment instructions, please see information listed at the bottom of this form.

License Number	3575960424790
License date	Feb 25, 2015
Licensed content publisher	Nature Publishing Group
Licensed content publication	Nature Reviews Molecular Cell Biology
Licensed content title	Self-consumption: the interplay of autophagy and apoptosis
Licensed content author	Guillermo Mariño, Mireia Niso-Santano, Eric H. Baehrecke, Guido Kroemer
Licensed content date	Jan 8, 2014
Volume number	15
Issue number	2
Type of Use	reuse in a dissertation / thesis
Requestor type	academic/educational
Format	print and electronic
Portion	figures/tables/illustrations
Number of figures/tables/illustrations	2
High-res required	no
Figures	Figures for autophagy and apoptosis from Box 1 and Box 2
Author of this NPG article	no
Your reference number	None
Title of your thesis / dissertation	Effect of Lipotoxicity on ER Stress, Autophagy and Apoptosis in Skeletal Muscle and Regulation by Adiponectin
Expected completion date	Feb 2015
Estimated size (number of pages)	111
Total	0.00 CAD

Terms and Conditions for Permissions

Nature Publishing Group hereby grants you a non-exclusive license to reproduce this material for this purpose, and for no other use,subject to the conditions below:

1. NPG warrants that it has, to the best of its knowledge, the rights to license reuse of this material. However, you should ensure that the material you are requesting is original to Nature Publishing Group and does not carry the copyright of another entity (as credited in the published version). If the credit line on any part of the material you have requested indicates that it was reprinted or adapted by NPG with permission from another source, then you should also seek permission from that source to reuse the material.

2. Permission granted free of charge for material in print is also usually granted for any electronic version of that work, provided that the material is incidental to the work as a whole and that the electronic version is essentially equivalent to, or substitutes for, the print version.Where print permission has been granted for a fee, separate permission must be obtained for any additional, electronic re-use (unless, as in the case of a full paper, this has already been accounted for during your initial request in the calculation of a print run).NB: In all cases, web-based use of full-text articles must be authorized separately through the 'Use on a Web Site' option when requesting permission.

3. Permission granted for a first edition does not apply to second and subsequent editions and for editions in other languages (except for signatories to the STM Permissions Guidelines, or where the first edition permission was granted for free).

4. Nature Publishing Group's permission must be acknowledged next to the figure, table or abstract in print. In electronic form, this acknowledgement must be visible at the same time as the figure/table/abstract, and must be hyperlinked to the journal's homepage.

5. The credit line should read:
   Reprinted by permission from Macmillan Publishers Ltd: [JOURNAL NAME] (reference citation), copyright (year of publication)
   For AOP papers, the credit line should read:
   Reprinted by permission from Macmillan Publishers Ltd: [JOURNAL NAME], advance online publication, day month year (doi: 10.1038/sj.[JOURNAL ACRONYM].XXXXX)

   Note: For republication from the *British Journal of Cancer*, the following credit lines apply.
   Reprinted by permission from Macmillan Publishers Ltd on behalf of Cancer Research UK: [JOURNAL NAME] (reference citation), copyright (year of publication)For AOP papers, the credit line should read:
   Reprinted by permission from Macmillan Publishers Ltd on behalf of Cancer Research UK: [JOURNAL NAME], advance online publication, day month year (doi: 10.1038/sj.[JOURNAL ACRONYM].XXXXX)

6. Adaptations of single figures do not require NPG approval. However, the adaptation should be credited as follows:

   Adapted by permission from Macmillan Publishers Ltd: [JOURNAL NAME] (reference citation), copyright (year of publication)

   Note: For adaptation from the *British Journal of Cancer*, the following credit line applies.
   Adapted by permission from Macmillan Publishers Ltd on behalf of Cancer Research UK: [JOURNAL NAME] (reference citation), copyright (year of publication)

7. Translations of 401 words up to a whole article require NPG approval. Please visit http://www.macmillanmedicalcommunications.com for more information.Translations of up to a 400 words do not require NPG approval. The translation should be credited as follows:

   Translated by permission from Macmillan Publishers Ltd: [JOURNAL NAME] (reference citation), copyright (year of publication).

   Note: For translation from the *British Journal of Cancer*, the following credit line applies.
   Translated by permission from Macmillan Publishers Ltd on behalf of Cancer Research UK: [JOURNAL NAME] (reference citation), copyright (year of publication)

We are certain that all parties will benefit from this agreement and wish you the best in the use of this material. Thank you.

Special Terms:

v1.1

Questions? customercare@copyright.com or +1-855-239-3415 (toll free in the US) or +1-978-646-2777.

Gratis licenses (referencing $0 in the Total field) are free. Please retain this printable license for your reference. No payment is required.